

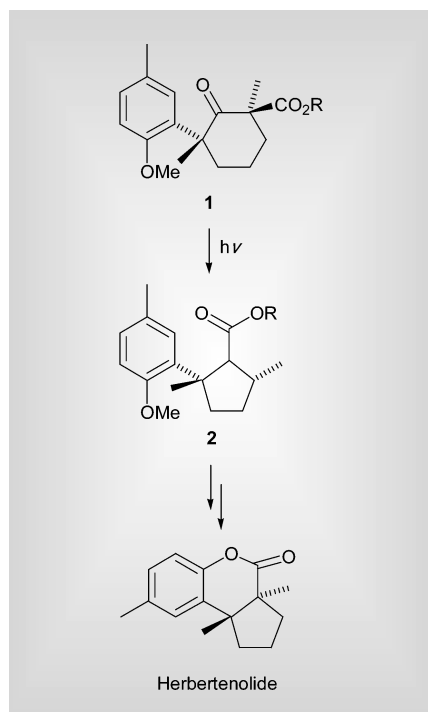


## Highlights

Markus Hölscher reviews some of the recent literature in green chemistry

### Chemo- and stereoselective solid state photodecarbonylation for the synthesis of natural products

Solvent free procedures can help to enlarge the pool of environmentally benign techniques in organic synthesis, as was shown by Garcia-Garibay *et al.* from the University of California - Los Angeles (*Org. Lett.* 2004, **6**, 645–647). During the seven step synthesis of ( $\pm$ )-herbertenolide, which was shown to suppress the growth of certain plant pathogenic fungi, they employed a photodecarbonylation in crystalline material as the key synthetic step for the introduction of vicinal quaternary centers. This technique was used for the first time in natural product synthesis.

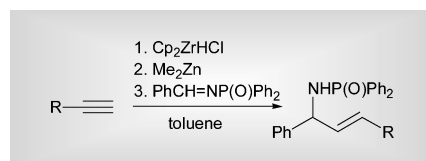


The reaction proceeded by irradiating crystalline ketone **1** at 0 °C for 6–12 h yielding cyclopentane **2** with remarkable chemo- and stereoselectivity (*ca.* 76% yield; at low conversions the *cis*-diastereomer could not be detected at all). The authors suggest the yield to be even

higher when lower reaction temperatures are used. Interestingly the same reaction did not afford the desired product when it was carried out in benzene solutions, emphasizing the potentially general importance of this method in natural product synthesis.

### One-pot process for the synthesis of allylic amines *via* microwave acceleration

Medicinal and organic chemists use allylic amines as valuable building blocks, and procedures for the synthesis of these include hydrozirconation of alkynes followed by zinc mediated addition of imines. Stephenson *et al.* from the University of Pittsburgh reported a facile one-pot synthesis which allows for rapid product formation by acceleration of reaction using microwave radiation (*Org. Biomol. Chem.* 2004, **2**, 443–445).

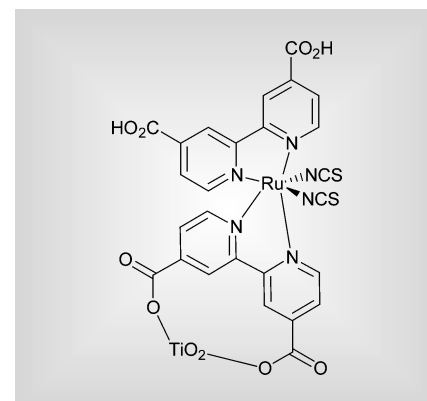


The authors sought to avoid chlorinated solvents and needed to overcome the drawback of low reaction rates for the hydrozirconation of alkynes in toluene. Microwave radiation solved both problems at once. Reaction times for the hydrozirconation of internal and terminal alkynes were brought down from more than 48 h under conventional heating (4-octyne) to *ca.* 5 min at 100 °C (under optimized conditions conversion was complete within 45 s). Subsequent reaction of the hydrozirconated products with imines yielded the desired allylic amines in good to excellent yields, with unsymmetrical internal alkynes proving to be the least reactive substrates for imine addition. Microwave radiation enables the use of a single solvent and yields overall reaction times of *ca.* 20 min.

### Heterogeneous mercury sensor

Chemical processes, medical applications and also environmental monitoring need

harmful species to be sensed, with the detection of mercury being of particular importance due to its biological toxicity. Mercury sensing devices in use suffer from disadvantages like high operation temperatures in the case of gold based films (150–300 °C) or limited sensitivity of polymer composites. Palomares *et al.* from Imperial College showed nanocrystalline, mesoporous TiO<sub>2</sub> films, which were treated with a ruthenium based dye (see below), to act as an appropriate mercury sensing device in aqueous solutions (*Chem. Commun.*, 2004, 362–363).



The dye was adsorbed on the TiO<sub>2</sub> film by simply soaking the material with acetonitrile-*tert*-butanol solutions of the ruthenium complex. The films were then exposed to aqueous solutions of metal salts including all metal cations mentioned by the Environmental Protection agency as 'drinking water contaminants' (Cd<sup>2+</sup>, Co<sup>2+</sup>, Cu<sup>2+</sup>, Hg<sup>2+</sup>, Ni<sup>2+</sup>, Pb<sup>2+</sup> and Zn<sup>2+</sup>). Remarkably, the film underwent a color change only in the presence of Hg<sup>2+</sup> ions, regardless of whether the solution applied contained only Hg<sup>2+</sup> or also all other metal cations. Reaction times varied between seconds and minutes at room temperature depending on the mercury concentrations. 'Naked eye' detection was possible down to 20 μM of Hg<sup>2+</sup>, and spectrophotometric detection allowed concentrations of down to *ca.* 0.3 μM (0.5 ppm) to be measured. The device operates selectively for mercury.

## Palladium nanoparticles as enantioselective catalysts for allylic alkylations

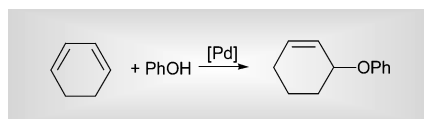
Metal nanoparticles are attracting more and more interest in catalytic applications and quite a few reactions have been shown to be efficiently catalyzed by these catalysts. As far as asymmetric catalysis is concerned, the field is still very open and much remains to be explored. A new example was lately added by the groups of Chaudret (Toulouse), Philippot (Toulouse) and Gómez (Barcelona) who reported on palladium nanoparticles which are catalytically active in enantioselective allylic alkylations (*J. Am. Chem. Soc.* 2004, **126**, 1592–1593). The authors claim to report the first asymmetric C–C coupling reaction using nanoparticles as catalysts. They used  $[\text{Pd}_2(\text{dba})_3]$  as precursor for decomposition by  $\text{H}_2$  at room temperature in the presence of chiral

xylofuranoside diphosphite as the ligand, which results in the formation of nanoparticles having a mean size of *ca.* 4 nm. Wide-angle X-ray analysis proved the bulk of the particles to consist of palladium metal.

For the evaluation of the catalytic performance the reaction of *rac*-3-acetoxy-1,3-diphenyl-1-propene with dimethyl malonate was studied in comparison with a molecular palladium complex generated by reaction of  $[\{\text{Pd}(\text{C}_3\text{H}_5\text{Cl})_2\}_2]$  with the ligand. Both systems yielded the expected alkylated product, but the molecular system catalyzed both enantiomers of the substrate with practically the same rate, whereas the nanoparticles showed a clear kinetic preference for the (*R*)-substrate (factors between 12 and 20 depending on the reaction conditions). Obviously the reaction mechanism varies according to the nature of the catalyst system.

## A green, catalytic way to ethers

The synthesis of ethers *via* substitution chemistry is usually accompanied by the generation of by-products. A recent development by Hartwig *et al.* from Yale University circumvents this by adding aromatic OH groups catalytically across cyclic and acyclic dienes yielding the desired ethers (*Angew. Chem., Int. Ed.* 2003, **42**, 5865–5868). Palladium catalysts are generated *in situ* from  $[\{\text{Pd}(\text{allyl})\text{Cl}\}_2]$  and appropriate ligands with the xantphos ligand yielding the most active system in the test reaction between cyclohexadiene and phenol.

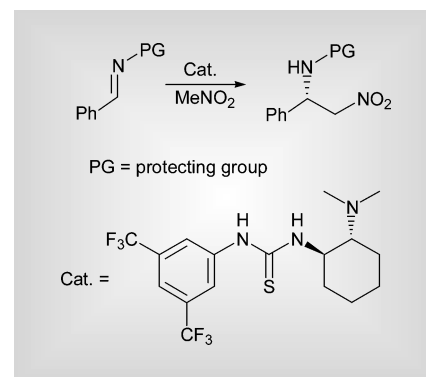


Both electron donating and withdrawing groups on the arene are tolerated with

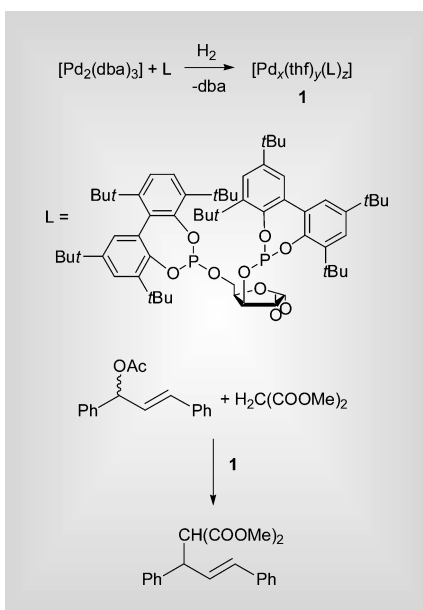
yields and conversion ranging from moderate to good and acyclic dienes can also be employed. The reaction is reversible with  $\Delta G \sim 0$ , indicating that small changes in the structures of the reactants can alter conversion and yield significantly.

## Metal free enantioselective aza-Henry reactions

The nucleophilic addition of nitroalkanes to imines known as the aza-Henry reaction is an interesting C–C bond forming process, since it yields  $\beta$ -nitroamine derivatives, which can be further transformed to 1,2-diamines and  $\alpha$ -amino acids. Takemoto *et al.* from Kyoto University showed that this reaction can be accomplished enantioselectively in a metal free way using bifunctional organocatalysts (*Org. Lett.* 2004, **6**, 625–627).



The reaction between different imines bearing protecting groups and MeNO<sub>2</sub> or other nitroalkanes proceeds with good to excellent yields (up to 91%) and moderate to good enantioselectivities (up to 76% *ee*), when an asymmetric thiourea is used as organocatalyst.





## Green Chemistry in Germany†

Andreas Förster from DECHEMA gives an overview of the current status of activities related to Green Chemistry within the major German funding agencies, public organisations, scientific societies and associations

### Introduction

The concept of Green Chemistry has seen a flourishing development in the last decade with interest increasing in both academic and industrial laboratories. To further implement Green Chemistry in research and education at different levels of society, several activities have been initiated, e.g. in the chemical industry, research institutions and universities, funding organisations and chemical societies. The scientific basis for the contribution of chemistry to a sustainable development are summarised in the book "Green Chemistry" by Paul Anastas.<sup>1</sup> Concepts of sustainable chemistry have also been recently discussed in two papers<sup>2,3</sup> and a Guest Editorial in issue 2, 2004 of *Green Chemistry*.<sup>4</sup>

This article will give an overview of ongoing or recently completed activities related to Green Chemistry within the major German funding agencies, public organisations, scientific societies and associations. The information provided will give an indication of the broad and high level work and is hoped to facilitate contacts and interactions between the described bodies, international organisations and individual experts.

### DECHEMA – Society for Chemical Engineering and Biotechnology



**Measuring the "greening" of chemistry**  
Measurement of the eco-efficiency or "sustainability" of chemical products and processes is important to assess and compare various approaches of Green Chemistry. Several measurement tools have been developed by organisations and companies. In 1999 DECHEMA (<http://www.dechema.de>) founded a working group "Sustainable Chemistry – Measurement and Metrics", integrating key players in this area in Germany. Industry,

institutes, universities and government agencies are involved. The aim of this working group is the continuous exchange of information to increase the transparency of existing measurement tools and to communicate the results within the community. In June 2001 the working group organised an International Conference on Measurement and Metrics in Frankfurt, Germany and participated in the preparation of the International Workshop "Tools, Needs, Metrics & Measurement for Dissemination Sustainable Manufacturing Practices", 24–25 June 2002, Washington DC, USA.

### Assessment of the sustainability of biotechnological processes

Biotechnology is often believed to be superior – in terms of sustainability – to established chemical production processes in many areas of the chemical industry. But up to now, an easy, and reliable assessment has still been difficult. The project "Simulation-based Assessment of the Sustainability of Biotechnological Production – BioBeN" aims to develop software that permits developers in industrial and academic research to evaluate the projected future biotechnological processes with respect to their economic, ecological and social impact. This project is being conducted by DECHEMA e.V., Department of Biochemical Engineering (<http://kwi.dechema.de/biovt>), within the "Sustainable BioProduction" programme of the BMBF.

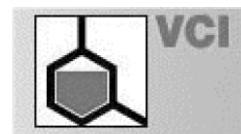
### Green Solvents for Catalysis

The use of environmentally benign reaction media is gaining an increasing importance for the future of Green Chemistry. Ionic liquids, supercritical reaction media, fluorinated phases or thermo-regulative systems: all these media are highly efficient solvents, have the potential to substitute classical organic solvents and may act as "green" and environmentally benign solvents. The innovative and fast developing research field on green solvents was the key theme of the 1st International Conference on "Green Solvents for Catalysis –

Environmentally Benign Reaction Media", which was held in Bruchsal, Germany, from 13–16 October 2002. The key topic was the comparison of various alternative solvents and their applications in homogeneous catalysis. The proceedings of the conference are available from DECHEMA e.V. Papers from the conference can also be found in a corresponding *Green Chemistry* special issue.<sup>5</sup> Due to the great success of the first conference the organisers have decided to organise a further meeting on "Green Solvents for Synthesis" from 3–6 October 2004 in Bruchsal, Germany. Further information is available on the web at <http://www.dechema.de/gsf2004>.

In addition DECHEMA has established a working group "Advanced Solvent Systems for Technical Applications (AS<sup>2</sup>TA)".

### VCI – German Chemical Industry Association



The chemical industry in Germany adopted the global Responsible Care initiative in 1991 and continuously improves labour safety, the high standard of safety in production plants and during transport, the reduction of emissions and the economical use of raw materials and energy. For example, energy related CO<sub>2</sub> emissions in the chemical industry in Germany were reduced from 65.4 million tons per year in 1990 to 44.0 million tons per year in 2001. Hence the use of energy in the German chemical industry decreased significantly during this period. To reach these goals the German chemical industry has not only improved its processes and technologies but has also developed an intensive educational and training system, conveying the ideas of Responsible Care to employees by simple experiments and demonstrations. In this context, too, a "Responsible Care game" has been developed by the German chemical industry association (VCI) (<http://www.vci.de>), the German

†The opinions expressed in the following article are entirely those of the author and do not necessarily represent the views of either the Royal Society of Chemistry, the Editor or the Editorial Board of *Green Chemistry*.

Federation of Chemical Employer's Associations, (BAVC) (<http://www.bavc.de>) together with the Trade Union for Mining, Chemicals and Energy, (IG BCE) (<http://www.igbce.de>).

### DBU – German Federal Environmental Foundation



The German Federal Environmental Foundation (<http://www.dbu.de>), the largest environmental foundation in Europe, promotes innovative, exemplary projects for the protection of the environment in the amount of approximately 40 million Euro per year. DBU supports activities related to Green Chemistry through personal scholarships to young researchers (mainly PhD students) as well as direct funding of medium to long term projects. Projects involving small and medium sized enterprises are the major target. In another project a network of six universities is developing a new curriculum for organic chemistry to teach students to apply "Green Chemistry" in their research (<http://www.oc-praktikum.de>).

### UBA – Federal Environmental Agency



The Federal Environmental Agency (<http://www.umweltbundesamt.de>) is the scientific environmental authority which comes under the jurisdiction of the Federal Ministry of the Environment, Nature, Conservation and Nuclear Safety (BMU) and is responsible for a diverse range of topics of environmental relevance, including safety management of chemicals in the chemical and other industries. UBA has funded and still is funding several projects involving Green Chemistry. UBA organised a workshop on "Sustainable Chemistry – integrated management of chemicals, products and processes" in Dessau, Germany, from 27–29 January 2004. The workshop provided a forum for representatives and experts from the authorities, research institutes and industry to discuss the next steps to be taken for the development of sustainable chemistry. The workshop focused on available criteria and indicators, methods and instruments for the evaluation of sustainability and aims to develop specific guidelines to implement sustainability for the management of chemicals. More than 120 experts participated at the event. Further information on this workshop can be found at <http://www.sustainable-chemistry.com>

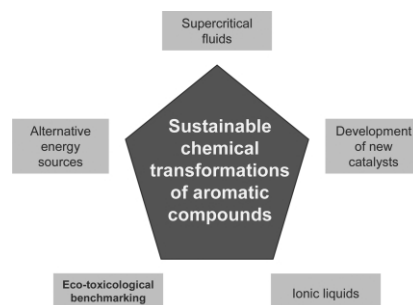
### BMBF – Federal Ministry of Education and Research



#### Lighthouse project "Sustainable Aromatic Chemistry"

In 1999 DECHEMA organised on behalf of the BMBF (<http://www.bmbf.de>) a status seminar "Sustainable Chemistry" for approximately 100 experts from industry, academia, organisations, ministries and the authorities. At this status seminar recommendations to the federal government for further activities in the area of sustainable chemistry were formulated. In the light of these considerations, in February 2001 the BMBF launched a programme "Sustainable Chemistry – research and development". As part of this programme a 'lighthouse' project on "Sustainable Aromatic Chemistry" is being funded. The participants comprise eight partners from research institutes and universities and four partners from industry. The project is focussed on alternatives for substitution reactions of aromatic chemicals in industry which usually involve stoichiometric and often wasteful organic reactions (*i.e.* nitrations, Friedel–Crafts reactions).

As depicted in the figure, the 'lighthouse' project applies different approaches for aromatic functionalisation reactions. In parallel to the chemical research the economic and environmental impact of the newly developed reactions are assessed and compared with the conventional reactions. This common approach, which is a novelty for research projects in chemistry funded by the BMBF, will help the researchers to decide at a very early stage of the process development which are the most environmentally benign and economically competitive solutions. The project is coordinated by Prof. Matthias Beller, IfoK Rostock (<http://www.ifo.uni-rostock.de>) and will end in March 2005.



#### ConNeCat – Competence Network Catalysis

In 2000 the BMBF started an initiative for the better combination of innovation-oriented research in the field of catalysis in

Germany. The Competence Network Catalysis ConNeCat (<http://www.conneecat.de>) was founded to close the gap between short term industrial R&D and basic research in universities and other research institutions. ConNeCat aims at assisting the scientific community in coordinating and optimising (pre-competitive) research in catalysis, encouraging cooperation between industrial and non-industrial research institutions, merging chemists, other natural scientists and engineers in interdisciplinary teams and providing a virtual and real platform for rapid exchange of information. Within the ConNeCat framework three lighthouse projects have been funded, one of them addressing main issues of Green Chemistry: "Tuneable Systems for Multiphase Catalysis – smart solvents/smart ligands" (Coordinator: Prof. Dr. Walter Leitner, RWTH Aachen)

### DFG – German Research Foundation



The German Research Foundation (<http://www.dfg.de>) is the central, self-governing research organisation that promotes research at universities and other publicly financed research institutions in Germany. The DFG serves all branches of science and the humanities by funding research projects and facilitating cooperation among researchers.

The DFG is also a member of the "Chairmen and directors of the European Research Councils' Chemistry Committees (CERC3)". CERC3's key objective is the coordination of national programmes and projects. CERC3 is trying to find ways to promote and fund transnational research in chemistry by inter-research Council cooperation. In May 2002, CERC3 decided to continue the "Transnational Research Initiative" and to initiate a new call for proposals in "Chemistry in Support of Sustainability". The focus of the call for proposals was on four main topics to be addressed by applicants:

- New Starting Materials and Reactions
- New Catalyst Systems
- New Reaction Media
- New Reactor Systems

27 joint proposals consisting of 67 sub-proposals were submitted. Nine joint projects were selected for funding, seven of them with the participation of German working groups. 22 teams from seven countries (Austria, Belgium, Denmark, France, Italy, Switzerland, Germany) are involved. Most of the projects deal with multi-step catalytic processes utilising



enzymes. Other topics are reactions in ionic liquids or microwave assisted synthesis. Further information can be found at the CERC 3 website (<http://www.cerc3.net>).

## GDCh – German Chemical Society



In 1990 the German Chemical Society (<http://www.gdch.de>) established a subject division on “Environmental Chemistry and Ecotoxicology”. Experts from academia and industry who are active in the respective topic work together, exchange ideas and foster the research area. The subject division is subdivided into five working parties, one of them focussing on “Resources and Environmentally Benign Synthesis in Processes”. This working party, chaired by Prof. Dieter Lenoir (GSF-National Research Center for Environment and Health, Oberschleißheim) organises and supports different events with respect to Green Chemistry. Since 1998 this working party organised biannual national conferences on this topic at several universities (Tübingen, Oldenburg, Jena). The next one will be held in 2005 in Rostock, Germany. Further information is available at <http://www.gdch.de/strukturen/fg/uoef.htm>.

## Conclusions

In Germany, activities relating to Green Chemistry are widespread throughout scientific and governmental organisations. At many research centres, universities and in industry R&D in Green Chemistry is being performed, but a comprehensive overview is outside of the scope of the present review.

Although the widespread activities in Green Chemistry described above are well accepted, a coherently structured and focused research infrastructure and community does not exist in Germany. The necessary cooperation between synthetic chemists and engineers as well as the support by industry is still to be improved in this research area. Therefore, Green Chemistry is not yet recognised as an independent research area and the visibility of Green Chemistry is not as prominent in Germany as it is in the UK, USA or Japan. There are, however, first attempts to implement Green Chemistry principles in the education and training of young chemists. It is hoped that the examples described above will further stimulate activities within individual university curricula. A possible approach to recognize and to support these efforts in research and education would be a Green Chemistry Award, which is already a well established practice, for instance, in the USA and UK.

To foster the visibility and acceptance of Green Chemistry in the German research

community, additional motivation of centres of scientific excellence in Green Chemistry is necessary as well as a coherent approach by the key players. Scientific organisations can provide support to the existing activities and form the nucleus of a coherent approach in Green Chemistry in Germany which will need to be supported and guided by the chemical industry.

**Dr. Andreas Förster**  
**DECHEMA – Society for Chemical**  
**Engineering and Biotechnology**  
**Theodor-Heuss Allee 25**  
**60486 Frankfurt**  
**Germany**  
**Phone: +49 69 7564409**  
**Fax: +49 69 7564117**  
**foerster@dechema.de**

## References

- 1 P. T. Anastas and J. C. Warner, *Green Chemistry*, Oxford University Press, Oxford, UK, 1998.
- 2 M. Eissen, J. O. Metzger, E. Schmidt and U. Schneidewind, 10 Years after Rio – Concepts on the Contribution of Chemistry to a Sustainable Development, *Angew. Chem.*, 2002, **114**, 402–425.
- 3 S. Bösch, D. Lenoir and M. Scheringer, Sustainable chemistry: starting points and prospects, *Angew. Chem., Int. Ed.*, 2002, **41**, 414–436.
- 4 J. O. Metzger, *Green Chem.*, 2004, **6**, G15–G16.
- 5 *Green Chem.*, 2003, **5**, (2), G28, G29, 99–239.



# New materials based on renewable resources: chemically modified highly porous starches and their composites with synthetic monomers

Krzysztof Milkowski, James H. Clark\* and Shinichi Doi

Green Chemistry Group, Clean Technology Centre, Department of Chemistry, University of York, Heslington, York, UK YO10 5DD. E-mail: jhc1@york.ac.uk; Fax: +44 1904 434550; Tel: +44 1904 432559

Received 16th December 2003, Accepted 23rd February 2004  
First published as an Advance Article on the web 5th March 2004

A range of novel starch based graft composites with synthetic polymers were prepared. These exhibit high surface areas as well as excellent thermal stabilities and useful wetting properties.

## Introduction

Starch is renewable, biodegradable and relatively inexpensive, which makes it attractive as an environmentally friendly polymer for general consumer applications, especially when modified physically or chemically<sup>1</sup> to improve properties such as hydrophobicity or thermal stability. Starches have been employed in blends or grafts with commercial polymers,<sup>2</sup> giving useful properties associated with biodegradability,<sup>3</sup> solubility in organic solvents, greater thermal or chemical stability or increased water affinity in hydrogels.<sup>4</sup>

In our previous communication<sup>5</sup> we have described new high surface area expanded corn starches (ECS), which have been chemically modified to give useful catalytic properties. Here we describe the first use of ECS for the absorption and subsequent graft-polymerisation of a range of synthetic monomers. The resulting composites exhibit novel characteristics, such as high porosity and interesting thermal properties.

## Experimental

The synthetic pathway can be divided into two parts: the preparation of expanded chemically modified corn starch networks and the subsequent graft copolymerisation with synthetic monomers. Firstly, high amylose or normal cornstarch is gelatinised and then retrograded to form an aqueous gel as described previously.<sup>5</sup> The water present in the system is then exchanged with a 3–5 fold excess ethanol. The resulting suspension is subsequently filtered and dried under vacuum to yield ECS. Chemical modification can be performed at the solvent exchange stage or on the ECS. The main chemical modifiers used were glycidyl methacrylate (GM) and epichlorohydrin (ECH). These were added to a basic suspension of ECS in 90–95% aqueous ethanol in molar ratios relative to alpha-glucan monomer units in the starch of 6 : 2 : 1 or 3 : 1 : 1 to the moles of modifier and NaOH respectively. Higher modification levels collapse the structure by degrading the starch polymer. After stirring overnight at room temperature, the suspension was filtered, washed with ethanol and vacuum dried to yield porous modified expanded starches (MECS) with surface areas (SA) in the range of 120–250 m<sup>2</sup> g<sup>-1</sup>.

For the composite preparation, three general pathways have been used for initiating the monomer grafting: (a) simple heating, (b) physically mixing 10–20% by weight of a radical initiator such as 1,1-Azobis(cyclohexanecarbonitrile) (VAZO) into the ECS/MECS and subsequent heating or (c) modifying the ECS with chlorosulfonic acid to initiate cationic polymerisation or sulfonate the monomers. The type of modifications performed and their effects on the SA of the starches are summarised in Table 1.

Four monomers were mainly employed for the grafting: styrene,  $\alpha$ -methyl styrene, indene and methyl acrylate. These were typically

**Table 1** Effect of chemical modifications, using glycidyl methacrylate (GM), epichlorohydrin (ECH) and chlorosulfonic acid, on the surface areas (SA) and pore volumes (PV) of high amylose corn starch

Materials	Modifier	Reaction molar ratio starch : mod : base	SA/m <sup>2</sup> g <sup>-1</sup>	PV/ml g <sup>-1</sup>
ECS	—		130	0.42
SGN621	GM	6 : 2 : 1	160	0.61
SGN311	GM	3 : 1 : 1	177	0.67
SEN621	ECH	6 : 2 : 1	230	0.82
SEN311	ECH	3 : 1 : 1	186	0.58
SSP313	CISO <sub>3</sub> H	3 : 1 : 3	88	0.35
SSP323	CISO <sub>3</sub> H	3 : 2 : 3	42	0.04

absorbed in a closed system from the gaseous phase over the starch powder at 20–100 °C at 50–1000 mbar for 10–48 h. The monomers polymerised around the starch matrix causing up to 500% weight gain. After thorough washing with the synthetic homopolymer solvent weight gains representing the grafted polymer were typically between 2–40%. Grafting was confirmed by DRIFT-IR, XPS and <sup>13</sup>C MAS-NMR.

## Results and discussion

The amount of monomer absorbed depended on the original SA, the amount of initiator used, the reaction temperature and the degree of chemical modification. The resulting composites retained high SA (Table 2). SEM analysis revealed that the expanded starch framework is coated with a synthetic polymer as shown in Fig. 1, but the composites retain porosity.

In general, as can be seen in Table 2, higher SA materials allowed more grafting as did using a radical initiator, instead of simple heat initiation. For styrene, modification with GM enhanced grafting with VAZO, but without it, the results were poorer than for unmodified starch (entries 2, 4 and 6 in Table 2). GM is capable of producing radicals with VAZO but not with styrene radicals or heat. Using VAZO also significantly decreased the SA, which is partially due to a greater integration of the synthetic polymer, but also due to possible cross-linking of two radically activated starch chains, in particular when modified by GM.

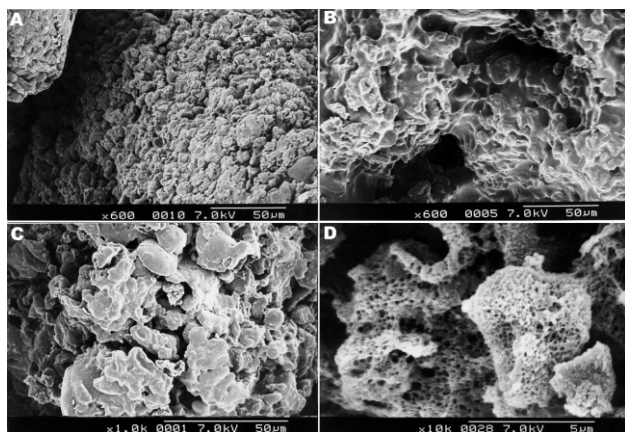
Unlike for styrene, modification with GM inhibited grafting of methyl acrylate. Although, as previously, higher SA gave more incorporation, this order was reversed with greater modification (entries 12–15 and 8–11 in Table 2). Moreover, significant grafting was achieved only in the presence of VAZO, but the incorporation levels were so high that the SA-s of the composites were negligible. The materials, however, are nearly uniform indicating intimate blending.

For polymerisations initiated by the SO<sub>3</sub>H group, more grafting was noted at higher temperatures and greater modification levels despite the significant difference in the SA-s of the two starches used. Grafting was generally lower than for the radical polymerisations, but subsequently the SA-s did not decrease by as much, except when modification levels and temperatures were high, degrading the starch (entry 24 in Table 2).

**Table 2** Comparison between the surface areas (SA) and amounts of grafting for a range of materials, monomers (M) and initiators (I). % SA is the % of the surface area of the composite in comparison to the SA before grafting. % in composite refers to synthetic polymer and is based on XPS measurements

Exp	I	Starch	SA/ m <sup>2</sup> g <sup>-1</sup>	M	Temp/ °C	% SA	% in composite
1	VAZO	SGN621	159		80	3.30	48.9
2		SGN621	159		80	34.0	15.0
3	VAZO	SGN311	165		80	9.10	54.3
4		SGN311	165	styrene	80	42.4	9.10
5	VAZO	ECS	170		80	15.3	44.8
6		ECS	170		80	36.5	34.9
7	VAZO	CS	—		80	78.1 <sup>a</sup>	8.2
<hr/>							
8	VAZO	SGN621	159		80	0.60	60.1
9		SGN621	159		80	12.6	14.3
10	VAZO	SGN311	165		80	0.70	42.7
11		SGN311	165		80	30.9	7.00
12	VAZO	ECS	134	methyl	80	0.01	58.5
13		ECS	134	acrylate	80	20.1	9.60
14	VAZO	ECS	170		80	0.01	67.8
15		ECS	170		80	28.8	14.0
16	VAZO	CS	—		80	56.0 <sup>a</sup>	4.8
<hr/>							
17		SSP313	85		80	48.2	21.7
18	SO <sub>3</sub> H	SSP313	85	styrene	20	41.2	8.10
19		SSP323	4		20	92.5	10.5
<hr/>							
20		SSP313	85	α-	80	32.9	14.4
21	SO <sub>3</sub> H	SSP313	85	methyl	20	50.6	6.90
22		SSP323	4	styrene	20	82.5	15.4
<hr/>							
23	SO <sub>3</sub> H	SSP313	85	indene	80	40.0	16.8
24		SSP323	4		80	0.75	31.0

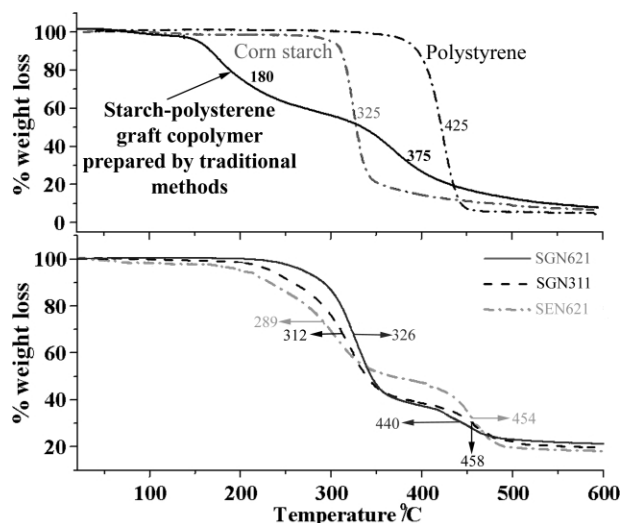
<sup>a</sup> Value represents surface area in m<sup>2</sup> g<sup>-1</sup> rather than %.



**Fig. 1** SEM pictures of ECS (A) and ECS-polystyrene graft copolymers with increasing magnification (B–D).

Porous composites can also be produced by adding the monomer and a radical initiator immediately after the gelatinisation of starch. After 24 h reaction at 80 °C, solvent exchange and drying produce porous composites (entries 7 and 16 in Table 2). However, greater grafting levels yield hard large agglomerates rather than fine powders.

In addition to high porosity, the composites prepared in this manner exhibit improved thermal properties in comparison to traditional grafts. Fig. 2 compares typical thermogravimetric curves of three composites prepared by gaseous absorption of styrene onto a blend of VAZO and MECS (lower graph) to curves for polystyrene, CS and their composite prepared in the traditional way (upper graph). Traditional grafting lowers the decomposition temperature for both the starch and the styrene component suggesting significant structural degradation. Moreover, the stability decreases with increasing amount of grafting. On the other hand,



**Fig. 2** Thermogravimetric curves of starch and polystyrene and their composite prepared in a traditional way as well as curves for composites prepared by gaseous absorption of monomers. The temperature values marked on the graphs represent the mid-decomposition temperatures for degradation segments in the homopolymers and composites.

for the new composites, the starch component degrades at higher temperature for comparable grafting levels and the polystyrene component is more stable even in comparison to polystyrene itself.

Additionally, as demonstrated in Table 2, with increasing level of starch modification more polystyrene is grafted, increasing not only the amount of the more stable composite fraction but also its degradation temperature. As shown by the case of SEN621 in Fig. 2, for a 50–50 composite mixture this temperature increases by nearly 30 °C.

Moreover, upon heating under nitrogen, normal or expanded starches increase several times in volume due to formation of CO<sub>2</sub> from partial combustion of chains. The composites, on the other hand, puff up to a lesser extent if at all. Although CO<sub>2</sub> is still generated, the composite holds the structure preventing swelling. This property can be useful in end use application.

## Conclusion

The low modification levels of starch employed in this study are unlikely to significantly affect toxicological properties. Furthermore, inclusion of starch into synthetic materials enhances environmental performance. Our composites exhibit excellent properties that can rival and hopefully replace some of the existing synthetic materials in end use applications.

## Acknowledgements

We gratefully acknowledge the financial support of the EPSRC (for a ROPA grant) and the Oji Paper Company (for a fellowship to S. D.).

## Notes and references

- J. Jane, *J. Macromol. Sci. – Pure Appl. Chem.*, 1995, **A32**, 751.
- G. J. L. Griffin, U.S. Patent: 1997, 4,021,388; V. D. Athwale and V. Lele, *Starch/Stärke*, 2001, **53**, 7; G. Fanta, D. Trimmell and J. Salch, *J. Appl. Polym. Sci.*, 1993, **49**, 1679; T. Trimmell, G. Fanta and J. Salch, *J. Appl. Polym. Sci.*, 1996, **60**, 285; A. Hebeish, M. Zahran, M. ElRafie and K. ElTahlawy, *Polym. Polym. Compos.*, 1996, **4**, 129; A. Hebeish, M. ElRafie, A. Higazy and M. Ramadan, *Starch/Stärke*, 1996, **48**, 175.
- J. Loercks, W. Pommeranz, H. Schmidt, R. Timmerman, E. Grigat and W. Schulz-Schlitte, US Patent 2001, 6,235,815 B1.
- C. Bastioli, *Starch/Stärke*, 2001, **53**, 351.
- S. Doi, J. H. Clark, D. J. Macquarrie and K. Milkowski, *Chem. Commun.*, 2002, **22**, 2632.



# Per-*O*-acetylation of sugars catalyzed by Ce(OTf)<sub>3</sub>

Giuseppe Bartoli,<sup>a</sup> Renato Dalpozzo,<sup>b</sup> Antonio De Nino,<sup>b</sup> Loredana Maiuolo,<sup>b</sup> Monica Nardi,<sup>b</sup> Antonio Procopio<sup>\*c</sup> and Antonio Tagarelli<sup>b</sup>

<sup>a</sup> Dipartimento di Chimica Organica, v.le Risorgimento 4, 40136 Bologna, Italy

<sup>b</sup> Dipartimento di Chimica Università della Calabria, Ponte Bucci, 87030, Arcavacata di Rende (CS), Italy

<sup>c</sup> Dipartimento Farmaco-Biologico, Università degli Studi della Magna Graecia, Complesso Nini Barbieri, Roccelletta di Borgia (CZ), Italy. E-mail: procopio@unicz.it; Fax: +39 (984) 492055

Received 20th January 2004, Accepted 24th February 2004

First published as an Advance Article on the web 10th March 2004

Ce(OTf)<sub>3</sub> is proposed as a valuable Lewis acid promoter in the per-*O*-acetylation reactions of sugars. The Ce(OTf)<sub>3</sub> is an environmentally friendly catalyst, used in very low percentage, and can be recovered after reaction and used without significant loss of activity.

## Introduction

An important part of our efforts toward more environmentally friendly chemistry<sup>1</sup> is aimed at developing new catalytic reagents for valuable protection/deprotection steps of functional groups.<sup>2</sup>

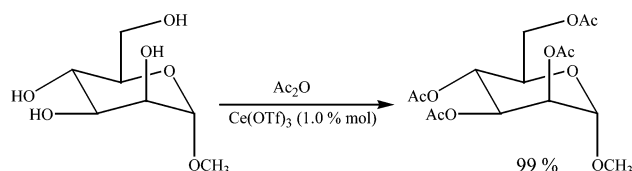
Per-*O*-acetylation is the most commonly used method for the protection of hydroxyl groups in sugars.<sup>3</sup> The structural elucidation of many natural products is very often realized through the per-*O*-acetylation of their saccharide moieties and fully acetylated sugars are inexpensive and useful starting materials for the synthesis of glycosides, oligosaccharides, and glycoconjugates. Moreover, it was recently reported that the acetylation of hydroxyl groups may be a valuable approach to CO<sub>2</sub>-philize polar compounds.<sup>4</sup> Thus, the per-*O*-acetylation of carbohydrates opens a wide range of opportunities for the exploitation of precious renewable compounds. Acetylation of sugars is usually carried out using acetic anhydride in presence of a basic or acid catalyst such as pyridine or other amines,<sup>5</sup> sodium acetate,<sup>5</sup> ZnCl<sub>2</sub>,<sup>6</sup> FeCl<sub>3</sub>,<sup>7</sup> toluene sulfonic acid,<sup>8</sup> montmorillonite,<sup>9</sup> iodine,<sup>10</sup> and molecular sieves.<sup>11</sup> However, many of these methods suffer from some drawbacks. The amines and pyridine, which is also used as solvent, present well known toxicity, have unpleasant odors, and are not easy to remove. Furthermore, many of these reactions are carried out under reflux, the promoter is used in none catalytic amounts or tedious work-up is required.

More recently, several triflate derivatives, such as Sc(OTf)<sub>3</sub>,<sup>12</sup> TMSOTf,<sup>13</sup> In(OTf)<sub>3</sub>,<sup>14</sup> Cu(OTf)<sub>2</sub>,<sup>15</sup> Bi(OTf)<sub>3</sub>,<sup>16</sup> and LiOTf<sup>17</sup> have been found to be effective as Lewis acid promoters in per-*O*-acetylation reactions of sugars. However, cost, availability, toxicity, and difficulty in handling can limit the widespread application of many of these triflate derivatives. Thus, despite a number of existing procedures, new efficient methodologies for per-*O*-acetylation reactions of sugars are still in strong demand. In the course of our investigations in the area of clean technologies using Lewis acid catalysts for atomic economic protection/deprotection steps of the hydroxyl function, we found that cerium salts are very active and environmentally friendly catalysts.<sup>2,18</sup> Particularly, we already reported that cerium(III) triflate is a valuable catalyst, readily recyclable *via* simple aqueous work-up, in the acetylation reactions of alcohols and phenols.<sup>2d</sup>

Now herein, we report a new mild and efficient protocol for the per-*O*-acetylation of a variety of carbohydrates using acetic anhydride in the presence of catalytic amounts of Ce(OTf)<sub>3</sub>.

## Results and discussion

The standard experimental procedure is reported for methyl- $\alpha$ -D-mannopyranoside (Scheme 1): a catalytic quantity of Ce(III)



trifluoromethanesulfonate (1.0% mol) was added to a suspension of methyl- $\alpha$ -D-mannopyranoside (1.0 mmol) in acetic anhydride (5.0 ml) and stirred at room temperature. After 1 hour, the solution was poured into water and stirred for few minutes; partition work-up with dichloromethane gives the methyl 2,3,4,6-tetraacetyl- $\alpha$ -D-mannopyranoside as essentially a single component (<sup>1</sup>H and <sup>13</sup>C NMR and mass spectrometry). After work-up, the aqueous phase was evaporated under reduced pressure and the Ce(III) salt was recovered as a white solid and reused after drying overnight over P<sub>2</sub>O<sub>5</sub>. This recycle protocol was repeated five times and the percentage of the catalyst recovery was always more than 90% (I.R. spectrum corresponding to the standard material<sup>19</sup>), while the yields of the peracetylated methyl- $\alpha$ -D-mannopyranoside were always more than 93%.

In order to extend the scope of this work, the described methodology was tested on different carbohydrate substrates. In all the cases, the per-*O*-acetylated sugars were obtained in very satisfactory yields and in relatively short times especially if the temperature was raised up to 50 °C for the less reactive substrates (Table 1).

The ratio of  $\alpha$ - and  $\beta$ -pyranose anomers for the per-*O*-acetylation products **4–13** in Table 1 was determined by 300 MHz <sup>1</sup>H-NMR spectral analysis which did not show the presence of  $\alpha$ - and  $\beta$ -furanose per-*O*-acetates since no chemical shifts up to 4.5 ppm were registered for H<sub>5</sub> signals. No substantial differences in  $\alpha/\beta$  ratio were registered respect to literature reported data.<sup>20</sup> It is noteworthy that a high yield was obtained in a very short time for per-*O*-acetylated cellobiose which gave only scarce results in other acetylation procedures.<sup>10</sup> Uridine (entry **14**) and thymidine (entry **15**) were transformed respectively into 2',3',5'-tri- and 3',5'-diacetylated products in the presence of Ce(OTf)<sub>3</sub>, and the subsequent chromatography column provided these valuable intermediates for the nucleoside chemistry. NMR spectra confirm that no N-acetylated pyrimidine base is present. Moreover, encouraged by the fact that acid labile groups such as isopropylidene and benzylidene survived the present conditions (entries **16** and **17** in Table 1), other substrates carrying different acid labile protecting groups were subjected to the Ce(OTf)<sub>3</sub> promoted acetylation. Methyl-6-trityl- $\alpha$ -D-glucopyranoside (entry



**Table 1** Per-*O*-acetylation of saccharidic compounds promoted by Ce(OTf)<sub>3</sub>

Entries <sup>a</sup>	T/°C	t/h	Yield (%)	α/β
methyl-α-D-mannopyranoside (1)	r.t.	1	99	—
methyl-α-D-glucopyranoside (2)	r.t.	3	95	—
methyl-α-D-galactopyranoside (3)	r.t.	20	96	—
D-mannose (4)	50	1	93	62/38
D-glucose (5)	50	2	94	86/14
D-galactose (6)	50	6	98	70/30
D-xylose (7)	50	7	93	80/20
D-ribose (8)	50	7	90	27/73
D-maltose (9)	50	3	88	28/72
D-lactose (10)	50	4	90	70/30
D-cellobiose (11)	50	3	75	31/69
sucrose (12)	50	1.5	99	87/13
<i>N</i> -Ac-D-glucosamine (13)	50	8	90	71/29
uridine (14)	50	1	96	—
thymidine (15)	50	1	95	—
methyl-4,6-benzyliden-α-D-glucopyranoside (16)	50	2	92	—
1,2:5,6-di- <i>O</i> -isopropyliden-α-D-glucofuranoside (17)	50	2	90	—
methyl-6-trityl-α-D-glucopyranoside (18)	50	2	89 <sup>b</sup>	—
methyl-6-TBDMS-α-D-glucopyranoside (19)	50	2	88 <sup>b</sup>	—

<sup>a</sup> All per-*O*-acetylated products were identified by comparison of their EIMS, <sup>1</sup>H and <sup>13</sup>C NMR spectral data with those of authentic compounds and literature reported data.<sup>20</sup> <sup>b</sup> Only fully acetylated product was obtained.

18) and methyl-6-TBDMS-α-D-glucopyranoside (entry 19) gave the fully acetylated compounds revealing that TBDMS and Tr groups are not compatible with the present acetylation method, as could be expected on the basis of previous reports.<sup>2b,21</sup>

## Conclusion

In conclusion, the per-*O*-acetylation of carbohydrates in acetic anhydride and catalytic amounts of cerium(III) trifluoromethanesulfonate presents, compared with the existing procedures, a series of advantages. Ce(OTf)<sub>3</sub> is commercially available at acceptable price<sup>19</sup> and the reaction is carried out in almost neutral conditions; in fact a 0.1 M solution of (Ce(OTf)<sub>3</sub> in water is only weakly acidic (pH = 6.0), and the aqueous layer from the work-up was also a weaker acid (pH = 6.7), which is compatible with some acid sensitive substrates. Moreover, the present method fulfils most of the 12 Principles of Green Chemistry.<sup>2</sup> In fact, cerium is not toxic, it is used in really catalytic amounts at room or modest temperature, and can be recovered and reused after reaction without significant loss of activity.

## Notes and references

- (a) P. T. Anastas and J. C. Warner, *Green Chemistry: Theory and Practice*, Oxford Science Publications, Oxford, 1998; (b) T. C. Collins, *Green Chemistry: Frontiers in Chemical Synthesis and Processes*, Oxford University Press, Oxford, 1998; (c) P. Tundo, P. Anastas StC., D. Black, J. Breen, T. Collins, S. Memoli, J. Miyamoto, M. Polyakoff and W. Tumas, *Pure Appl. Chem.*, 2000, **72**, 1207; (d) P. T. Anastas and M. M. Kirchhoff, *Acc. Chem. Res.*, 2002, **35**, 68.
- (a) G. Bartoli, G. Cupone, R. Dalpozzo, A. De Nino, L. Maiuolo, E. Marcantoni and A. Procopio, *Synlett*, 2001, 1897; (b) G. Bartoli, G.

- Cupone, R. Dalpozzo, A. De Nino, L. Maiuolo, A. Procopio, L. Sambri and A. Tagarelli, *Tetrahedron Lett.*, 2002, **43**, 5945; (c) R. Dalpozzo, A. De Nino, L. Maiuolo, A. Procopio, A. Tagarelli, G. Sindona and G. Bartoli, *J. Org. Chem.*, 2002, **67**, 9093; (d) R. Dalpozzo, A. De Nino, L. Maiuolo, A. Procopio, M. Nardi, G. Bartoli and R. Romeo, *Tetrahedron Lett.*, 2003, **44**, 5621.
- P. M. Collins and R. J. Ferrier, *Monosaccharides. Their Chemistry and Their Roles in Natural Products*, John Wiley & Sons, New York, 1995, pp. 360.
  - P. Raveendran and S. L. Wallen, *J. Am. Chem. Soc.*, 2002, **124**, 7274.
  - (a) M. L. Wolfrom and A. Thompson, *Methods Carbohydr. Chem.*, 1963, **2**, 211; (b) W. Steglich and G. Höfle, *Angew. Chem., Int. Ed. Engl.*, 1969, **8**, 981.
  - R. H. Baker and F. G. Bordwell, *Organic Syntheses Collective*, vol III, Wiley, New York, 1955, pp. 141.
  - F. Dasgupta, P. P. Singh and H. C. Srivastava, *Carbohydr. Res.*, 1980, **80**, 346.
  - A. C. Cope and E. C. Herrick, *Org. Synth.*, 1963, **4**, 304.
  - P. M. Bhaskar and D. Loganathan, *Tetrahedron Lett.*, 1998, **39**, 2215.
  - K. P. R. Kartha and R. A. Field, *Tetrahedron*, 1997, **53**, 11753.
  - A. Adinolfi, G. Barone, A. Iadonis and M. Schiattarella, *Tetrahedron Lett.*, 2003, **44**, 4661.
  - (a) A. G. M. Barrett and D. C. Braddock, *Chem. Commun.*, 1997, 351; (b) J. C. Lee, C. A. Tai and S. C. Hung, *Tetrahedron Lett.*, 2002, **43**, 851; (c) K. Ishira, M. Kubota, H. Kuvihara and H. Yamamoto, *J. Am. Chem. Soc.*, 1995, **117**, 4413.
  - P. A. Procopiou, S. P. D. Baugh, S. S. Flack and G. G. A. Inglis, *J. Org. Chem.*, 1998, **63**, 2342.
  - K. K. Chauhan, C. G. Frost, I. Love and D. Waite, *Synlett.*, 1999, 1743.
  - K. L. Chandra, P. Saravanan, R. K. Singh and V. K. Singh, *Tetrahedron*, 2002, **58**, 1369.
  - (a) A. Orita, C. Tanahashi, A. Kakuda and J. Otera, *J. Org. Chem.*, 2001, **66**, 8926; (b) I. Mohammadpoor-Baltork, H. Aliyan and A. R. Khosropour, *Tetrahedron*, 2001, **57**, 5851.
  - B. Karimi and J. Maleki, *J. Org. Chem.*, 2003, **68**, 4951.
  - (a) E. Marcantoni, F. Nobili, G. Bartoli, M. Bosco and L. Sembri, *J. Org. Chem.*, 1997, **62**, 4183; (b) A. Cappa, E. Marcantoni, E. Torregiani, G. Bartoli, M. C. Bellocci, M. Bosco and L. Sembri, *J. Org. Chem.*, 1999, **64**, 5696; (c) R. Dalpozzo, A. De Nino, L. Mariuolo, A. Procopio, A. Tagarelli, G. Sindona and G. Bartoli, *J. Org. Chem.*, 2002, **67**, 9093.
  - Ce(OTf)<sub>3</sub> was purchased from Acros (31.19 € per 1.0 g), I.R. Spectrum (KBr): 521 (54.23); 586 (43.79); 644 (22.13); 1037 (20.56); 1249 (5.4); 1627 (40.42); 1634 (47.22); 3449 (18.83).
  - NMR references for peracetylated derivatives of compounds 1–17 of Table 1: (1) C. Morat, F. R. Taravel and M. Vignon, *Magn. Reson. Chem.*, 1988, **26**, 264 (2) W. J. Goux and C. J. Unkefer, *Carbohydr. Res.*, 1987, **159**, 191; N. Ikemoto, O. K. Kim, C. L. Lo, V. Satyanarayana, M. Chang and K. Nakanishi, *Tetrahedron Lett.*, 1992, **33**(30), 4295 (3) V. Petrovic, S. Tomic and M. Matanovic, *Carbohydr. Res.*, 2002, **337**, 863 (4–6,8) R. U. Lemieux and J. D. Stevens, *Can. J. Chem.*, 1965, **43**, 2059 (7) J. Borowiecka and M. Michalska, *Synthesis*, 1996, 858; P. L. Durette and D. Horton, *J. Org. Chem.*, 1971, **36**(18), 2658 (9–11) S. S. Allavudeen, B. Kuberan and D. Loganathan, *Carbohydr. Res.*, 2002, **337**, 965; G. T. Ong, K. Y. Chang, S. H. Wu and K. T. Wang, *Carbohydr. Res.*, 1994, **265**(2), 311 (10) A. J. Ross, I. A. Ivanova, M. A. J. Ferguson and A. V. Nicolaev, *J. Chem. Soc., Perkin Trans. 1*, 2001, **1**, 72; A. Hasegawa, M. Marita, Y. Kojirna, H. Ishida and M. Kiso, *Carbohydr. Res.*, 1991, **214**, 43 (12) T. Nishida, C. R. Enzell and G. A. Morris, *Magn. Reson. Chem.*, 1986, **24**, 179; G. Descartes, G. Muller and J. Mentech, *Carbohydr. Res.*, 1984, **134**, 313; Ě. Kupče and R. Freeman, *J. Magn. Reson.*, 1992, **100**, 208 (13) ref. 10; (14,15) R. Saladino, C. Crestini, F. Occhionero and R. Nicoletti, *Tetrahedron*, 1995, **51**(12), 3607(156) M. Adinolfi, L. De Napoli, G. Di Fabio, A. Iadonis, D. Montesarchio and G. Piccialli, *Tetrahedron*, 2002, **58**, 6697 (17) H. C. Tsui and L. A. Paquette, *J. Org. Chem.*, 1998, **63**(26), 9968.
  - A. K. Nezhad and R. F. Alamdari, *Tetrahedron*, 2001, **57**, 6805.

# Base catalysts immobilised on silica coated reactor walls for use in continuous flow systems

Toby Jackson,<sup>a</sup> James H. Clark,<sup>\*a</sup> Duncan J. Macquarrie<sup>a</sup> and John H. Brophy<sup>b</sup>

<sup>a</sup> Clean Technology Centre, Department of Chemistry, University of York, Heslington, York, UK YO10 5DD. E-mail: jhc1@york.ac.uk; Fax: +44 1904 434550; Tel: +44 1904 432559

<sup>b</sup> Velocys Inc., 7950 Corporate Blvd., Plain City, OH 43064, USA. E-mail: jhbrophy@yahoo.com; Tel: +44 117 9732649

Received 3rd December 2003, Accepted 8th March 2004  
First published as an Advance Article on the web 23rd March 2004

The walls of a flowcell reactor were modified by coating with silica, which was subsequently modified by attachment of aminopropyl groups. The reactor was then utilised in Knoevenagel and Michael reactions

## Introduction

Liquid phase continuous flow reactors are a response to the drive towards cleaner, safer and more intensified processes in the chemical industry.<sup>1</sup> Compared to traditional batch processes continuous flow regimes are more efficient in terms of overall operation (e.g. energy and labour) as well as allowing minimisation of hazards. For example, continuous flow reactors reduce the volumes of hazardous chemicals that must be handled. In addition, continuous removal of heat provides greater control for highly exothermic reactions. The efficiency of catalysis in continuous flow processes is greatly enhanced if the catalytic species can be tethered to, or trapped inside, the reactor, which removes the need for downstream separation. Examples of such catalytic systems have been developed for microreactors<sup>2</sup> and membrane reactors,<sup>3</sup> however few examples of a covalently anchored organic based catalyst exist for continuous flow systems.<sup>4</sup> Organic based supported catalysts have been widely reported for conventional heterogeneous catalysis in batch systems using polymers<sup>5</sup> and silicas<sup>6</sup> as supports.

The Knoevenagel reaction typically involves the base catalysed condensation of aldehydes and activated methylene compounds and is one of the most important carbon-carbon bond forming reactions available to synthetic chemists. Heterogeneous catalysis of this reaction has been previously undertaken using alumina,<sup>7</sup> zeolites,<sup>8</sup> aminopropyl modified silicas<sup>9</sup> and silica supported guanidines.<sup>10</sup> A membrane microreactor system utilising a basic zeolite catalyst coated on the reactor walls is the only current literature example of fixed heterogeneous catalysis of the Knoevenagel reaction in a continuous flow system.<sup>3</sup> Here we report a novel example of a continuous flow system incorporating an organic based catalyst tethered to the reactor walls.

## Results and discussion

The prototype flowcell reactor for the solid base catalysed Knoevenagel reactions consisted of two aluminium plates, one containing input and output holes and both with wells to accommodate a porous silica coating (see Fig. 1).

The plates were sealed using a 0.7 mm viton gasket and connected to a syringe pump. To heat the cell an electrical heating element connected to a variable resistor to allow for temperature control was clamped under the bottom plate. The device was lagged with cotton wool.

Prior to the fabrication of the flowcell the plates were coated with silica and an organic base was tethered to this support. Initially the

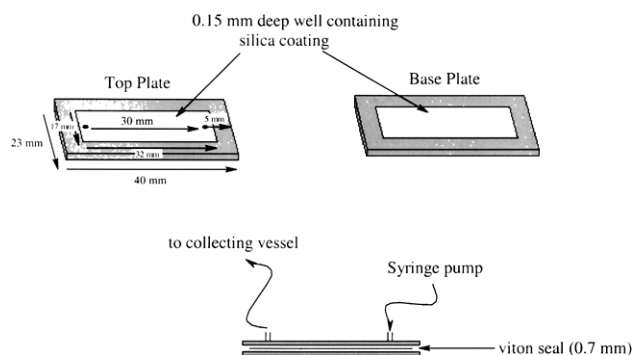
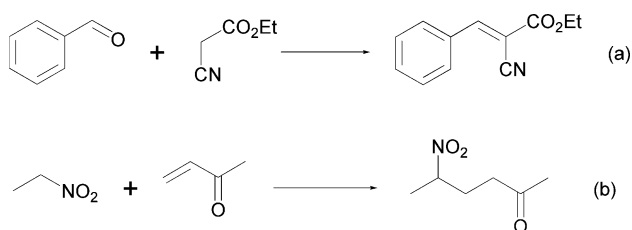


Fig. 1 Flowcell reactor constructed from silica coated aluminium plates sealed with a viton spacer.

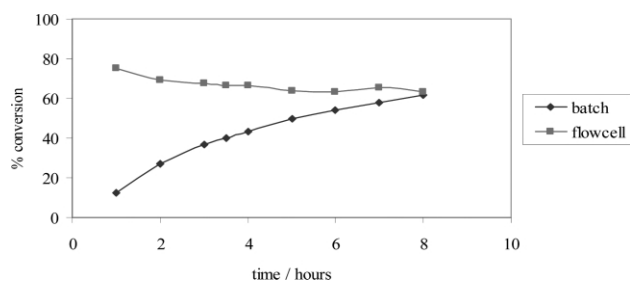
plates were cleaned with toluene and etched with hydrochloric acid. Sodium silicate solution was added dropwise to the plate wells and dilute sulfuric acid was added to form a gelatinous coating. The plates were then baked at 200 °C to leave an excess of white particulate material, which was carefully removed to leave a well adhered thin layer of silica on the metal surface. Soaking in water further removed any loose material and sodium sulfate. SEM revealed the coating to be of an open porous nature and the surface area was measured at 112 m<sup>2</sup> g<sup>-1</sup>. Organic modification to tether the base catalyst was accomplished using 3-aminopropyltrimethoxysilane giving a 0.5 mg cm<sup>-2</sup> loading of the modified silica coating on the plates. CHN analysis revealed a 0.9 mmol g<sup>-1</sup> loading of basic aminopropyl groups. Diffuse Reflectance Infrared Fourier Transform Spectroscopy (DRIFTS) showed evidence of aliphatic C-H stretching at 2937 cm<sup>-1</sup> and 2870 cm<sup>-1</sup> as well as two N-H bands at 3357 cm<sup>-1</sup> and 3289 cm<sup>-1</sup> and N-H bending at 1607 cm<sup>-1</sup>. Si-O stretching was also evident at 1185 cm<sup>-1</sup> and 1011 cm<sup>-1</sup>.

Once the flowcell was assembled, a solventless reaction mixture (solventless reactions are regarded to be a more efficient, greener approach to organic synthesis than the use of traditional toxic and volatile media<sup>11</sup>) of ethyl cyanoacetate (1 equivalent), benzaldehyde (1 equivalent) and 1,3-dibromobenzene (0.165 equivalents, as internal GC standard) was injected into the heated flowcell (90 °C) at 6.6 μl min<sup>-1</sup>.<sup>†</sup> The flowcell output was analysed periodically by GC and conversions calculated with respect to the consumption of benzaldehyde. (Fig. 2 reaction (a)) No evidence of any other product apart from α-cyanocinnamic acid ethyl ester (confirmed by GC-MS) was obtained. As can be seen in Fig. 3, the flowcell exhibited a constant level of conversion once a steady state had been realised after the first hour. No evidence of particulate material was observed in the eluted reaction mixture and there was no evidence of weight loss from the plates on disassembly.

<sup>†</sup> This equates to a residence time of 1 h.



**Fig. 2** Test reactions utilised in the evaluation of the flow reactor.



**Fig. 3** The conversion of benzaldehyde to  $\alpha$ -cyanocinnamic acid ethyl ester determined by GC for the batch and flowcell reactors.

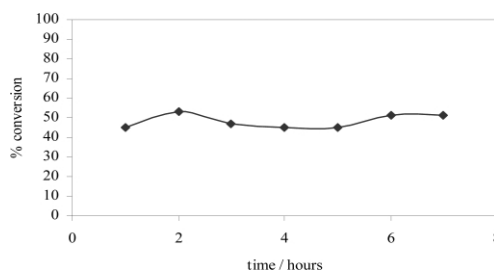
A stirred batch reaction was run under the same conditions with an equivalent quantity of catalyst and volume of reaction mixture.<sup>‡</sup> The results of this are also displayed in Fig. 3. Coincidentally the conversion of benzaldehyde in the two systems was similar after an 8 hour period, but the non-linear reaction order would suggest that rate in the flowcell reactor with higher catalyst concentration would be superior. Indeed the consistent levels of conversion of the flowcell would prove advantageous when applied to “scale out” synthesis allowing for long term feed without decline in activity. Continuous use of this catalyst is particularly beneficial because the catalyst appears to undergo a significant degree of deactivation on isolation and reuse when used in batch and continuous systems. In both cases conversions were observed to fall to between 20% and 30% on reuse. This is consistent for these type of silica supported catalyst used in Knoevenagel reactions.<sup>9</sup>

Poisoning of heterogeneous primary amine base catalysts in Knoevenagel reactions has previously been ascribed to a slow reaction of the ester groups present in the reactant/product with the active centres of the catalyst.<sup>9</sup> This process results in an irreversible loss in activity. On disassembly of the flowcell small patches of yellow discoloration were evident near the corners of the plates. On analysis, DRIFTS showed the yellow areas to have new peaks at 3056  $\text{cm}^{-1}$ , 2207  $\text{cm}^{-1}$ , 1663  $\text{cm}^{-1}$  and 1545  $\text{cm}^{-1}$ , in addition to the disappearance of the N–H bands at 3357  $\text{cm}^{-1}$  and 3289  $\text{cm}^{-1}$ . This corresponds to the spectrum expected for the poisoned catalyst. However, analysis of the other areas of the plates indicate that no poisoning has occurred. Indeed imine stretching was evident at 1652  $\text{cm}^{-1}$  from the condensation of benzaldehyde with the surface amine centres and it is this species that is believed to be the active catalyst for this reaction.<sup>12</sup> The regions of poisoning on the flowcell plates can be attributed to non-uniform flow which results in localised areas of stationary flow and these areas are susceptible to poisoning. However, due to consistent activity the reaction must be taking place away from these “dead zones” in a continuous flow environment. We therefore believe that if this catalytic coating was applied to a reactor with well-defined channels with uniform laminar flow then continuous flow would inhibit the slow poisoning process and extend the life of these catalysts.

The catalysis of the Michael reaction (Fig. 2, reaction (b)) has also been investigated using a similar catalytic system in the

flowcell. Previous studies have shown the successful use of silica supported tertiary amines for the catalysis of conjugate addition of nitroalkanes to  $\alpha,\beta$ -unsaturated carbonyl compounds.<sup>13</sup> Flowcell plates with a silica coating were prepared and *N,N*-dimethyl-3-aminopropyltrimethoxysilane were tethered to this support using *N,N*-dimethyl-3-aminopropyltrimethoxysilane. Alkyl C–H stretching could be clearly determined at 2930  $\text{cm}^{-1}$  in addition to C–H stretching from the N–CH<sub>3</sub> groups at 2760  $\text{cm}^{-1}$  by DRIFTS. The plates were then assembled into the flowcell reactor and heated to 98 °C. A Michael reaction mixture of nitroethane (8.7 equivalents), used in excess as both reactant and solvent, methyl vinyl ketone (1 equivalent) and *n*-dodecane (0.06 equivalents, as internal GC standard) was injected into the flowcell *via* a syringe pump at a rate of 6.6  $\mu\text{l min}^{-1}$ .

GC analysis showed consistent conversion of the reactants to 5-nitrohexane-2-one in good yields over a 7 hour period with no evidence of other products (see Fig. 4). Some weight loss was



**Fig. 4** The conversion of methyl vinyl ketone to 5-nitrohexane-2-one determined by GC for the flowcell reactor.

measured from the plates (7%) once they had been disassembled and cleaned, however, no loss in activity was apparent from these results nor was any increase in activity, which might have been expected due to loose particulates catalysing the reaction, observed over a prolonged period of flow. No change in conversion was noted upon heating of solutions obtained after passing through the reactor, indicating that no active species was leached from the plates.

## Conclusion

It has been shown for the first time that alkyl amines can be covalently anchored to a silica coating on the walls of a continuous flow reactor. These catalytic surfaces have been shown to be active as base catalysts for both Knoevenagel and Michael reactions with good yields and with consistent continuous conversions. While the flow rates for these reactions are quite slow, reasonable rates of production could be achieved through the use of multichannel parallel reactors.

## Acknowledgements

We would like to express thanks to Velocys Inc. for funding this study. D. J. M. thanks the Royal Society for a University Research Fellowship.

## Notes and references

- R. Jachuck, *Handbook of Green Chemistry & Technology*, ed. J. H. Clark and D. J. Macquarrie, Blackwell Publishing, Oxford, 2002.
- P. D. I. Fletcher, S. J. Haswell, E. Pombo-Villar, B. H. Warrington, P. Watts, S. Y. F. Wong and X. Zhang, *Tetrahedron*, 2002, **58**, 4735; D. W. Hall, G. Grigoropoulou, J. H. Clark, K. Scott and R. J. J. Jachuck, *Green Chem.*, 2002, **4**, 459.
- S. M. Lai, R. Martin-Aranda and K. L. Yeung, *Chem. Commun.*, 2003, 218.
- S. J. Haswell, B. O'Sullivan and P. Styring, *Lab Chip*, 2001, **1**, 164; G. H. Seong and R. M. Crooks, *J. Am. Chem. Soc.*, 2002, **124**, 13360.
- C. A. McNamara, M. J. Dixon and M. Bradley, *Chem. Rev.*, 2002, **102**, 3275.

<sup>‡</sup> The catalyst for the batch reaction was acquired from an aluminium sheet that was derivatised with the catalytic coating in an identical fashion to the flowcell plates. 5.4 mg of catalyst was used with 3168  $\mu\text{l}$  of reaction mixture – the equivalent volume of 8 hours flow through the continuous flow reactor.

- 
- 6 P. M. Price, J. H. Clark and D. J. Macquarrie, *J. Chem. Soc., Dalton Trans.*, 2000, 101.
- 7 J. Muzart, *Synth. Commun.*, 1985, **15**, 285.
- 8 M. L. Kantum, B. M. Choudary, C. V. Reddy, K. K. Rao and F. Figueras, *Chem. Commun.*, 1998, 1033; A. Corma, R. M. Martin-Aranda, V. Fornés and F. Rey, *J. Catal.*, 1992, **134**, 58.
- 9 D. J. Macquarrie, J. H. Clark, A. Lambert, J. E. G. Mdoe and A. Priest, *React. Funct. Polym.*, 1997, **35**, 153.
- 10 A. C. Blanc, D. J. Macquarrie, S. Valle, G. Renard, C. R. Quinn and D. Brunel, *Green Chem.*, 2000, **2**, 283.
- 11 G. W. V. Cave, C. L. Raston and J. L. Scott, *Chem. Commun.*, 2001, 2159.
- 12 K. A. Utting and D. J. Macquarrie, *New J. Chem.*, 2000, **24**, 591.
- 13 J. E. Mdoe, J. H. Clark and D. J. Macquarrie, *Synlett*, 1998, 625; R. Ballini, G. Bosica, D. Livi, A. Palmieri, R. Maggi and G. Sartori, *Tetrahedron Lett.*, 2003, **44**, 2271.

# Photochemical removal of uranium from a phosphate waste solution†

Caroline J. Evans,\* Graeme P. Nicholson, Douglas A. Faith and Mark J. Kan

Materials Science Research Division, AWE, Aldermaston, Reading, Berkshire, UK RG7 4PR

Received 22nd October 2003, Accepted 6th February 2004

First published as an Advance Article on the web 23rd February 2004

A photochemical method to remove uranium from a phosphate containing waste in high yield is reported. The solution resulting from the titrimetric assay of uranium consists of approximately  $1 \text{ g dm}^{-3}$  uranium in phosphoric acid ( $3 \text{ mol dm}^{-3}$ ). UV illuminated titanium dioxide in a deaerated and 25 fold diluted waste solution (40 ppm uranium) containing a hole scavenger (methanol) almost completely (98%) removed uranium from solution at pH 2 in six hours. The product was found to be free of phosphate and resulted in a grey colouration of the titania. Re-dissolution of the uranium occurred in an aerated environment over the course of a week. These results demonstrate the basis for an environmentally friendly method to photochemically reduce and remove uranium from solutions containing strongly co-ordinating ligands.

## Introduction

The Davies and Gray analytical method as modified by Eberle *et al.*<sup>1</sup> is a well-established multi-step potentiometric titration procedure utilised internationally as a standard technique for the highly precise and accurate assay of uranium materials.<sup>2</sup> The method is specific to uranium and is based upon the ability of a strong phosphoric acid medium to facilitate the reduction of uranium (vi) or  $\text{UO}_2^{2+}$  to U(iv) by a mild reducing agent Fe (ii) through an increase in the U(vi)/U(iv) and decrease in Fe (iii)/Fe (ii) formal potentials.<sup>3</sup> Excess Fe (ii) is catalytically oxidised by nitric acid in the presence of Mo(vi). Dilution of the phosphoric medium and associated change in the Gibbs free energy of the system supports the oxidation of U(iv) by the addition of V(iv). The resulting V (iii) is titrated with cerium dichromate and hence allows the concentration of uranium in solution to be determined indirectly.

This complex titration has the practical advantages of speed and automation but the disadvantage that the resulting solution contains uranium in phosphoric acid ( $3 \text{ mol dm}^{-3}$ ). Uranium recovery from the resulting solution is required to significantly reduce toxicity and radioactivity for waste disposal purposes. Conventional separation techniques (ion exchange and solvent extraction) offer no practical solution to recovering uranium from the vast molar excess ( $> 700$ ) of the strongly coordinating phosphate ligands.

Previous studies have demonstrated that UV illuminated titania powders can photocatalytically reduce and deposit metals including heavy metal ions such as uranyl from solution.<sup>4–6</sup> The work presented here demonstrates the application of this technology to selectively remove uranium from waste solutions containing strong complexing agents.

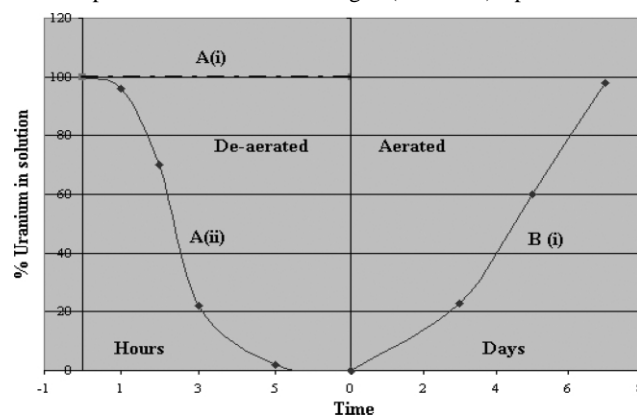
## Experimental

A standard water-cooled immersion well photochemical reactor ( $600 \text{ cm}^3$  volume) as supplied by Photochemical Reactors, Reading, UK was used. A porous gas inlet at the bottom of the vessel allowed sample de-gassing and titania agitation. The UV source was a 400 W mercury discharge lamp. Degussa P25 titania and BDH Analar grade methanol were used throughout. Davies and Gray solutions were generated in-house and contain approximately U ( $1 \text{ g dm}^{-3}$ ), Fe ( $1.3 \text{ g dm}^{-3}$ ), Mo, Cr, V ( $0.1 \text{ g dm}^{-3}$ ) in  $3 \text{ mol dm}^{-3}$  phosphoric acid and lower concentrations of other anions. All photochemical reactions were undertaken at  $\text{pH } 2 \pm 0.1$  following a 25 times dilution (solution concentration 40 parts per million

(ppm)) in order to prevent uranium phosphate precipitation. The separation of U from phosphoric acid by titania was followed by heavy metal analysis utilising inductively coupled plasma optical emission and mass spectrometry (ICP-OES and ICP-MS). Holes generated during the photochemical process must be neutralised by reducing agents. In this work methanol was utilised as the hole scavenger. Reduction in methanol concentration was monitored by gas chromatography.

## Results and discussion

Fig. 1 illustrates the effect of illumination with UV light, deaeration and the presence of a hole scavenger (methanol) upon an initial



**Fig. 1** Uranium concentration as a function of time, initially at 40 ppm and pH, A(i) dark experiment (no UV), and illumination experiment but no methanol, both de-aerated; A(ii) illumination in the presence of methanol and de-aerated; B(i) no illumination, titania aerated to remove uranium.

uranium concentration of 40 ppm at pH 2. Several observations were made including (i) no adsorption of uranium was observed in the dark experiment, A(i) (no UV), as indicated by the constant uranium solution concentration. This is consistent with the work of Cerrillos *et al.*<sup>5</sup> Additionally speciation studies<sup>7</sup> have calculated that  $\text{UO}_2(\text{H}_2\text{PO}_4)_2$  and  $\text{UO}_2(\text{H}_2\text{PO}_4)^+$  are the dominant species at pH 2 and therefore as the titania is positively charged (isoelectric point 6.48) no adsorption is expected. (ii) Unless a hole scavenger such as methanol is added no photodeposition of uranium occurs. (iii) Uranium can be almost completely photodeposited ( $> 98\%$ ) onto titania (observed as a grey coloration) from the waste solution within six hours. During this period the pH remained constant, methanol depleted to below the gas chromatograph limit of detection ( $\sim 10 \text{ ppm}$ ) and the solution concentration of Fe, V and Cr remained unchanged. The Mo concentration reduced by  $\sim 40\%$ .

† © British Crown Copyright 2001/MOD. Published with the permission of the Controller of Her Britannic Majesty's Stationery Office.



Following photoreduction, the uranium completely redissolves in an aerated environment (no UV illumination) at a rate consistent with uranium oxide (either  $\text{UO}_2$  or  $\text{U}_3\text{O}_8$ ). The photodeposit on titania was dissolved in nitric acid ( $8 \text{ mol dm}^{-3}$ ) and analysed for phosphorus. The mole ratio of uranium : phosphorus was reduced from 1 : 700 in solution to 50 : 1, that is the product does not contain phosphate ligands.

The flat band potential of titania is sufficiently negative ( $-0.40 \text{ V}$  relative to a standard calomel reference electrode)<sup>9</sup> to thermodynamically reduce uranium(vi) to uranium(iv) but not to lower oxidation states as indicated in the following reduction–oxidation couples (Table 1).

**Table 1** Reduction of U(vi) to lower oxidation states (w.r.t. SCE)

$\text{UO}_2^{2+} + \text{e}^- \rightarrow \text{UO}_2^+$	+0.31 V	(a)
$\text{UO}_2^{2+} + 4\text{H}^+ + 2\text{e}^- \rightarrow \text{U}^{4+} + 2\text{H}_2\text{O}$	+0.57 V	(b)
$\text{UO}_2^{2+} + 2\text{e}^- \rightarrow \text{UO}_2(\text{s})$	+0.67 V	(c) basic solution
$\text{UO}_2 + 4\text{H}^+ + \text{e}^- \rightarrow \text{U}^{4+} + 2\text{H}_2\text{O}$	+0.86 V	(d)

(a), (b), (d),<sup>10</sup> (c)<sup>11</sup>

The formal potential of the U(vi)/U(iv) couple is comparable to that observed in dilute phosphoric acid by Rao and Sagi of  $+0.7 \text{ V}$ .<sup>3</sup> As the photodeposit cannot readily be washed off the titania a surface adsorption step must occur to allow electron transfer and reduction of uranium from vi to iv either in a two electron process or *via* U(v) disproportionation. The adsorption of uranium on titania as a function of pH would not initially appear to be a good indicator of the mechanism at pH 2. Unlike previous studies (approximately 60% uranium removal),<sup>4</sup> uranium is almost completely removed (>98%) from the waste solution at pH 2 in this work.

The dependence of pH upon adsorption as previously reported by Amadelli *et al.*<sup>6</sup> and Cuerillos and Ollis<sup>5</sup> indicates a decrease in reaction rate as the pH and degree of adsorption increases from pH 2 to pH 7.<sup>5</sup> pH dependence was attributed to the charge on titania particles and degree of solvation of uranyl. Our system does not show the same pH dependence, however enhanced adsorption of metal ions in the presence of co-ordinating ligands is frequently mentioned in the literature with several authors suggesting synergistic adsorption effects in the presence of co-ordinating species in the solution or pre-adsorbed on the surface.<sup>12</sup> This work suggests an interplay between a series of complex reactions at the

photo-excited titania surface which promote the photoreduction process at pH 2. The large  $\text{UO}_2(\text{H}_2\text{PO}_4)^+$  species are expected to be less solvated than uranyl ions and thus more easily adsorbed. This is promoted by the simultaneous abstraction of  $\text{H}^+$  from  $\text{TiOH}_2^+$  by the phosphate ligand and consequential breaking of bonds with uranium. A mechanism supported by the absence of phosphate ligands in the product. Reduction of uranyl occurs at the substrate surface either by a two electron transfer process or *via* U(v) disproportionation.

## Conclusions

A practical photoreduction process based upon titania and UV illumination of uranium waste solutions which is highly selective towards uranium in solutions containing strongly co-ordinating ligands can be developed from this work reported. This process allows uranium to be separated from aqueous waste solutions previously deemed as intractable by routine separation techniques such as ion exchange. Once adsorbed on titania the uranium can easily be recovered in small volumes of nitric acid, the standard matrix used in the Nuclear Industry and the titania potentially re-used.

## References

- 1 A. R. Eberle, M. W. Lerner, C. G. Goldbeck and C. J. Rodden, Report NBL-252, New Brunswick Laboratory, USA, July 1970.
- 2 W. Davies and W. Gray, *Talanta*, 1964, **11**, 1203.
- 3 G. G. Rao and S. R. Sagi, *Talanta*, 1962, **9**, 715.
- 4 J. Chien, D. F. Ollis, W. H. Rulkens and H. Bruning, *Colloids Surf. A: Physicochem. Eng. Aspects*, 1999, **151**, 339–349.
- 5 C. Cerrillos and D. F. Ollis, *J. Adv. Oxid. Technol.*, 1998, **3**(2), 167–173.
- 6 R. Amadelli, A. Maldotti, S. Sostero and V. Carassiti, *J. Chem. Soc., Faraday Trans.*, 1991, **87**(19), 3267–3273.
- 7 E. E. Barker, *MPhil Thesis*, University of Wales College of Cardiff, 1993.
- 8 B. Ohtani, Y. Okugawa, S. Nishimoto and T. Kagiya, *J. Phys. Chem.*, 1987, **91**, 3550–3555.
- 9 M. D. Ward and A. J. Bard, *J. Phys. Chem.*, 1982, **86**, 3599–3605.
- 10 *CRC Handbook of Chemistry and Physics*, 78<sup>th</sup> edn., ed. in chief D. R. Lide, CRC Press Inc., Boca Raton, FL, USA, 1997.
- 11 S. Ahrland, J. O. Liljenzin and J. Ryberg, 'The Chemistry of the Actinides', *Comprehensive Inorganic Chemistry*, Pergamon Press, Oxford, England, UK, 1975, ch. 45, pp. 465–635.
- 12 M. Mlakar and M. Brianca, *J. Electroanal. Chem.*, 1998, **256**, 269.



# Reductive total chlorine free photochemical bleaching of cellulosic fabrics, an energy conserving process†

Akihiko Ouchi,\*<sup>a</sup> Toru Obata,<sup>a</sup> Takeshi Oishi,<sup>a</sup> Hitoshi Sakai,<sup>a</sup> Teruyuki Hayashi,<sup>a</sup> Wataru Ando<sup>a</sup> and Jun Ito<sup>b</sup>

<sup>a</sup> Research Institute for Green Technology, National Institute of Advanced Industrial Science and Technology, Tsukuba, Ibaraki 305-8565, Japan. E-mail: [ouchi.akihiko@aist.go.jp](mailto:ouchi.akihiko@aist.go.jp)

<sup>b</sup> Textile Research & Development Center, Nisshinbo Industries, Inc., Miai, Okazaki, Aichi 444-8510, Japan

Received 1st December 2003, Accepted 11th February 2004  
First published as an Advance Article on the web 5th March 2004

Water-insoluble natural colored compounds adsorbed or chemically bound on cellulosic fabrics were bleached effectively at room temperature by a selective photolysis of the colored compounds using various excimer lasers (ArF, KrF, XeCl, XeF), a low-pressure mercury lamp, and a black-light fluorescent lamp in the presence of aqueous solutions of various reducing reagents. Sodium borohydride gave the best efficiency on the bleaching when KrF, XeCl, XeF excimer lasers or a low-pressure mercury lamp were used as light sources and the efficiency of the bleaching was found to be comparable to that of the conventional thermal bleaching processes.

## 1 Introduction

Bleaching is one of the most important chemical processes for the utilization of natural cellulosic fabrics. In textile<sup>1</sup> and paper<sup>2</sup> industries, halogenated oxidizing reagents are widely used in large quantities for bleaching. However, such halogenated oxidizing reagents are reported to form harmful compounds known as adsorbable organically bound halogens.<sup>3,4</sup> To avoid the use of such halogenated oxidizing reagents, hydrogen peroxide is partly used in conventional TCF (total chlorine free) bleaching processes. Peracids, which are considered as an activated form of hydrogen peroxide, are also used in the bleaching of cotton fabrics. However, the main drawback of these peroxides is the efficiency of the bleaching;<sup>1</sup> the efficiency is not as good as those obtained by using chlorinated oxidizing reagents. Ozone–oxygen gas mixtures have also been tested for bleaching but a considerable decrease of the tensile strength was observed at the high degree of bleaching,<sup>5</sup> and the use of such gas mixtures has some problems of safety when it is used in production sites.

Another problem in the present thermal processes is the necessity for a large amount of energy because long processing times at high temperature are required in the conventional processes.<sup>1</sup> The consumption of energy implies the generations of gases that have negative effects on the environment through combustion of fuels. Therefore, the reduction of the processing energy is also a requisite for environmentally friendly processes.

As a new TCF bleaching process for cotton fabrics that fulfill these two requirements, a room-temperature oxidative photochemical process using aqueous solutions of sodium peroxocarbonate (or a mixture of hydrogen peroxide and sodium carbonate) and irradiation with a black-light fluorescent lamp have been reported.<sup>6</sup> Although some attempts on the photochemical

bleaching of cotton fabrics have been conducted, they were found to be much less effective than the conventional processes<sup>7</sup> or even resulted in significant damage to the fabric.<sup>8</sup> In contrast to the previous reports, our oxidative TCF photochemical bleaching gave the same or better efficiency as that of conventional thermal bleachings using halogenated oxidizing reagents without any decrease in the tensile strength of the fabrics.

In the photochemical bleaching, the main consumption of energy is due to the operation of light sources. In the oxidative process, the best light source that satisfied the bleaching efficiency and the energy consumption was a black-light fluorescent lamp. However, the efficiency of the conversion of electric energy to light energy is rather low with the black-light fluorescent lamp.<sup>9</sup> If a light source that has a higher efficiency of conversion is used, further reduction of the necessary processing energy will be accomplished. A candidate for the light source that is easily accessible at the moment is the low-pressure mercury lamp; its efficiency of conversion of electric energy to light energy is *ca.* 2.7-fold higher than that of the black-light fluorescent lamp.<sup>9</sup> Unfortunately, low-pressure mercury lamps (main emission: 254 nm) cannot be used in combination with peroxide reagents because the peroxides have considerable absorption at 254 nm so that hydroxyl radicals are generated by irradiation with the low-pressure mercury lamps resulting in considerable damage to cotton fabrics.<sup>6</sup> Therefore, the use of other bleaching reagents is necessary when low-pressure mercury lamps are used for the light sources.

The present work reports a detailed study on the further reduction of energy in the bleaching of cotton fabrics by a reductive TCF photochemical process using aqueous solutions of various halogen free reducing reagents and irradiation of light from various sources,<sup>10</sup> including a low-pressure mercury lamp.

## 2 Results

### 2.1 Effect of reductive bleaching reagents

Scoured cotton fabric (SF) was subjected to laser bleachings using 250 mM aqueous solutions of six different halogen-free reducing reagents, namely, sodium borohydride (NaBH<sub>4</sub>), sodium hydro-sulfite (Na<sub>2</sub>S<sub>2</sub>O<sub>4</sub>), sodium hydrogensulfite (NaHSO<sub>3</sub>), sodium sulfite (Na<sub>2</sub>SO<sub>3</sub>), thiourea dioxide [H<sub>2</sub>NC(=NH)SO<sub>2</sub>H], and rongalite (formaldehyde sodium sulfoxylate, HOCH<sub>2</sub>SO<sub>2</sub>Na). The pHs of the solutions were 9.84 for NaBH<sub>4</sub>, 4.27 for NaHSO<sub>3</sub>, 9.52 for Na<sub>2</sub>SO<sub>3</sub>, 4.32 for H<sub>2</sub>NC(=NH)SO<sub>2</sub>H, and 9.41 for HOCH<sub>2</sub>SO<sub>2</sub>Na.

† Electronic supplementary information (ESI) available: UV absorption spectrum of the aqueous solutions of NaBH<sub>4</sub>, Na<sub>2</sub>S<sub>2</sub>O<sub>4</sub>, NaHSO<sub>3</sub>, Na<sub>2</sub>SO<sub>3</sub>, H<sub>2</sub>NC(=NH)SO<sub>2</sub>H, and HOCH<sub>2</sub>SO<sub>2</sub>Na. The results on the whiteness and the yellow index of KrF laser bleached cotton fabrics using EtOH solutions of various silyl hydride reagents [(MeO)<sub>3</sub>SiH, (EtO)<sub>3</sub>SiH, *n*-Bu<sub>3</sub>SiH, *n*-C<sub>8</sub>H<sub>17</sub>SiH<sub>3</sub>, (HMe<sub>2</sub>Si)<sub>2</sub>O, (HMe<sub>2</sub>SiO)<sub>4</sub>Si, Me<sub>3</sub>SiO(HMeSiO)<sub>20</sub>SiMe<sub>3</sub>, (MeO)<sub>3</sub>Si(CH<sub>2</sub>)<sub>3</sub>NH<sub>2</sub>, SM8707, SRX310]. Additive effects of amines and ammonium salts in the KrF laser bleaching using an aqueous solution of NaBH<sub>4</sub>. The KrF laser bleaching in alcohol-, amine-, ammonium salt-, and amide–H<sub>2</sub>O mixtures. Emission spectra of the low-pressure mercury lamp and the black-light fluorescence lamp. See <http://www.rsc.org/suppdata/gc/b3/b315580c/>

The pH of  $\text{Na}_2\text{S}_2\text{O}_4$  was 6.87 when the solution was freshly prepared but the pH changed to 2.82 and then to 3.37 under continuous stirring in the air.

Among four major excimer lasers, *i.e.*, ArF (193 nm), KrF (248 nm), XeCl (308 nm), and XeF (351 nm) lasers, a KrF laser was used for the bleaching because this wavelength was found to be most effective in the preliminary laser bleaching experiments using  $\text{NaBH}_4$  aqueous solution.<sup>10</sup> Fig. 1 shows the whiteness and the yellow index of the KrF laser bleached cotton fabrics (LF) as a function of laser irradiation time. The figure shows that  $\text{NaBH}_4$  gave the highest whiteness and the smallest yellow index. In the cases of  $\text{Na}_2\text{S}_2\text{O}_4$ ,  $\text{NaHSO}_3$ ,  $\text{H}_2\text{NC(=NH)SO}_2\text{H}$ , and  $\text{HOCH}_2\text{SO}_2\text{Na}$ , back coloration was observed with prolonged laser irradiations, especially in the cases with the first two reagents.

The back coloration seemed to be attributed to reactive species generated by the decomposition of the reagents with KrF laser and successive reactions of the reactive species with the cotton fabrics because these reagents showed considerable absorptions at KrF laser emission line (248 nm)<sup>11</sup> but no absorption by the cotton fabric itself. Therefore, to avoid the generation of such undesirable reactive species similar laser bleaching experiments using XeF excimer laser (351 nm) were also conducted. The reagents showed no absorptions at the XeF laser emission line so the decomposition of the reagents can be avoided.

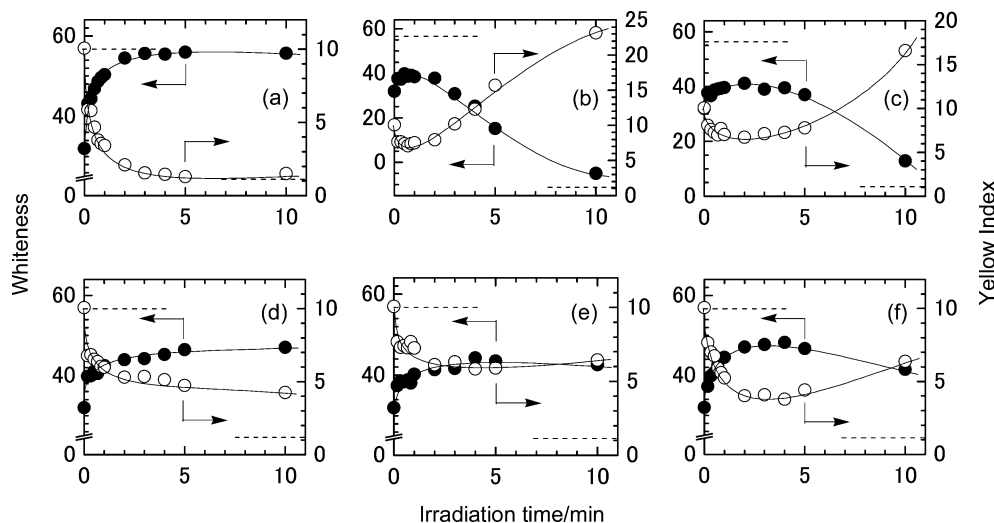
Fig. 2 shows the whiteness and the yellow index of XeF laser bleached cotton fabrics (LF) as a function of laser irradiation time. The figure also showed that  $\text{NaBH}_4$  gave the highest whiteness and the smallest yellow index. As expected, the back coloration of LF with prolonged laser irradiation was not observed for all the reagents utilized for the bleaching. However, the rate of the bleaching using  $\text{NaBH}_4$  became slower than that with the KrF laser.

Fig. 3 shows the whiteness and the yellow index of thermally bleached cotton fabrics (TF) at room temperature using the same six reducing reagents without laser irradiations. The figure clearly shows that the laser irradiation is essential for efficient bleaching.

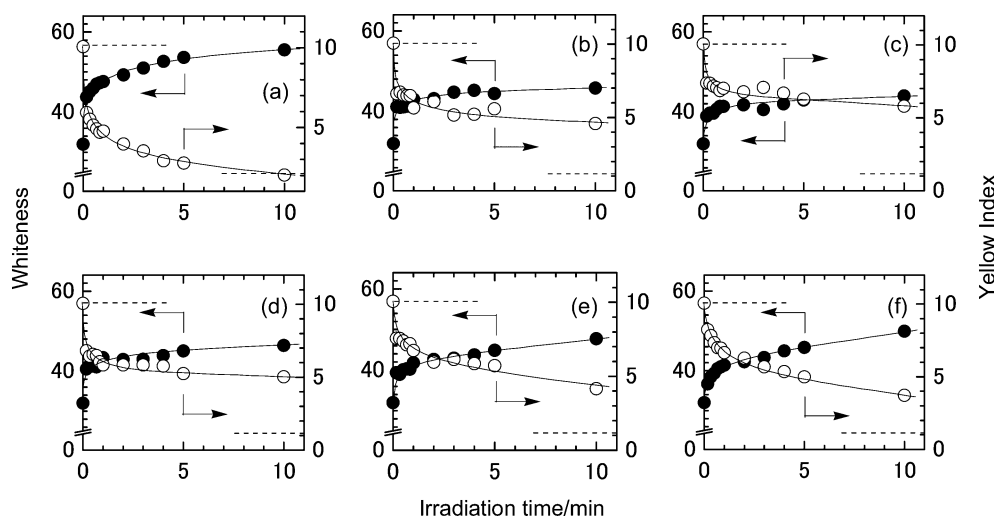
In addition to the above six reducing reagents, EtOH solutions of 10 different silyl hydrides were also used for the laser bleaching using KrF excimer laser.<sup>11</sup> However, the efficiency of the bleaching was almost the same as that in pure EtOH.

## 2.2 Effect of laser wavelength in the bleaching using $\text{NaBH}_4$

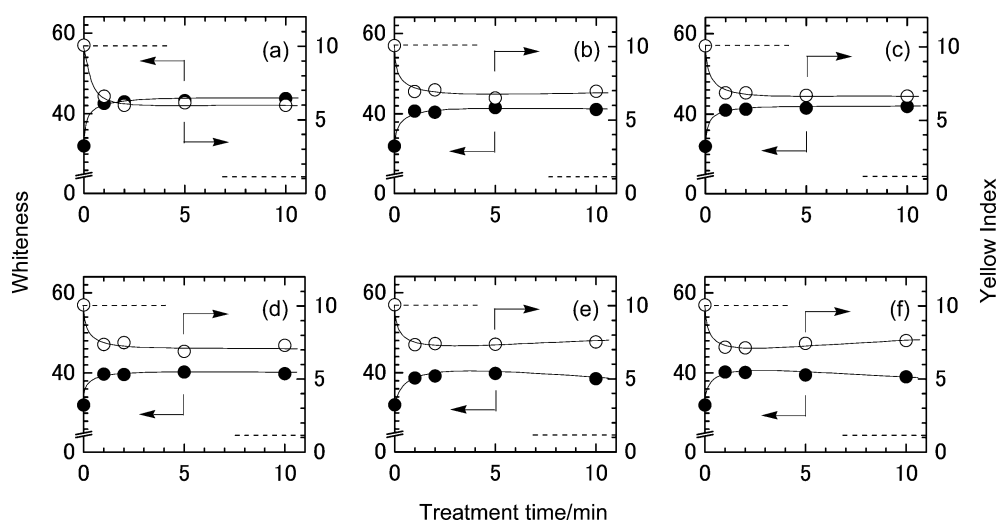
From Figs. 1 and 2,  $\text{NaBH}_4$  was selected as a promising reagent for the laser bleaching. For the optimization of the bleaching condition, the effect of laser wavelength was tested.



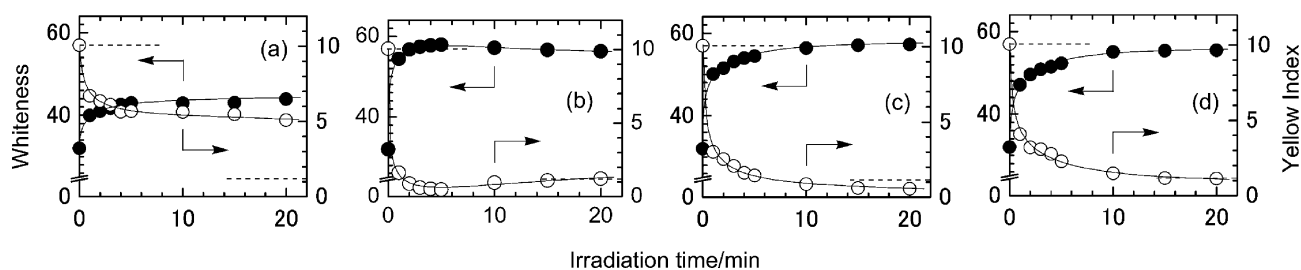
**Fig. 1** Whiteness and yellow index of KrF excimer laser bleached cotton fabrics (LF) as a function of irradiation time. Reagents: (a)  $\text{NaBH}_4$ , (b)  $\text{Na}_2\text{S}_2\text{O}_4$ , (c)  $\text{NaHSO}_3$ , (d)  $\text{Na}_2\text{SO}_3$ , (e)  $\text{H}_2\text{NC(=NH)SO}_2\text{H}$ , and (f)  $\text{HOCH}_2\text{SO}_2\text{Na}$ . Whiteness: black symbols, yellow index: white symbols. Laser bleaching conditions:  $40 \text{ mJ cm}^{-2} \text{ pulse}^{-1}$ , 5 Hz, room temperature. Reagent: 250 mM aqueous solution. Number of cotton cloths: 1 sheet.<sup>17</sup> Whiteness and yellow index of conventionally bleached fabric (CF) are shown in the figures as horizontal broken lines.



**Fig. 2** Whiteness and yellow index of XeF excimer laser bleached cotton fabrics (LF) as a function of irradiation time. Reagents: (a)  $\text{NaBH}_4$ , (b)  $\text{Na}_2\text{S}_2\text{O}_4$ , (c)  $\text{NaHSO}_3$ , (d)  $\text{Na}_2\text{SO}_3$ , (e)  $\text{H}_2\text{NC(=NH)SO}_2\text{H}$ , and (f)  $\text{HOCH}_2\text{SO}_2\text{Na}$ . Whiteness: black symbols, yellow index: white symbols. Laser bleaching conditions:  $40 \text{ mJ cm}^{-2} \text{ pulse}^{-1}$ , 5 Hz, room temperature. Reagent: 250 mM aqueous solution. Number of cotton cloths: 1 sheet.<sup>17</sup> Whiteness and yellow index of conventionally bleached fabric (CF) are shown in the figures as horizontal broken lines.



**Fig. 3** Whiteness and yellow index of thermally bleached cotton fabrics (TF) as a function of treatment time. Reagents: (a)  $\text{NaBH}_4$ , (b)  $\text{Na}_2\text{S}_2\text{O}_4$ , (c)  $\text{NaHSO}_3$ , (d)  $\text{Na}_2\text{SO}_3$ , (e)  $\text{H}_2\text{NC(=NH)SO}_2\text{H}$ , and (f)  $\text{HOCH}_2\text{SO}_2\text{Na}$ . Whiteness: black symbols, yellow index: white symbols. Treatment temperature: room temperature. Reagent: 250 mM aqueous solution. Number of cotton cloths: 1 sheet.<sup>17</sup> Whiteness and yellow index of conventionally bleached fabric (CF) are shown in the figures as horizontal broken lines.



**Fig. 4** Wavelength dependence on the whiteness and yellow index of excimer laser bleached cotton fabrics (LF) by  $\text{NaBH}_4$  (aq) as a function of irradiation time. Utilized lasers, (a) ArF (193 nm), (b) KrF (248 nm), (c) XeCl (308 nm), and (d) XeF (351 nm) excimer lasers. Whiteness: black symbols, yellow index: white symbols. Laser bleaching conditions:  $40 \text{ mJ cm}^{-2} \text{ pulse}^{-1}$ , 5 Hz, 6 wt%  $\text{NaBH}_4$  (aq), room temperature. Number of cotton cloths: 1 sheet.<sup>17</sup> Whiteness and yellow index of conventionally bleached fabric (CF) are shown in the figures as horizontal broken lines.

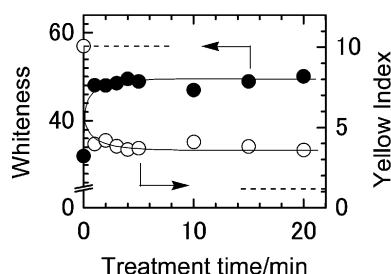
Fig. 4 shows the whiteness and the yellow index of LF as a function of laser irradiation time. The bleaching was conducted by using 6 wt%  $\text{NaBH}_4$  aqueous solution and four different excimer lasers. In the case of KrF laser irradiation, the efficiency of the bleaching reached the level of conventional thermal bleaching with  $\text{NaClO}_2$  after 2 min irradiation, and reached its maximum at 5 min, giving a maximum whiteness of 58 and minimum yellow index of 0.5. However, a slight back coloration proceeded with further irradiation.

In contrast to the case of the KrF laser, a continuous improvement of the bleaching efficiency was observed with ArF, XeCl, and XeF lasers. In the cases of XeCl and XeF laser bleedings, the whiteness and the yellow index reached the level of the conventional thermal bleaching at 15 and 10 min, respectively, for the XeCl laser and >20 min and 20 min for the XeF laser. However, the bleaching with ArF laser was ineffective, which can

be explained by the absorption of the ArF laser emission (193 nm) by cotton fabric itself.

Fig. 5 shows the whiteness and the yellow index of TF as a function of bleaching time. As seen in the figure, the whiteness and the yellow index leveled off after 4 min and did not show considerable change with further treatment. This result confirms that the irradiation of the lasers is essential for fast bleedings.

Table 1 shows the tensile strengths of LF obtained by the ArF, KrF, XeCl, and XeF laser bleedings using  $\text{NaBH}_4$  aqueous solutions. The result shows that no decrease of the tensile strength was observed in all cases. This is a big advantage to the reported photochemical bleaching of cotton fabrics using aqueous  $\text{H}_2\text{O}_2$  that showed considerable degradation of the fabric although the bleaching was accelerated.<sup>8</sup>



**Fig. 5** Whiteness and yellow index of thermally bleached cotton fabrics (TF) as a function of bleaching time. Whiteness: black symbols, yellow index: white symbols. Bleaching conditions: 6 wt%  $\text{NaBH}_4$  (aq), room temperature. Number of cotton cloths: 1 sheet.<sup>17</sup> Whiteness and yellow index of conventionally bleached fabric (CF) are shown in the figure as horizontal broken lines.

**Table 1** Tensile strength of the fabrics obtained by different bleaching methods

Bleaching method		Tensile strength <sup>a</sup> /kg
ArF laser <sup>b</sup>	6 wt% $\text{NaBH}_4$ (aq)	32
KrF laser <sup>b</sup>	6 wt% $\text{NaBH}_4$ (aq)	33
XeCl laser <sup>b</sup>	6 wt% $\text{NaBH}_4$ (aq)	32
XeF laser <sup>b</sup>	6 wt% $\text{NaBH}_4$ (aq)	32
Low-pressure Hg lamp <sup>c</sup>	6 wt% $\text{NaBH}_4$ (aq)	33
Black-light lamp <sup>c</sup>	6 wt% $\text{NaBH}_4$ (aq)	32
Thermal	$\text{NaClO}_2$ (aq) <sup>d</sup>	34
None <sup>e</sup>		33

<sup>a</sup> Average of five independent runs. <sup>b</sup> Laser bleaching condition:  $40 \text{ mJ cm}^{-2} \text{ pulse}^{-1}$ , 5 Hz, 3 min, room temperature. <sup>c</sup> Bleaching condition:  $0.93 \text{ mW cm}^{-2}$ , 60 min, room temperature. <sup>d</sup> Conventionally bleached fabric (CF), Ref. 6b. <sup>e</sup> Scoured fabric (SF), Ref. 6b.

**Table 2** Back coloration of the fabrics obtained by different bleaching methods. The test on the color fastness to light

Bleaching method		Before test <sup>a</sup>		After test <sup>a</sup>	
		Whiteness <sup>b</sup>	Yellow index <sup>b</sup>	Whiteness <sup>b</sup>	Yellow index <sup>b</sup>
ArF laser <sup>c</sup>	6 wt% NaBH <sub>4</sub> (aq)	45	5.2	49	3.7
KrF laser <sup>c</sup>	6 wt% NaBH <sub>4</sub> (aq)	58	0.7	58	0.7
XeCl laser <sup>c</sup>	6 wt% NaBH <sub>4</sub> (aq)	55 (58) <sup>d</sup>	1.7 (0.6) <sup>d</sup>	55 (58) <sup>d</sup>	1.7 (0.7) <sup>d</sup>
XeF laser <sup>c</sup>	6 wt% NaBH <sub>4</sub> (aq)	55 (56) <sup>d</sup>	1.8 (1.1) <sup>d</sup>	54 (56) <sup>d</sup>	1.9 (1.3) <sup>d</sup>
Low-pressure Hg lamp <sup>e</sup>	6 wt% NaBH <sub>4</sub> (aq)	57	0.8	57	0.9
Black-light lamp <sup>e</sup>	6 wt% NaBH <sub>4</sub> (aq)	54	2.0	54	2.0
Thermal	NaClO <sub>2</sub> (aq) <sup>f</sup>	57	1.1	58	0.6
None <sup>g</sup>		33	10.1	45	5.6

<sup>a</sup> Test method for color fastness to xenon arc lamp light. <sup>b</sup> Number of cotton cloths: 1 sheet, average of five independent runs. <sup>c</sup> Laser bleaching condition: 40 mJ cm<sup>-2</sup> pulse<sup>-1</sup>, 5 Hz, 3 min, room temperature. <sup>d</sup> Laser bleaching condition: 40 mJ cm<sup>-2</sup> pulse<sup>-1</sup>, 5 Hz, 10 min, room temperature. <sup>e</sup> Bleaching condition: 0.93 mW cm<sup>-2</sup>, 60 min, room temperature. <sup>f</sup> Conventionally bleached fabric (CF), Ref. 6b. <sup>g</sup> Scoured fabric (SF), Ref. 6b.

Table 2 shows the results on the back coloration of LF from the test of the color fastness to light. The bleached fabrics obtained by KrF, XeCl, and XeF laser irradiation showed no back coloration under the utilized test. On the contrary, in the case of the ArF laser bleaching, further improvement in the whiteness and the yellow index was observed by the test.

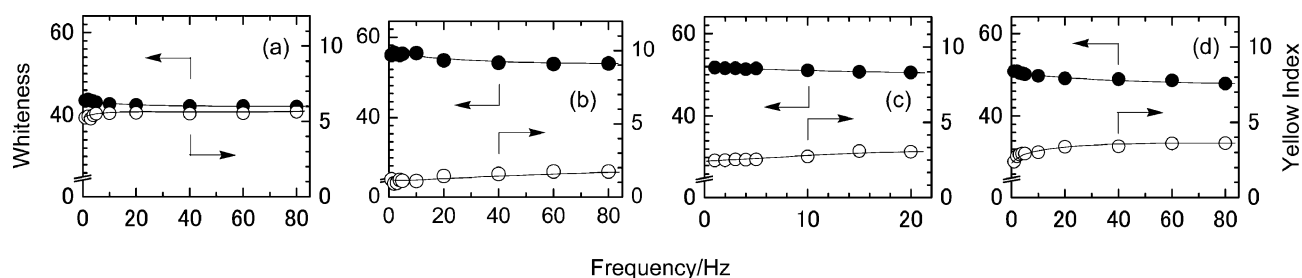
It should be noted that the KrF laser bleaching only required 2 min irradiation and was operated at room temperature, in contrast to the standard thermal processes used in production.<sup>1</sup>

### 2.3 Effect of laser bleaching conditions in the bleaching using NaBH<sub>4</sub>

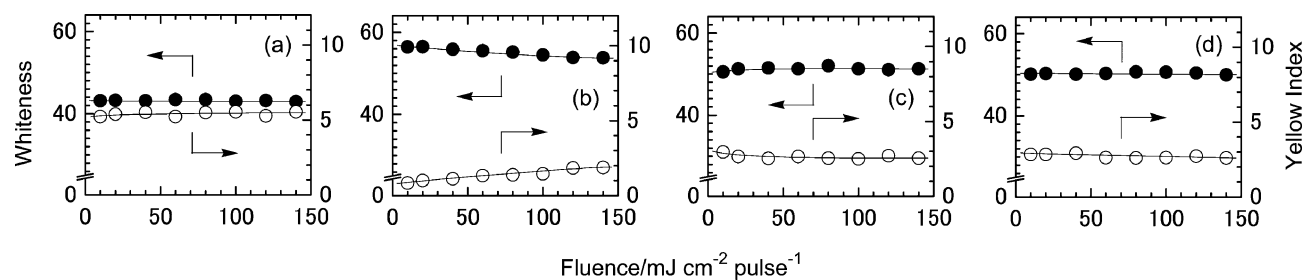
The effect of laser frequency and pulse energy was tested in order to improve the efficiency of the bleaching. The effect of NaBH<sub>4</sub> concentration was also studied to minimize the amount of the reagent used for the bleaching.

Fig. 6 shows the whiteness and the yellow index of LF as a function of laser frequency. In all laser irradiations, a slight decrease of the whiteness and a slight increase of the yellow index were observed with the increase of the laser frequency.

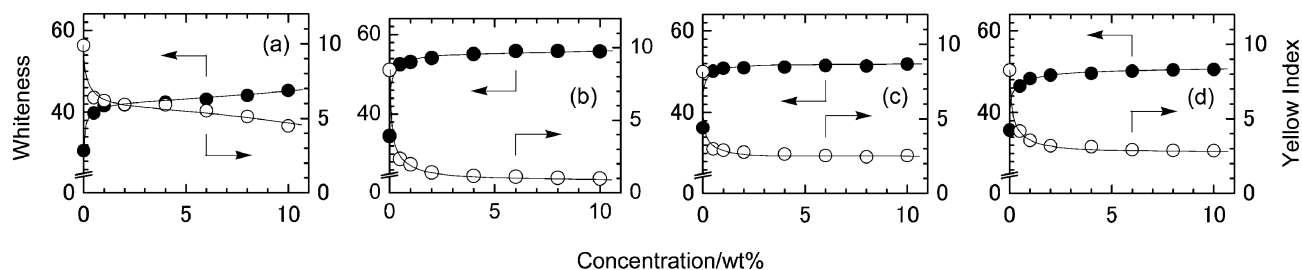
Fig. 7 shows the whiteness and the yellow index of LF as a function of the laser pulse energy; in this experiment, total energy irradiated to a unit area was kept constant so that the number of laser pulses decreased with the increase of the laser pulse energy. The figure shows that the efficiency of the bleaching decreased with the increase of the KrF laser pulse energy but it remained



**Fig. 6** Wavelength dependence on the whiteness and yellow index of excimer laser bleached cotton fabrics (LF) by NaBH<sub>4</sub> as a function of laser frequency. Utilized lasers, (a) ArF (193 nm), (b) KrF (248 nm), (c) XeCl (308 nm), and (d) XeF (351 nm) excimer lasers. Whiteness: black symbols, yellow index: white symbols. Laser bleaching conditions: 40 mJ cm<sup>-2</sup> pulse<sup>-1</sup>; 600 pulses; 6 wt% NaBH<sub>4</sub> (aq), room temperature. Number of cotton cloths: 1 sheet.<sup>17</sup>



**Fig. 7** Wavelength dependence on the whiteness and yellow index of excimer laser bleached cotton fabrics (LF) by NaBH<sub>4</sub> as a function of laser pulse energy. Utilized lasers, (a) ArF (193 nm), (b) KrF (248 nm), (c) XeCl (308 nm), and (d) XeF (351 nm) excimer lasers. Whiteness: black symbols, yellow index: white symbols. Laser bleaching conditions: 5 Hz, 24 J cm<sup>-2</sup>, 6 wt% NaBH<sub>4</sub> (aq), room temperature. Number of cotton cloths: 1 sheet.<sup>17</sup>



**Fig. 8** Wavelength dependence on the whiteness and yellow index of excimer laser bleached cotton fabrics (LF) as a function of NaBH<sub>4</sub> concentration. Utilized lasers, (a) ArF (193 nm), (b) KrF (248 nm), (c) XeCl (308 nm), and (d) XeF (351 nm) excimer lasers. Whiteness: black symbols, yellow index: white symbols. Laser bleaching conditions: 40 mJ cm<sup>-2</sup> pulse<sup>-1</sup>, 5 Hz, 2 min, room temperature. Number of cotton cloths: 1 sheet.<sup>17</sup> Whiteness and yellow index of conventionally bleached fabric (CF) are shown in the figures as horizontal broken lines.



almost constant in the cases of the ArF, XeCl, and XeF laser irradiations.

These results indicate that the necessary time for the bleaching can be shortened by increasing the laser frequency and/or the laser pulse energy, especially in the cases of the XeCl and XeF laser irradiations.

Fig. 8 shows the whiteness and the yellow index of LF as a function of the NaBH<sub>4</sub> concentration. Considerable improvement of the whiteness and the yellow index was observed by increasing the reagent concentration but they leveled off in the cases of KrF, XeCl and XeF laser bleedings after reaching their maximum and minimum, respectively, but continuous increase was observed in the case of ArF laser bleaching.

## 2.4 Additive effect on the laser bleaching

The effect of various additives in the KrF laser bleaching using NaBH<sub>4</sub> was tested in order to improve the efficiency of the bleaching.

Fig. 9 shows the effect of alcohols (MeOH, EtOH, *iso*-PrOH, *tert*-BuOH) on the whiteness and the yellow index in the KrF laser bleaching using aqueous NaBH<sub>4</sub>. As seen in the figure, all the alcohols showed a slight retardation of the bleaching efficiency at the initial stage of the bleaching. However, the suppression of back colorations by further laser irradiation was observed in the presence of alcohols. All the four alcohols showed practically the same effect on the bleaching.

The effects of amines (NH<sub>3</sub>, *iso*-Pr<sub>2</sub>NH, Et<sub>3</sub>N, Et<sub>2</sub>NH, EtNH<sub>2</sub>) and ammonium salts [(NH<sub>4</sub>)<sub>2</sub>B<sub>4</sub>O<sub>7</sub>, (NH<sub>4</sub>)<sub>2</sub>SO<sub>4</sub>, (NH<sub>3</sub>OH)<sub>2</sub>SO<sub>4</sub>] on the whiteness and the yellow index of the KrF laser bleaching using aqueous NaBH<sub>4</sub> were also tested.<sup>11</sup> The additive effect of amines was similar to that of alcohols; all the amines showed a slight retardation of the bleaching efficiency at the initial stage of the bleaching but back colorations by further laser irradiations were suppressed at the same time. Among the five amines, NH<sub>3</sub> showed largest retardation of the reaction rate but the effect of other amines were almost the same. As for the ammonium salts, (NH<sub>3</sub>OH)<sub>2</sub>SO<sub>4</sub> showed some retardation of the bleaching but the other ammonium salts did not show considerable effect.

The KrF laser bleaching was also conducted in the additive–water mixtures or in alcohols without using any reducing reagents.

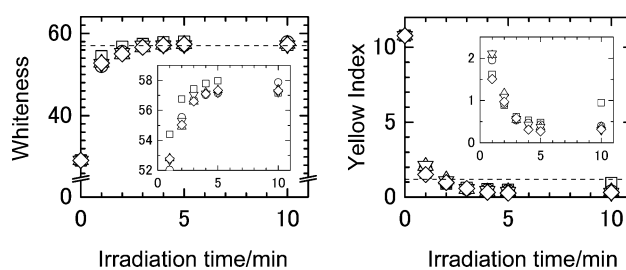
The KrF laser bleaching in alcohol–water mixtures was conducted using four kinds of alcohols, MeOH, EtOH, *iso*-PrOH, and *tert*-BuOH but the whiteness and the yellow index of LFs were practically the same as those in H<sub>2</sub>O and no significant effect of the alcohols was observed.<sup>11</sup> However, when pure alcohols were used, the efficiency of the bleaching was increased compared with that in water (*cf.* Fig. 10). Among the four alcohols, EtOH showed the best result but the efficiency was much less than the cases when aqueous NaBH<sub>4</sub> was used.

The KrF laser bleaching in amine (NH<sub>3</sub>, *iso*-Pr<sub>2</sub>NH, Et<sub>3</sub>N, Et<sub>2</sub>NH, EtNH<sub>2</sub>)–water mixtures showed only a small effect on the bleaching except for NH<sub>3</sub>, which showed a considerable decrease in the efficiency.

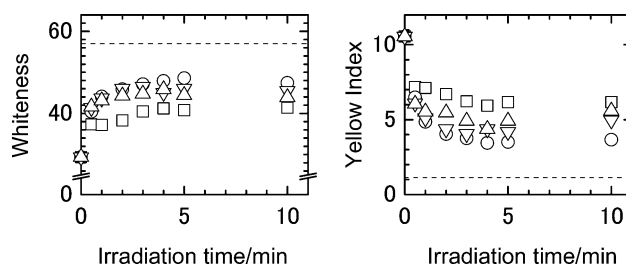
The KrF laser bleaching in ammonium salt– and amide–water mixtures was also conducted.<sup>11</sup> Mixtures of seven kinds of ammonium salts, (NH<sub>4</sub>)<sub>2</sub>B<sub>4</sub>O<sub>7</sub>, (NH<sub>4</sub>)<sub>2</sub>SO<sub>4</sub>, (NH<sub>3</sub>OH)<sub>2</sub>SO<sub>4</sub>, NH<sub>4</sub>Cl, (NH<sub>4</sub>)<sub>2</sub>CO<sub>3</sub>, CH<sub>3</sub>COONH<sub>4</sub>, and HCOONH<sub>4</sub>, and an amide, HCONH<sub>2</sub>, were tested. A slight acceleration of the bleaching was observed, especially in the cases of (NH<sub>4</sub>)<sub>2</sub>SO<sub>4</sub>, HCOONH<sub>4</sub>, and HCONH<sub>2</sub> but the efficiency was much less than the cases when NaBH<sub>4</sub> was used.

Fig. 11 shows the whiteness and the yellow index of the KrF laser bleaching in acid–water mixtures. Mixtures of three kinds of acids, HCl, CH<sub>3</sub>COOH, and HCOOH, were tested. As seen in the figure, the efficiency of the bleaching was accelerated at the initial stage of the bleaching but considerable back coloration started with

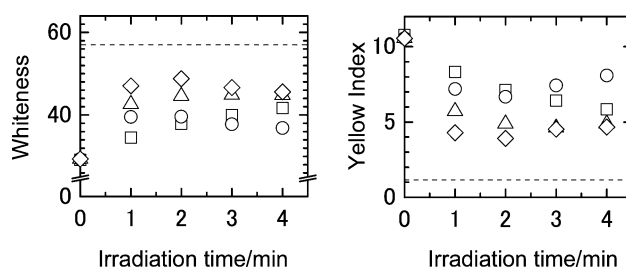
prolonged irradiation. The efficiency of the bleaching was also much less than that with aqueous NaBH<sub>4</sub>.



**Fig. 9** Additive effect of alcohols on the whiteness and yellow index of excimer laser bleached cotton fabrics (LF) by NaBH<sub>4</sub> (aq) as a function of irradiation time. Alcohols, □: none; ○: MeOH; △: EtOH; ▽: *iso*-PrOH; ◇: *tert*-BuOH. Laser bleaching conditions: KrF laser, 40 mJ cm<sup>-2</sup> pulse<sup>-1</sup>, 5 Hz, 6 wt% NaBH<sub>4</sub> in various solvents (6 wt% alcohols in H<sub>2</sub>O), room temperature. Number of cotton cloths: 1 sheet.<sup>17</sup> Whiteness and yellow index of conventionally bleached fabric (CF) are shown in the figures as horizontal broken lines.



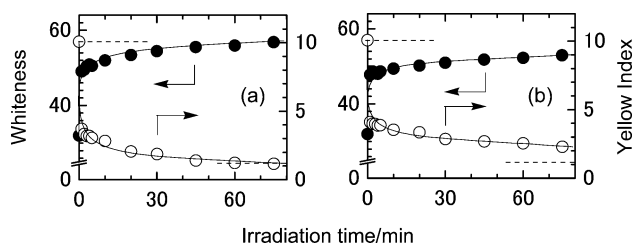
**Fig. 10** Whiteness and yellow index of excimer laser bleached cotton fabrics (LF) in water and in alcohols as a function of irradiation time. Solvents, □: H<sub>2</sub>O; ○: EtOH; △: *n*-PrOH; ▽: *iso*-PrOH. Laser bleaching conditions: KrF laser, 40 mJ cm<sup>-2</sup> pulse<sup>-1</sup>, 5 Hz, room temperature. Number of cotton cloths: 1 sheet.<sup>17</sup> Whiteness and yellow index of conventionally bleached fabric (CF) are shown in the figures as horizontal broken lines.



**Fig. 11** Whiteness and yellow index of excimer laser bleached cotton fabrics (LF) in acid–H<sub>2</sub>O mixtures as a function of irradiation time. Acids, □: none; ○: HCl; △: CH<sub>3</sub>COOH; ◇: HCOOH. Laser bleaching conditions: KrF laser, 40 mJ cm<sup>-2</sup> pulse<sup>-1</sup>, 5 Hz, 6 wt% acid in H<sub>2</sub>O, room temperature. Number of cotton cloths: 1 sheet.<sup>17</sup> Whiteness and yellow index of conventionally bleached fabric (CF) are shown in the figures as horizontal broken lines.

## 2.5 Bleaching with conventional light sources

Instead of using lasers, the use of more common light sources was investigated. Fig. 12 shows the whiteness and the yellow index of the photochemically bleached fabrics (PF) using a low-pressure mercury lamp (major emission: 254 nm) and a black-light fluorescent lamp (352 nm).<sup>11</sup> In the case of the bleaching using the low-pressure mercury lamp, the whiteness and the yellow index reached the level of CF after 60 min. When the black-light fluorescent lamp was used, the whiteness and the yellow index did not reach the level of CF even after 75 min irradiation although a continuous improvement was observed.



**Fig. 12** Whiteness and yellow index of photochemically bleached cotton fabrics (PF) by  $\text{NaBH}_4$  as a function of irradiation time. Irradiation conditions: (a) low-pressure Hg lamp ( $0.93 \text{ mW cm}^{-2}$ ) and (b) black-light fluorescent lamp ( $0.93 \text{ mW cm}^{-2}$ ). Whiteness: black symbols, yellow index: white symbols. Reaction conditions: 6 wt%  $\text{NaBH}_4$  (aq), room temperature. Number of cotton cloths: 1 sheet.<sup>17</sup> Whiteness and yellow index of conventionally bleached fabric (CF) are shown in the figures as horizontal broken lines.

The tensile strength of PF did not show any decrease when the low-pressure mercury lamp or the black-light fluorescent lamp was used for the bleaching (cf. Table 1). Back coloration of both PF was also tested by the test on the color fastness to light (cf. Table 2), which showed no significant change in the whiteness and the yellow index of the fabrics in both cases.

## 2.6 UV-vis spectra of cellulosic fabrics

Fig. 13 shows the absorbance and absorbance difference of various cotton fabrics. Figs. 13A–D show the absorbance of SF, LF, and LF after the test of color fastness to light (LFT). Figs. 13E,F show the absorbance of SF, PF, and PF after the test of color fastness to light (PFT). In all cases, a considerable decrease of the absorption was observed after the bleaching (cf. SF – LF and SF – PF in Figs. 13a–f). In the cases of the bleaching using KrF and XeCl lasers, and the low-pressure mercury lamp, the efficiency of the bleaching was better than that of the conventional thermal bleaching using  $\text{NaClO}_2$  (cf. LF – CF and PF – CF in Figs. 13b,c,e). However, in the cases of the bleaching using XeF laser and black-light

fluorescent lamp, the efficiency of the bleaching was lower than that of the conventional thermal bleaching using  $\text{NaClO}_2$  at  $< 230 \text{ nm}$  (cf. LF – CF and PF – CF in Figs. 13d,f) and in the case of ArF laser bleaching, better efficiency of the bleaching was obtained by the conventional thermal bleaching (cf. LF – CF in Fig. 13a).

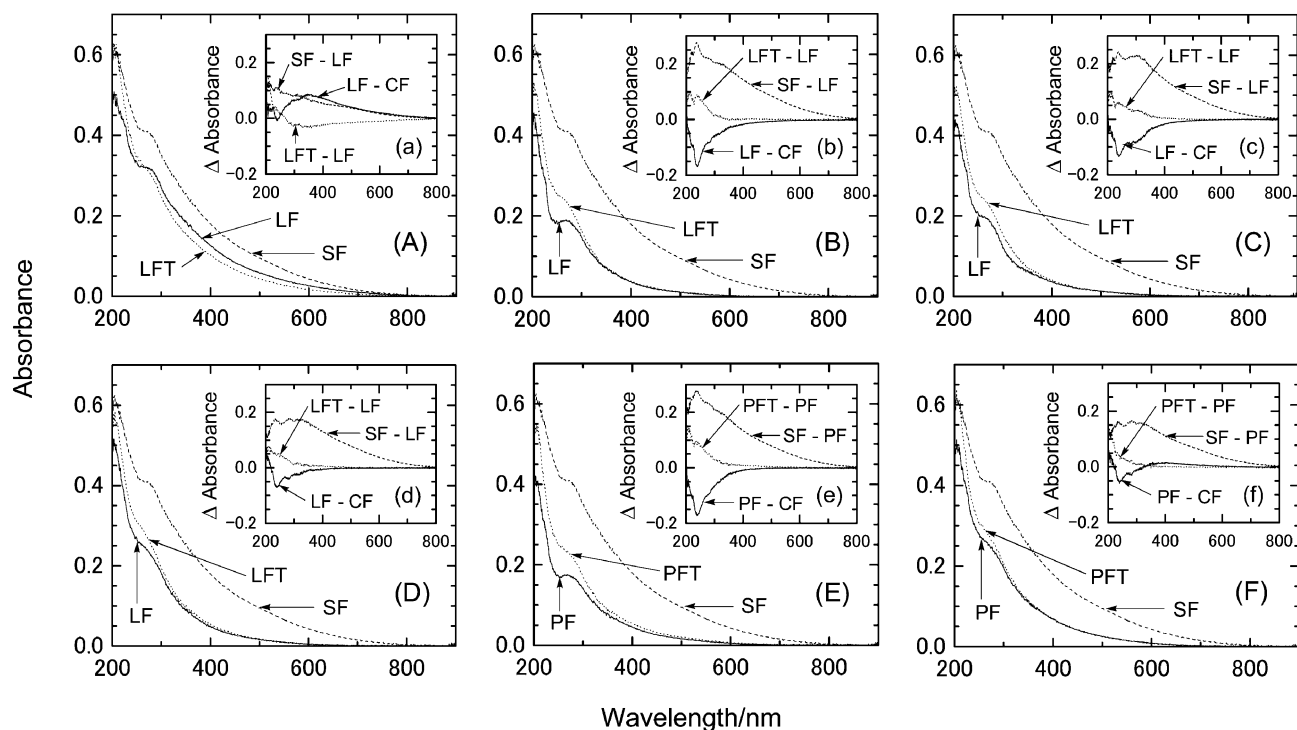
Although the structures of the natural colored compounds remaining on the scoured cotton fabrics are still not clarified, this decrease of the absorbance by the bleaching indicates that the colored compounds have broad absorption in the UV to visible region. The presence of this broad absorption is evidence for the existence of extended  $\pi$ -electron systems in the colored compounds. The decrease of this absorption by the bleaching implies the decomposition or the shortening of the extended  $\pi$ -electron systems of the colored compounds.

It should be also noted that, in all cases, the absorbance spectrum of LF and PF showed an absorption maximum or a shoulder at ca. 250 nm. The corresponding shoulder was also observed in the absorption spectrum of SF. This absorption maximum can be assigned as a substituted benzene moiety.<sup>12</sup> The presence of this maximum in LF and in PF indicates the difficulty in the further reduction of the substituted benzene moieties by photochemical processes. However, the decrease of this absorption by the photochemical bleaching was larger than that by the conventional thermal bleaching except for the case with the ArF laser bleaching (cf. LF – CF and PF – CF in Fig. 13 b–f).

The recovery of this absorption band after the test on the color fastness to light, except for the case with the ArF laser bleaching, implies photochemical regenerations of the substituted benzene moieties (cf. LFT – LF and PFT – LF in Fig. 13 b–f).

## 3 Discussion

Bleaching of cotton fabrics can be considered as a decolorization of natural dyes remaining on the surface of cotton fibers. The structure of the natural colored compounds remaining on the scoured cotton fabrics is still not identified. However, the structures of the



**Fig. 13** Absorption (A–F) and absorbance difference (a–f) spectra of cotton fabrics. Bleaching conditions: (A, a) ArF laser [ $40 \text{ mJ cm}^{-2} \text{ pulse}^{-1}$ , 5 Hz, 3 min, 6 wt%  $\text{NaBH}_4$  (aq), room temperature], (B, b) KrF laser [ $40 \text{ mJ cm}^{-2} \text{ pulse}^{-1}$ , 5 Hz, 3 min, 6 wt%  $\text{NaBH}_4$  (aq), room temperature], (C, c) XeCl laser [ $40 \text{ mJ cm}^{-2} \text{ pulse}^{-1}$ , 5 Hz, 10 min, 6 wt%  $\text{NaBH}_4$  (aq), room temperature], (D, d) XeF laser [ $40 \text{ mJ cm}^{-2} \text{ pulse}^{-1}$ , 5 Hz, 10 min, 6 wt%  $\text{NaBH}_4$  (aq), room temperature], (E, e) low-pressure Hg lamp [ $0.93 \text{ mW cm}^{-2}$ , 60 min, 6 wt%  $\text{NaBH}_4$  (aq), room temperature], (F, f) black-light fluorescent lamp [ $0.93 \text{ mW cm}^{-2}$ , 60 min, 6 wt%  $\text{NaBH}_4$  (aq), room temperature]. (A–F) -----: scoured fabric (SF), —: laser bleached fabric (LF) or photochemically bleached fabric (PF), .....: LF or PF after the test of color fastness to light (LFT, PFT, respectively). (a–f) —: LF – CF or PF – CF (CF: conventionally bleached fabric), -----: SF – LF or SF – PF, .....: LFT – LF or PFT – PF. Number of cotton cloths: 5 sheets.<sup>17</sup>

remaining colored compounds are expected to have extended  $\pi$ -electron systems so that the decolorization of the colored compounds can be accomplished by cleaving such extended  $\pi$ -electron systems.

For all utilized reducing reagents, the bleaching was largely accelerated by the irradiation of light. Except for the ArF excimer laser, the light used in our experiments was not absorbed by the cotton fabric itself, which can avoid direct photochemical damage of the fabrics. However, a considerable back coloration was observed when the reducing reagents have absorptions at the wavelength of the utilized light. This can be explained by the photochemical generation of reactive species from the reagents and their successive reactions with the fabrics.

The function of the photo irradiation on the large acceleration of the bleaching can be explained by the increase of the oxidizing power of the natural colored compounds. In thermal bleachings, the bleachings initiate when an electron is transferred from the reducing reagents to one of the unoccupied molecular orbitals of the natural colored compounds. However, in the excited states, the electron can be transferred to a singly occupied orbital that has lower energy than the LUMO of the ground state. Such singly occupied orbitals have larger oxidizing power than the LUMO of the ground state, which explains the facilitation of the reduction by the irradiation of light to the colored compounds.

The effect of the bleaching was the same when the lasers and conventional lamps were used as light sources. However, the efficiency of the conversion of electric energy to light energy is much higher for conventional lights. Therefore, to reduce the amount of the necessary energy for bleaching, a low-pressure mercury lamp was tested as a light source, which was found to be very effective (*cf.* Fig. 12a). The time profile of the improvement of the whiteness and the yellow index was almost the same as those in the oxidative photochemical bleaching<sup>6b</sup> using aqueous solutions of sodium peroxocarbonate and a black-light fluorescent lamp. The output energy of the low-pressure mercury lamp and the black-light fluorescent lamp was the same ( $0.93 \text{ mW cm}^{-2}$ ), which means that the required energy for both bleaching methods was the same. However, the efficiency of the conversion of electric energy to light energy is *ca.* 2.7-fold higher for the low-pressure mercury lamp than the black-light fluorescent lamp.<sup>9</sup> This means that the necessary processing energy of the reductive photochemical bleaching can be reduced to 1/2.7 of that of the oxidative photochemical bleaching. A brief assessment of the necessary energy for the bleaching using the low-pressure mercury lamp and  $\text{NaBH}_4$  revealed that the photochemical process only needed *ca.* 8% of the energy required in the conventional thermal bleaching.<sup>13</sup>

Although the present reductive photochemical TCF bleaching has an advantage over a previously reported oxidative photochemical TCF process in the standpoint of energy consumption, the use of sodium borohydride was necessary to obtain high bleaching efficiency. Although boron compounds exist in natural sea water ( $4.44 \text{ mg-B L}^{-1}$ ),<sup>14</sup> they are reported to have some toxicity but it is generally lower than that of many adsorbable organically bound halogens that are often generated from bleaching using halogenated reagents.<sup>15</sup> The boron wastes, however, can be removed by appropriate waste water treatment and the removed boron compounds could be used in other applications such as in the preservation of wood.<sup>16</sup>

## 4 Experimental

The sample used for the laser and photochemical bleaching was a scoured cotton fabric (SF) [G poplin (J6220), scoured by Awazu Rensen Kogyo]. A sheet of SF (*ca.*  $5 \times 5 \text{ cm}^2$ ) was padded in the aqueous solutions of  $\text{NaBH}_4$ ,  $\text{Na}_2\text{S}_2\text{O}_4$ ,  $\text{NaHSO}_3$ ,  $\text{Na}_2\text{SO}_3$ ,  $\text{H}_2\text{NC(=NH)SO}_2\text{H}$ , and  $\text{HOCH}_2\text{SO}_2\text{Na}$ . The uptake of the solutions by the 1-g SF was  $2.5 \pm 0.3 \text{ g}$ . The sheet was then irradiated with a light source at room temperature, washed with water, and dried.

The light sources used were a Lambda Physik LPX210i [ArF (193 nm), KrF (248 nm), and XeF (351 nm)] and a Lambda Physik COMPex102 [XeCl (308 nm)] excimer lasers, a 15 W low-pressure mercury lamp (National Germicidal Lamp GL-15), and a 15 W black-light blue fluorescent lamp (National FL15BL-B). The pulse energy of the lasers was measured by a Gentec ED-500 joulemeter and a digital storage oscilloscope (Gould Classic 9500, 500 MHz, 2GS/s). The light intensities and the emission spectra of the low-pressure mercury lamp and the black-light fluorescent lamp were measured by an Ushio USR-40D Spectroradiometer.

Conventionally bleached fabric (CF) was obtained by bleaching the same batch of SF used in the photochemical bleaching experiments by using  $\text{NaClO}_2$  [G poplin (J6220), bleached by Awazu Rensen Kogyo].

Reflectance and absorption spectra, whiteness, and yellow index of the fabrics were measured by a UV-vis spectrophotometer (Shimadzu UV-2400PC) equipped with an integration sphere (Shimadzu ISR-2200) using  $\text{BaSO}_4$  (Merck, for white standard DIN 5033) as a reference. The whiteness and the yellow index were those defined in JIS Z 8715 (CIE 1986c) and JIS K 7103, respectively (larger whiteness and smaller yellow index indicate better bleaching). The tensile strength of the fabrics was measured by "breaking strength method A (raveled strip method)" defined in JIS L 1096 A (ISO 5081) using a Schopper's type tensile strength tester (Toyo Seiki Seisaku-sho, Ltd., No. 551 model C). The tensile strength was obtained by the average of 5 independent runs. Color fastness to light was measured by "test method for color fastness to xenon arc lamp light" defined in JIS L 0843 (ISO 105 B-02) using a xenon long life fade meter (Suga Test Instruments Co., Ltd., FAL-25AX). The data was obtained by the average of 5 independent runs. The pH of the aqueous solutions was measured by a Sartorius PT-15 Portable Meter equipped with a pH/ATC electrode [standardized by pH buffer solutions (DKK-TOA Corp.) at pH 4.01, 6.86, and 9.18].

## Acknowledgement

We thank the Ministry of Economy, Trade and Industry, Japan for financial support. We thank Mr. Sadao Tamura for conducting some preliminary experiments on the laser bleaching. T. Oishi thanks the New Energy and Industrial Technology Development Organization for a fellowship.

## References and notes

- 1 M. Lewin, in *Handbook of Fiber Science and Technology, Chemical Processing of Fibers and Fabrics, Fundamentals and Preparation*, ed. M. Lewin and S. B. Sello, Marcel Dekker, Inc., New York, 1984, vol. 1, Part B, ch. 2.
- 2 V. Lorás, in *Pulp and Paper*, ed. J. P. Casey, John Wiley & Sons, Inc., New York, 1980, vol. 1, ch. 5.
- 3 For textiles: see, for example G. Schulz, H. Herlinger and P. Schäfer, *Textilveredlung*, 1992, **27**, 167.
- 4 For pulps: see, for example J. Rutkowski, *Cellul. Chem. Technol.*, 1997, **31**, 485.
- 5 M. Prabakaran, R. C. Nayar, N. S. Kumar and J. V. Rao, *J. Soc. Dyers Colour.*, 2000, **116**, 83.
- 6 (a) A. Ouchi and H. Sakai, *Green Chem.*, 2003, **5**, 329–331; (b) A. Ouchi, H. Sakai, T. Oishi, T. Hayashi, W. Ando and J. Ito, *Green Chem.*, 2003, **5**, 516–523.
- 7 J. Ludwig, J. P. Fouassier, R. Freytag and P. Viallier, *Bull. Sci. Inst. Text. Fr.*, 1982, **11**, 81.
- 8 I. Ruzsnák, I. Kovács, B. Losonczy and J. Morgós, *Textilveredlung*, 1979, **14**, 442.
- 9 The efficiency of the conversion of electric energy to light energy is 50% for a low-pressure mercury lamp (40 W germicidal lamp, National GL-40) and 18% for a black-light fluorescent lamp (40 W black-light blue fluorescent lamp, National FL40S-BL-B).
- 10 Preliminary result on the bleaching with  $\text{NaBH}_4$  (aq) and a KrF excimer laser: A. Ouchi, T. Obata, H. Sakai and M. Sakuragi, *Green Chem.*, 2001, **3**, 221.
- 11 The experimental data are shown in the electronic supplementary information†.

- 
- 12 H. H. Jaffé and M. Orchin, *Theory and Application of Ultraviolet Spectroscopy*, John Wiley & Sons, Inc., New York, 1962, ch. 12.
  - 13 Photon energy required in the bleaching using a low-pressure mercury lamp and NaBH<sub>4</sub> in our experiments was *ca.* 8 kcal m<sup>-2</sup> cotton cloth, which corresponds to an electric energy<sup>9</sup> of *ca.* 16 kcal m<sup>-2</sup> cotton cloth. The necessary energy for the standard conventional thermal bleaching is 213 kcal m<sup>-2</sup> cotton cloth, which was obtained from the Japan Textile Finishers Association.
  - 14 *Handbook of Chemistry and Physics*, ed. D. R. Lide, 81st edn., 2000–2001, CRC Press, Boca Raton, FL, 2000, p. 14.
  - 15 (a) *The Merck Index*, ed. S. Budavari, 12th edn., Merck & Co., Inc., Whitehouse Station, NJ, 1996; (b) *Comprehensive Toxicology*, ed. I. G. Sipes, C. A. McQueen and A. J. Gandolfi, Pergamon, Oxford, 1997.
  - 16 We thank the referee for the suggestion of using boron wastes in other applications such as in the preservation of wood.
  - 17 When the number of the sheets of **SF** was varied from one to ten, the reflectance increased with the increase of the number of the sheets until four but it leveled off over five. The increase of the reflectance by increasing the number of the sheets was due to the suppression of transmitted light.

# Catalytic performance and properties of ceria based catalysts for cyclic carbonate synthesis from glycol and carbon dioxide

Keiichi Tomishige,\* Hiroaki Yasuda, Yuichi Yoshida, Mohammad Nurunnabi, Baitao Li and Kimio Kunimori

Institute of Materials Science, University of Tsukuba, 1-1-1, Tennodai, Tsukuba, Ibaraki 305-8573, Japan

Received 27th January 2004, Accepted 24th February 2004  
First published as an Advance Article on the web 12th March 2004

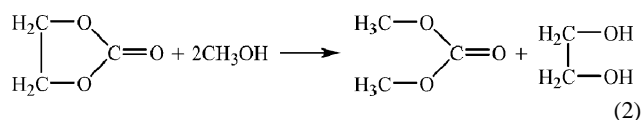
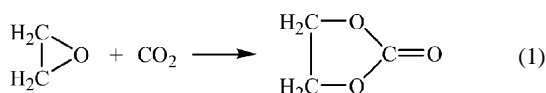
Ceria based catalysts are very effective for the synthesis of cyclic carbonate such as ethylene carbonate (EC) and propylene carbonate (PC) by the reaction of CO<sub>2</sub> with ethylene glycol and propylene glycol. In these reactions, polycarbonate and ethers (diethylene glycol and dipropylene glycol) were not detected under optimum reaction conditions. This indicates that the PC and EC formation over CeO<sub>2</sub>-ZrO<sub>2</sub> catalysts is highly selective. Catalytic activity was much dependent on the composition and calcination temperature of catalysts. On the basis of catalyst characterization by means of surface area measurement, X-ray diffraction, thermogravimetric analysis, and temperature programmed desorption of NH<sub>3</sub> and CO<sub>2</sub>, the relations between catalytic performance and properties are discussed.

## Introduction

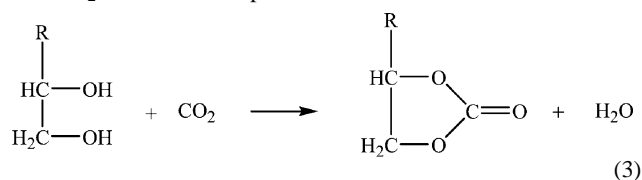
Cyclic alkylene carbonates such as ethylene carbonate (EC) and propylene carbonate (PC) have been available commercially, and they have been used as both a reactive intermediate and an inert solvent.<sup>1,2</sup> In addition to their biodegradability and high solvency, they have high boiling and flash points, low odor levels and evaporation rate and low toxicities. Furthermore, the use of EC and PC as a solvent in degreasing, paint stripping, and cleaning applications has increased drastically in the past few years. At the same time, they are also finding increased utility as diluents epoxy and isocyanate components of resin systems, and they have become the electrolytes of choice in the production of lithium ion batteries.

Carbon dioxide insertion into propylene oxide is the commercial method for the industrial production of propylene carbonate.<sup>1</sup> Recently, a lot of studies have been reported on the development of catalysts, especially heterogeneous catalysts, such as polymer-supported quaternary onium salts,<sup>3</sup> magnesia,<sup>4,5</sup> Mg-Al mixed oxide,<sup>6</sup> and Cs-loaded zeolite and alumina,<sup>7,8</sup> and lanthanide oxychloride.<sup>9</sup>

Furthermore, a possible utilization of cyclic alkylene carbonates such as EC and PC is the transesterification with methanol to form dimethyl carbonate (DMC) and corresponding glycols. It is known that this is one of the industrial synthetic processes utilizing CO<sub>2</sub> as a raw material.<sup>10</sup> The conversion of carbon dioxide to useful industrial compounds has recently raised much interest in view of "Green Chemistry".<sup>11-13</sup> Especially, DMC has attracted much attention in terms of a non-toxic substitute for dimethyl sulfate and phosgene, which are toxic and corrosive methylating agents.<sup>14</sup> In addition, DMC is considered to be an option for meeting the oxygenate specifications for transportation fuel.<sup>15</sup> The traditional synthesis of DMC used to require phosgene as a reagent. Two processes based on the oxy-carbonylation of methanol have already been successfully developed up to larger scale: (1) the oxidative carbonylation of CH<sub>3</sub>OH with carbon monoxide and oxygen catalyzed by cuprous chloride,<sup>16</sup> and (2) an oxidative carbonylation process using a palladium catalyst and methyl nitrite promoter.<sup>17</sup> The utilization of carbon dioxide as the raw material of the DMC synthesis process has been developed.<sup>10</sup> The reaction scheme is EC formation from ethylene oxide and CO<sub>2</sub> (eqn. (1)),<sup>18,19</sup> and the transesterification of EC with methanol (eqn. (2)).<sup>20-22</sup>

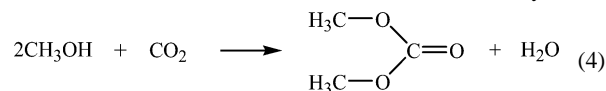


In this system, ethylene glycol (EG) is always co-produced with DMC. If ethylene carbonate can be synthesized from EG and CO<sub>2</sub>, the reaction scheme becomes more valuable since EG can be reused. From this viewpoint, the synthesis of cyclic carbonate from CO<sub>2</sub> and corresponding glycols can be more important (eqn. (3)). However, the synthesis of EC and PC by the reaction of EG and PG with CO<sub>2</sub> has not been reported.



(EG: R=H, PG: R=CH<sub>3</sub>)

Our group has developed heterogeneous catalysts for selective DMC synthesis from CH<sub>3</sub>OH and CO<sub>2</sub> (eqn. (4)) such as ZrO<sub>2</sub>,<sup>23,24</sup> H<sub>3</sub>PO<sub>4</sub>/ZrO<sub>2</sub>,<sup>25-27</sup> and CeO<sub>2</sub>-ZrO<sub>2</sub> solid solution<sup>28,29</sup> catalysts.



In this article, we investigate whether CeO<sub>2</sub>-ZrO<sub>2</sub> solid solution can be applied to the EG+CO<sub>2</sub> and PG+CO<sub>2</sub> reactions to form EC and PC, respectively. Furthermore, we characterize the catalyst structure and acid-base properties, and the relation between the characterization results and catalyst performance in the carbonate synthesis reaction.

## Experimental

CeO<sub>2</sub>-ZrO<sub>2</sub>, CeO<sub>2</sub> and ZrO<sub>2</sub> were prepared by calcining the hydroxides (available from Daiichi Kigenso, Japan) for 3 h under air atmosphere at various temperatures (673–1473 K). The preparation method of the hydroxides was on the basis of the patent.<sup>30</sup> The molar ratios Ce/(Ce + Zr) of the catalysts were 0, 0.2, 0.33, 0.5 and 1.0. The reaction was carried out in a stainless-steel autoclave reactor with an inner volume of 70 ml. The standard procedure in the case of PG+CO<sub>2</sub> reaction is as follows: 7.60 g propylene glycol (PG, 100 mmol, Wako Pure Chemical Industries, 99.5% min, dehydrated), 4.92 g CH<sub>3</sub>CN (AN, solvent, 120 mmol,



Wako Pure Chemical Industries, 99%, dehydrated) and 0.05 or 0.5 g catalyst were put into an autoclave, and then the reactor was purged with CO<sub>2</sub>. After that, the autoclave was pressurized with CO<sub>2</sub> (200 mmol, Takachiho Trading Co. Ltd. 99.99%). The reactor was heated and magnetically stirred constantly during the reaction. After the reaction, 2-propanol was added to the liquid phase as a standard for the quantitative analysis. In the case of EG+CO<sub>2</sub> reaction, EG (EG, 100 mmol, Wako Pure Chemical Industries, 99.5% min, dehydrated) was used instead of PG.

Products in the liquid phase were analyzed by a gas chromatograph (GC) equipped with FID. The capillary column TC-WAX was used for the separation column. In the analysis of the liquid phase, PC and EC were observed as a product. Diethylene glycol (DEG) and dipropylene glycols (DPGs), which are expected by-products in this reaction, were measured as the products by means of GC analysis. In the GC analysis, the sensitivity was determined using pure chemicals such as PC (Wako Pure Chemical Industries, 97.0%), EC (Wako Pure Chemical Industries, 98.0%), DPG (mixture of isomers, Wako Pure Chemical Industries, 90.0%), and DEG (Aldrich, 99%). Furthermore, all the products in the gas phase were below the detection limit of FID-GC. Products were also identified by GC-MS.

In the experiments for the solvent effect, we tested various kinds of solvent such as diethyl ether (Wako Pure Chemical Industries, 99.5% min, dehydrated), tetrahydrofuran (Wako Pure Chemical Industries, 99.5% min, dehydrated), chloroform (Wako Pure Chemical Industries, 99.0% min), dimethyl sulfoxide (Wako Pure Chemical Industries, 99.0% min, dehydrated), *N,N*-dimethylformamide (Wako Pure Chemical Industries, 99.5% min, dehydrated), and propionitrile (Wako Pure Chemical Industries, 98.0% min). These solvents were used without further purification.

The surface area of the catalyst was measured with the BET method (N<sub>2</sub> adsorption) using Gemini (Micromeritics). In order to evaluate the formation of poly(propylene carbonate) and poly(ethylene carbonate), FTIR spectra of the liquid phase after the reaction test were obtained using a liquid IR cell with CaF<sub>2</sub> window and Magna 550 (Nicolet) in transmission mode. FTIR measurement was carried out after the separation of solid catalysts from the liquid phase.

X-Ray diffraction (XRD) measurement was carried out by an X-ray diffractometer (PHILIPS, Philips X'Pert MRD) with Cu K $\alpha$  (40 kV, 20 mA) radiation.

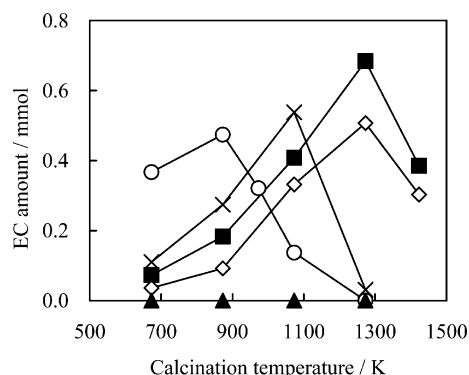
The amount of CO<sub>2</sub> and NH<sub>3</sub> adsorption was measured by a volumetric method using a vacuum line, which has a 30-cm<sup>3</sup> dead volume. Sample pretreatment was evacuation at 773 K for 0.5 h. The pressure of the gas phase at the equilibrium state was about 6.6 kPa of CO<sub>2</sub> and NH<sub>3</sub>. The adsorption was carried out at room temperature. Temperature programmed desorption (TPD) profiles of CO<sub>2</sub> and NH<sub>3</sub> were obtained by the mass spectrometer (Balzers, Prisma QMS 200). A mass signal of *m/z* = 44 and 16 was monitored in the CO<sub>2</sub> and NH<sub>3</sub> TPD, respectively. Sample pretreatment and gas adsorption were performed in a closed circulating vacuum system. Before the measurement of TPD profiles, the sample was evacuated for 1 h at room temperature. Sample weight was 0.1 g. Heating rate was about 7 K min<sup>-1</sup>. NH<sub>3</sub> (99.999%) and CO<sub>2</sub>(99.99%) were purchased from Takachiho Trading Co. Ltd. and they were used without further purification.

Thermogravimetric and differential thermal analyses (TGA and DTA) were performed using DTG-60 (Shimadzu). A platinum basket was used as a sample holder and the samples were about 10 mg of hydroxides. The reference compound in DTA measurement was  $\alpha$ -Al<sub>2</sub>O<sub>3</sub>. TGA and DTA profiles were measured in the air flow (20 ml min<sup>-1</sup>) at the heating rate 15 K min<sup>-1</sup>.

## Results and discussion

### EG+CO<sub>2</sub> reaction

Fig. 1 shows the calcination temperature dependence of EC formation starting from EG and CO<sub>2</sub> catalyzed by CeO<sub>2</sub>, ZrO<sub>2</sub>, and



**Fig. 1** Calcination temperature dependence of the amount of EC formation in EG+CO<sub>2</sub> reaction. ○: CeO<sub>2</sub>, ▲: ZrO<sub>2</sub>, ◇: CeO<sub>2</sub>-ZrO<sub>2</sub> (Ce/(Ce+Zr) = 0.20), ■: CeO<sub>2</sub>-ZrO<sub>2</sub> (Ce/(Ce+Zr) = 0.33), ×: CeO<sub>2</sub>-ZrO<sub>2</sub> (Ce/(Ce+Zr) = 0.5). Reaction conditions: reaction temperature 423 K, EG : CO<sub>2</sub> : CH<sub>3</sub>CN = 100 : 200 : 120 mmol, reaction time 2 h, catalyst weight 0.05 g.

CeO<sub>2</sub>-ZrO<sub>2</sub> (Ce/(Ce + Zr) = 0.0, 0.2, 0.33 and 0.5). No EC formation was detected over ZrO<sub>2</sub> with various calcination temperatures (673, 873, 1073 and 1273 K). As shown later, the EC amount at the equilibrium level is 1.18 mmol under these reaction conditions. The EC amount shown in Fig. 1 did not reach the equilibrium level. This means that the results were determined by the catalytic activities in the EG+CO<sub>2</sub> reaction. In the case of CeO<sub>2</sub>, the EC amount reached a maximum on the catalyst calcined at 873 K, and decreased on CeO<sub>2</sub> calcined at a temperature higher than 873 K. This behaviour can be explained by the low surface area of CeO<sub>2</sub> at 1073 K (7 m<sup>2</sup> g<sup>-1</sup>). The BET surface areas of the catalysts are listed in Table 1. A maximum of the EC amount as a function of

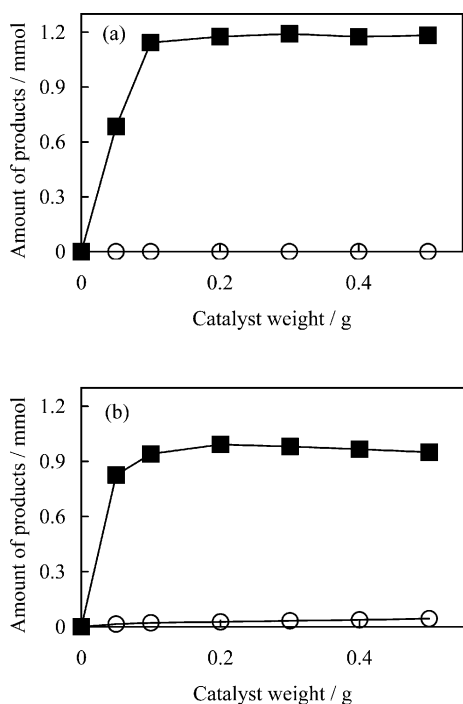
**Table 1** BET surface area of CeO<sub>2</sub>-ZrO<sub>2</sub> catalysts calcined at various temperatures

Ce/(Ce+Zr)	Calcination temperature/K	Surface area/m <sup>2</sup> g <sup>-1</sup>
0	673	93
	873	36
	1073	17
	1273	9
0.2	673	98
	873	49
	1073	33
	1273	19
	1423	10
0.33	673	109
	873	64
	1073	42
	1273	20
	1423	11
0.5	673	105
	873	66
	1073	34
	1273	5
1.0	673	56
	873	37
	1073	7
	1273	3

calcination temperature was observed over all the catalysts except ZrO<sub>2</sub>. This strongly suggests that the active species of the catalysts is cerium ions. The calcination temperature, where the EC amount reached a maximum, was much dependent on the composition of the catalysts. The maximum appeared at 1073 K over CeO<sub>2</sub>-ZrO<sub>2</sub> (Ce/(Ce+Zr) = 0.5), and at 1273 K over CeO<sub>2</sub>-ZrO<sub>2</sub> (Ce/(Ce+Zr) = 0.2 and 0.33). This indicates that the maximum temperature becomes higher over the catalyst with higher Zr content. According to Table 1, regarding surface area of catalysts calcined at the same temperature, the catalyst with higher Zr content had higher surface area. These behaviours agree with the previous reports.<sup>31,32</sup> This is because ZrO<sub>2</sub> addition to CeO<sub>2</sub> inhibited the sintering of CeO<sub>2</sub>. The

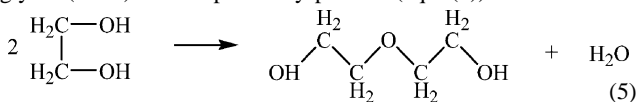
behaviour of the maximum temperature is thought to be related to the surface area of catalysts. The sintering proceeded drastically under calcination at higher temperature (1273 K) even on CeO<sub>2</sub>-ZrO<sub>2</sub> (Ce/(Ce+Zr) = 0.33). The relation between the catalyst structure and activity is discussed later. It is very interesting that the CeO<sub>2</sub>-ZrO<sub>2</sub> (Ce/(Ce+Zr) = 0.33) catalyst calcined at higher temperature exhibited higher activity.

Fig. 2 shows the effect of catalyst weight on the amount of products in the EG+CO<sub>2</sub> reaction over CeO<sub>2</sub>-ZrO<sub>2</sub> (Ce/(Ce+Zr) =



**Fig. 2** Effect of catalyst weight on amount of products in the EG+CO<sub>2</sub> reaction over CeO<sub>2</sub>-ZrO<sub>2</sub> (Ce/(Ce+Zr) = 0.33) calcined at 1273 K. ■: ethylene carbonate, ○: diethylene glycol. (a) reaction temperature 423 K, (b) reaction temperature 463 K EG : CO<sub>2</sub> : CH<sub>3</sub>CN = 100 : 200 : 120 mmol, reaction time 2 h.

0.33) calcined at 1273 K. In the EG+CO<sub>2</sub> reaction, diethylene glycol (DEG) is an expected by-product (eqn. (5)).



At 423 K, the formation of DEG was not detected by GC at all. In this case, the EC amount increased with the catalyst weight in the range of 0.05–0.10 g, and it was almost constant in the range of 0.1–0.5 g-cat. This indicates that the reaction of EG and CO<sub>2</sub> to form EC reached equilibrium and the EC amount was limited. On the other hand, the formation of DEG was observed and its amount increased with the catalyst weight at 463 K. The EC amount over 0.05 g-cat approached the level of the plateau, however, it decreased gradually with increasing catalyst weight in the range of 0.1–0.5 g-cat. This is because H<sub>2</sub>O formed with DEG decreases EC formation (eqn. (3)). In addition, it is found that a lower reaction temperature is more favourable for the selective synthesis of EC from EG+CO<sub>2</sub>.

On the basis of the data shown above, we can compare the EC amount with the total amount of Ce and Zr in the catalyst. In 0.05-g CeO<sub>2</sub>-ZrO<sub>2</sub> (Ce/(Ce+Zr) = 0.33), the total amount of Ce and Zr ions is estimated to be about 0.36 mmol, which is smaller than EC formation (0.68 mmol). The turnover number (TON) is at least 1.9, and in fact it must be much higher because the number of surface active sites is much smaller than the total amount of Ce and Zr ions.

Table 2 shows the dependence of the amount of EC and DEG formation on various reaction conditions over CeO<sub>2</sub>-ZrO<sub>2</sub> (Ce/

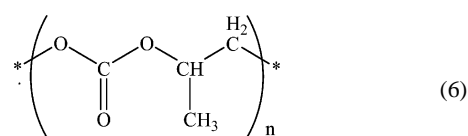
**Table 2** Results of EG+CO<sub>2</sub> reaction over CeO<sub>2</sub>-ZrO<sub>2</sub> (Ce/(Ce+Zr) = 0.33) under various reaction conditions

Reaction temperature/K	Catalyst weight	Reaction time/g	Formation amount/mmol	
			EC	DEG
383	0.05	2	0.16	n. d.
383	0.5	2	0.86	n. d.
403	0.05	2	0.42	n. d.
403	0.5	2	0.96	n. d.
403	0.5	8	1.09	n. d.
423	0.05	2	0.68	n. d.
423	0.5	2	1.18	n. d.
423	0.5	8	1.12	0.01
443	0.05	2	0.78	n. d.
443	0.5	2	1.07	0.01
443	0.5	8	0.90	0.04
463	0.05	2	0.83	0.02
463	0.5	2	0.95	0.04
463	0.5	8	0.68	0.11

Reaction conditions: EG : CO<sub>2</sub> : CH<sub>3</sub>CN = 100 : 200 : 120 mmol. Catalyst: CeO<sub>2</sub>-ZrO<sub>2</sub>(Ce/(Ce+Zr) = 0.33), calcination temperature 1273 K. n. d.; not detected by FID-GC.

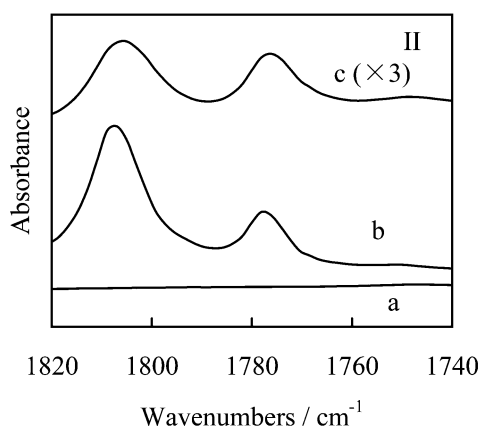
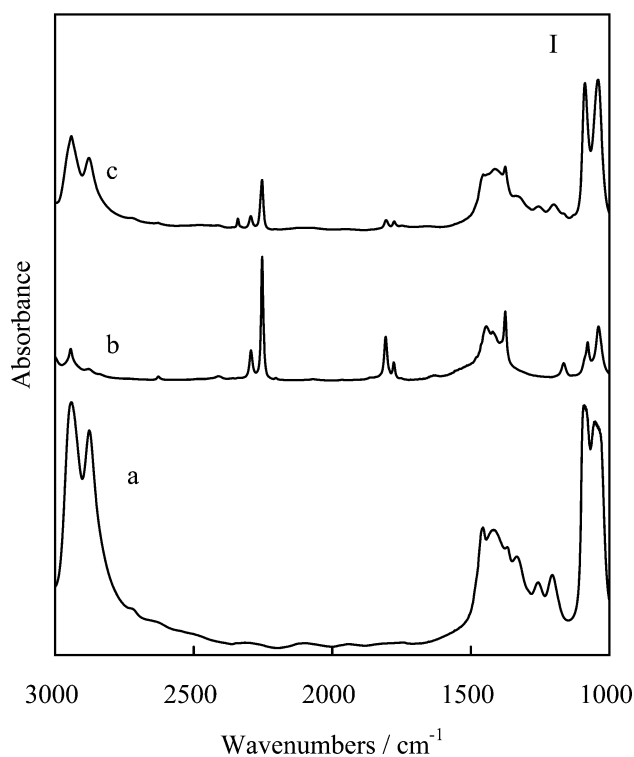
(Ce+Zr) = 0.33) calcined at 1273 K. It is clear that the formation of DEG was not observed at lower reaction temperatures (383 and 403 K) even after 8 h using 0.5-g cat. This indicates that the formation of EC is highly selective in this temperature range. At 403 K, the observed equilibrium level of EC formation is determined to be 1.09 mmol because of no DEG formation. In contrast, at higher reaction temperature, the formation of DEG became more significant. When DEG formation is observed, the EC amount is decreased by H<sub>2</sub>O formed in eqn. (5). This is observed in the results at higher reaction temperature (423–443 K). In the case of the result using 0.5 g-cat, DEG amount increased with the reaction time whereas EC amount decreased. This relation indicates that EC formation is very sensitive to this kind of by-reaction.

Furthermore, we measured the FTIR spectra of the liquid phase after the reaction in order to recognize the formation of poly(ethylene carbonate). It has been reported that poly(propylene carbonate) can be synthesized from propylene oxide and CO<sub>2</sub> using chromium salen derivatives as catalysts.<sup>33</sup> According to this reference, it is easy to distinguish between poly(propylene carbonate) as shown in eqn. (6) and cyclic propylene carbonate by means of FTIR measurement.



It is known that the absorbance at 1752 cm<sup>-1</sup> is due to poly(propylene carbonate) and that at 1802 cm<sup>-1</sup> is assigned to propylene carbonate. Fig. 3 shows the FTIR spectra of the liquid phase after the reaction as well as the reference samples. In Fig. 3(a), no peak was observed in the range of 1600–1900 cm<sup>-1</sup>. In Fig. 3(b), two peaks due to EC at 1807 and 1778 cm<sup>-1</sup> were observed. The previous reports have pointed out that the splitting into these two peaks is considered to be Fermi resonance of the C=O stretching mode with an overtone of the ring breathing mode.<sup>34,35</sup> In Fig. 3(c), two peaks were also observed at 1805 and 1776 cm<sup>-1</sup>, and these can be assigned to EC formed by the reaction of EG with CO<sub>2</sub>, and this was also supported by GC analysis. A small peak shift can be due to the difference of solvent. Furthermore, no peaks near 1750 cm<sup>-1</sup> were observed at all in Fig. 3(c), and this indicates no formation of polycarbonate during the reaction. In addition, the IR peaks at 2293 and 2252 cm<sup>-1</sup> are due to AN, and the peak at 2341 cm<sup>-1</sup> can be assigned to CO<sub>2</sub> dissolved in the liquid of the sample.

From the results listed in Table 2, we can approximately estimate the EG-based selectivity of EC formation (EC/(EC+2DEG)). In this



**Fig. 3** FTIR spectra of liquid phase in EG+CO<sub>2</sub> reaction. (I) Wavenumbers range: 3000–1000 cm<sup>-1</sup>, (II) Wavenumbers range: 1820–1740 cm<sup>-1</sup> (a) EG, (b) AN : EC = 120 : 1.2 mmol, (c) After the reaction at 423 K (0.5 g CeO<sub>2</sub>-ZrO<sub>2</sub> (Ce/(Ce+Zr) = 0.33) calcined at 1273 K, EG: CH<sub>3</sub>CN:CO<sub>2</sub> = 100 : 120 : 200 mmol, 2-Propanol (2.6 mmol) was added the liquid phase after the reaction as a standard. The thickness of liquid phase was 0.015 mm.

case, we have to estimate the formation rate of EC on the basis of the formation amount. Here, the formation amount of EC is not so far from the equilibrium level, and strictly speaking, it is difficult to estimate the formation rate and the selectivity accurately. In fact, it will be possible to estimate the accurate formation rate under shorter reaction time and using a smaller amount of catalyst. We think that it is important to show the estimation, although it is approximate. For example, at 423 K, the formation rate of EC can be approximately estimated to be 6.8 mmol h<sup>-1</sup> g-cat<sup>-1</sup> (= 0.68 mmol/(2 h × 0.05 g)), although it appears that the real formation rate can be higher than this estimation. On the other hand, the formation rate of DEG can be estimated to be 0.005 mmol h<sup>-1</sup> g-cat<sup>-1</sup> (= 2 × 0.01 mmol/(8 h × 0.5 g)). The selectivity for EC can be calculated to be higher than 99.9% on the basis of the estimation above with some approximations. Furthermore, the selectivity can be higher than at lower reaction temperatures like 383 and 403 K. This estimation strongly suggests that the selectivity of EC

formation from the EG+CO<sub>2</sub> reaction over CeO<sub>2</sub>-ZrO<sub>2</sub> (Ce/(Ce+Zr) = 0.33) calcined at 1273 K was very high.

The effect of the amount of CO<sub>2</sub> and EG reactants in EG+CO<sub>2</sub> reaction over CeO<sub>2</sub>-ZrO<sub>2</sub> (Ce/(Ce+Zr) = 0.33) calcined at 1273 K is listed in Table 3. Considering the effect of CO<sub>2</sub> amount, the EC

**Table 3** Effect of the amount of CO<sub>2</sub> and EG reactants in EG+CO<sub>2</sub> reaction over CeO<sub>2</sub>-ZrO<sub>2</sub> (Ce/(Ce+Zr) = 0.33) calcined at 1273 K

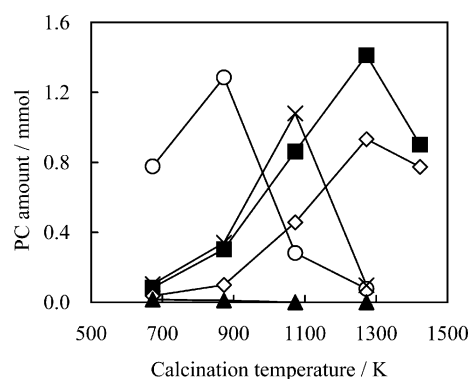
Catalyst weight/g	Reactant/mmol		Product amount/mmol	
	EG	CO <sub>2</sub>	EC	DEG
0.05	100	100	0.32	n. d.
0.5	100	100	0.71	n. d.
0.05	100	200	0.68	n. d.
0.5	100	200	1.18	n. d.
0.05	100	300	0.76	n. d.
0.5	100	300	1.25	n. d.
0.05	100	400	0.81	n. d.
0.5	100	400	1.33	n. d.
0.5	25	200	0.28	n. d.
0.5	50	200	0.54	n. d.
0.5	100	200	1.18	n. d.
0.5	200	200	1.12	0.01

Reaction conditions: temperature 423 K, reaction time 2 h, 120 mmol AN was used as a solvent.

amount produced over 0.05 g catalyst was lower than that on 0.5 g catalyst. Therefore, it is interpreted that the result over 0.05 g catalyst corresponds to the formation rate and that over 0.5 g catalyst represents the equilibrium level. The formation rate of EC and the equilibrium EC amount were almost proportional to the CO<sub>2</sub> amount in the range of 0–200 mmol of CO<sub>2</sub>. The effect of CO<sub>2</sub> amount was not so significant in the range of 200–400 mmol CO<sub>2</sub>. A similar tendency was observed in the case of dimethyl carbonate formation in CH<sub>3</sub>OH+CO<sub>2</sub> reaction.<sup>24</sup> Furthermore, the EC amount over 0.5 g catalyst proportionally increased with the EG amount in the range of 0–100 mmol EG. In contrast, the EC amount was saturated at 200 mmol EG.

### PG+CO<sub>2</sub> reaction

Fig. 4 shows the calcination temperature dependence of PC formation starting from PG and CO<sub>2</sub> over various catalysts at 423 K. The formation of PC and H<sub>2</sub>O from PG and CO<sub>2</sub> is a reversible



**Fig. 4** Calcination temperature dependence of the amount of PC formation in PG+CO<sub>2</sub> reaction. ○: CeO<sub>2</sub>, ▲: ZrO<sub>2</sub>, ◇: CeO<sub>2</sub>-ZrO<sub>2</sub> (Ce/(Ce+Zr) = 0.20), ■: CeO<sub>2</sub>-ZrO<sub>2</sub> (Ce/(Ce+Zr) = 0.33), ×: CeO<sub>2</sub>-ZrO<sub>2</sub> (Ce/(Ce+Zr) = 0.5). Reaction conditions: reaction temperature 423 K, PG : CO<sub>2</sub> : CH<sub>3</sub>CN = 100 : 200 : 120 mmol, reaction time 2 h, catalyst weight 0.05 g.

reaction (eqn. (3)), and PC amount can be limited by the equilibrium. Under these reaction conditions, the equilibrium yield can be estimated to be 2.0 mmol as described later. Therefore, the PC amount shown in Fig. 4 did not reach the PC amount at the equilibrium and the results can reflect the catalytic activity. The PC amount was very low over ZrO<sub>2</sub> calcined at various calcination

temperatures (673–1273 K), and this indicates that ZrO<sub>2</sub> exhibited almost no activity in this reaction as well as EG+CO<sub>2</sub> reaction. Regarding CeO<sub>2</sub> catalyst, maximum PC amount was obtained over the catalyst calcined at 873 K. On the other hand, maximum PC yield was obtained on CeO<sub>2</sub>-ZrO<sub>2</sub> (Ce/(Ce+Zr) = 0.5) calcined at 1073 K and CeO<sub>2</sub>-ZrO<sub>2</sub> (Ce/(Ce+Zr) = 0.2 and 0.33) calcined at 1273 K. Although the PC formation rate in the PG+CO<sub>2</sub> reaction was higher than the EC formation rate in the EG+CO<sub>2</sub> reaction, the dependence of catalytic activity on the catalyst composition and calcination temperature is very similar.

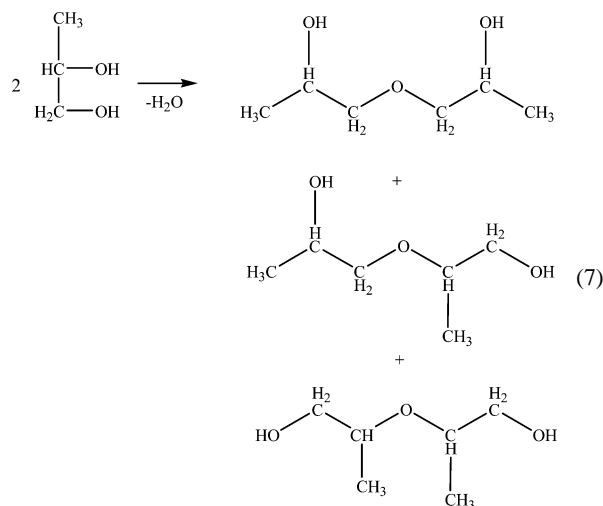
Table 4 shows the dependence of the amount of PC formation under various reaction conditions over CeO<sub>2</sub>-ZrO<sub>2</sub> (Ce/(Ce+Zr) =

**Table 4** Results of PG+CO<sub>2</sub> reaction over CeO<sub>2</sub>-ZrO<sub>2</sub> (Ce/(Ce+Zr) = 0.33) under various reaction conditions

Reaction temperature/ K	Catalyst weight/g	Reaction time/h	Formation amount/mmol	
			PC	DPGs
383	0.05	2	0.16	n. d.
383	0.5	2	1.1	n. d.
383	0.5	8	2.0	n. d.
403	0.05	2	0.67	n. d.
403	0.5	2	2.0	n. d.
403	0.5	8	2.0	n. d.
423	0.05	2	1.4	n. d.
423	0.5	2	2.0	n. d.
423	0.5	8	2.0	n. d.
443	0.05	2	1.6	n. d.
443	0.5	2	2.0	n. d.
443	0.5	8	1.9	n. d.
463	0.05	2	1.5	n. d.
463	0.5	2	1.9	n. d.
463	0.5	8	1.9	n. d.

Reaction conditions: PG : CO<sub>2</sub> : CH<sub>3</sub>CN = 100 : 200 : 120 mmol. Catalyst: CeO<sub>2</sub>-ZrO<sub>2</sub>(Ce/(Ce+Zr) = 0.33), calcination temperature 1273 K. n. d.; not detected by FID-GC.

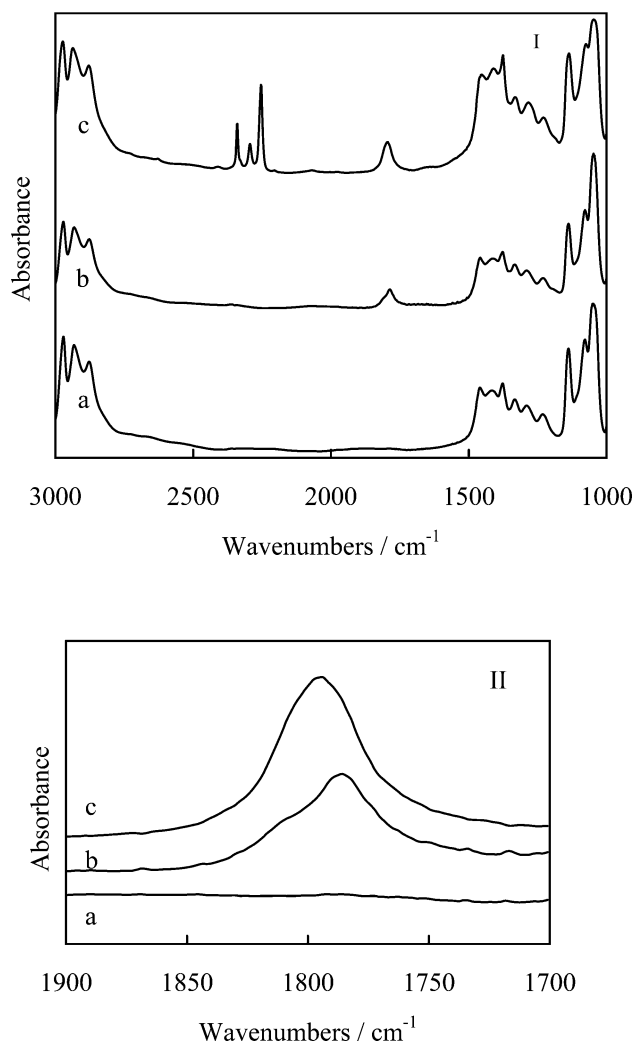
0.33) calcined at 1273 K. Dipropyleneglycols (DPG) are an expectable by-products in PG+CO<sub>2</sub> reaction (eqn. (7)). DPGs have three isomers as shown below.



As a result, DPGs were not detected by GC analysis under these reaction conditions as listed in Table 4. Especially, DPGs were not detected even at high temperature (443 and 463 K), where DEG was formed in the EG+CO<sub>2</sub> reaction. This indicates that PC synthesis from PG+CO<sub>2</sub> is more selective than EC from EG+CO<sub>2</sub>. At present, the reason for the different behaviour in ether formation between the EG+CO<sub>2</sub> and PG+CO<sub>2</sub> reactions is not clear. Further investigation is necessary for the elucidation of this difference.

Furthermore, we also measured the FTIR spectra of the liquid phase after the reaction in order to recognize the formation of poly(propylene carbonate). Fig. 5 shows the FTIR spectra of the

liquid phase after the PG+CO<sub>2</sub> reaction as well as the reference samples. In the case of propylene glycol, no peak was observed near 1800 cm<sup>-1</sup> (Fig. 5(a)). On the other hand, the peak at 1782 cm<sup>-1</sup> was observed in the reference sample (Fig. 5(b)). The sample



**Fig. 5** FTIR spectra of the liquid phase in the PG+CO<sub>2</sub> reaction. (I) Wavenumbers range: 3500–1000 cm<sup>-1</sup>, (II) Wavenumbers range: 1900–1700 cm<sup>-1</sup> (a) PG, (b) PG : PC = 100 : 2 mmol, (c) After the reaction at 403 K (0.5 g CeO<sub>2</sub>-ZrO<sub>2</sub> (Ce/(Ce+Zr) = 0.33) calcined at 1273 K, PG : CH<sub>3</sub>CN : CO<sub>2</sub> = 100 : 120 : 200 mmol. 2-Propanol (2.6 mmol) was added to the liquid phase after the reaction as a standard. The thickness of the liquid phase was 0.015 mm for (a) and (b), and 0.045 mm for (c).

contained PC and the peak is assigned to PC. Furthermore, the peak at 1790 cm<sup>-1</sup> was observed in the liquid phase after the reaction. This can also be assigned to PC formed from the reaction of PG and CO<sub>2</sub>, which was supported by GC analysis. The difference in peak positions between Fig. 5(b) and (c) is due to difference of solvents. It should be noted that no peak was observed at 1750 cm<sup>-1</sup> due to poly(propylene carbonate) at all, and this indicates that poly(propylene carbonate) is not formed at all. In addition, the peaks at 2293 and 2252 cm<sup>-1</sup> can be assigned to AN, and the peak at 2341 cm<sup>-1</sup> can be assigned to CO<sub>2</sub> dissolved in the liquid after the reaction. From the analysis of the liquid phase after the reaction by GC and FTIR, it is also concluded that the only detected product is PC and the selectivity of PC formation is very high.

The amount of PC formation over CeO<sub>2</sub>-ZrO<sub>2</sub> (Ce/(Ce+Zr) = 0.33) calcined at 1273 K after 8 h was almost the same as that after 2 h at reaction temperatures higher than 403 K as listed in Table 4. It is thought that the amount of PC reaches the equilibrium level. A similar phenomenon was also observed in the case of EG+CO<sub>2</sub> reaction. These results indicate that the amount of PC over 0.05 g catalyst after 2 h is controlled by the catalytic activity of PC

formation. In 0.05 g  $\text{CeO}_2\text{-ZrO}_2$  ( $\text{Ce}/(\text{Ce}+\text{Zr}) = 0.33$ ), the total amount of Ce and Zr ions is estimated to be about 0.36 mmol, which is smaller than PC formation (1.6 mmol at 443 K). The turnover number (TON) can be calculated to be 4.4, and in fact it must be much higher because the number of surface active sites is much smaller than the total amount of Ce and Zr ions judging from the BET surface area. This is supported by the result that  $\text{CeO}_2\text{-ZrO}_2$  solid solution works as a heterogeneous catalyst in DMC formation from methanol and  $\text{CO}_2$ .<sup>29</sup> The formation rate of PC at 443 K over  $\text{CeO}_2\text{-ZrO}_2$  ( $\text{Ce}/(\text{Ce}+\text{Zr}) = 0.33$ ) calcined at 1273 K can be calculated to be 16 mmol  $\text{g-cat}^{-1} \text{h}^{-1}$ . On the other hand, the formation rate of DPGs is below  $[(2 \times 0.01 \text{ mmol})/0.5 \text{ g}]/8 \text{ h}$  ( $= 0.005 \text{ mmol g-cat}^{-1} \text{h}^{-1}$ ) since the detection limit of DPGs in GC analysis is 0.01 mmol. The selectivity of PC formation on the basis of this estimation is above 99.9%. It can be said that PC can be selectively synthesized from propylene glycol and  $\text{CO}_2$  over  $\text{CeO}_2\text{-ZrO}_2$  solid solution catalysts.

We also investigated the effect of solvent in PG+ $\text{CO}_2$  reaction, and we tested diethyl ether, tetrahydrofuran, chloroform, dimethyl sulfoxide, *N,N*-dimethylformamide, and propionitrile. The results are listed in Table 5. Regarding the results of non-solvent and

**Table 5** Effect of solvent in PG+ $\text{CO}_2$  reaction at 403 K

Solvent	Catalyst weight/g	Reaction time/h	Formation amount/mmol	
			PC	DPGs
None	0.05	2	0.37	n. d.
	0.5	2	0.50	n. d.
Acetonitrile	0.05	2	0.67	n. d.
	0.5	2	2.0	n. d.
Diethyl ether	0.5	2	0.41	n. d.
Tetrahydrofuran	0.5	2	0.58	n. d.
Chloroform	0.5	2	0.62	n. d.
Dimethyl sulfoxide	0.5	2	1.56	n. d.
<i>N,N</i> -Dimethylformamide	0.5	2	1.77	n. d.
Propionitrile	0.5	2	1.68	n. d.

Reaction conditions: PG :  $\text{CO}_2$  : solvent = 100 : 200 : 120 mmol. Catalyst:  $\text{CeO}_2\text{-ZrO}_2$  ( $\text{Ce}/(\text{Ce}+\text{Zr}) = 0.33$ ), calcination temperature 1273 K. n. d.; not detected by FID-GC.

acetonitrile (AN), PC amount over 0.05 g catalyst without solvents (0.37 mmol) was a little smaller than that using AN (0.67 mmol), however, PC amount over 0.5 g catalyst using AN (2.0 mmol) was about four times as large as that without solvents (0.5 mmol). This comparison suggests that the effect of solvent on the equilibrium is more significant than that on the formation rate. Although the mechanism of this solvent effect is not clear at present, a possible interpretation is the difference of solubility of  $\text{CO}_2$  in the liquid phase. We monitored the pressure during the reaction. In the case of non-solvent reaction, the total pressure was 6.8 MPa, and in contrast, it was 6.3 MPa when the AN solvent was used. A cause of the difference in the total pressure could be due to the difference in  $\text{CO}_2$  solubility. The solvents such as diethyl ether, tetrahydrofuran and chloroform were not effective; in contrast, solvents such as dimethyl sulfoxide, *N,N*-dimethylformamide, acetonitrile, and propionitrile were very effective in promoting of PC formation. At present, it is difficult to explain these solvent effects clearly. Further investigation is necessary for the elucidation. However, it is concluded that AN was the most effective solvent in PG+ $\text{CO}_2$  reaction. Furthermore, we also investigated the effect of AN amount in PG+ $\text{CO}_2$  reaction as listed in Table 6. The formation rate of PC on the basis of PC amount over 0.05 g-cat increased with the additive amount of AN in the range of 0–120 mmol; at the same time, the PC amount at equilibrium level on the basis of that over 0.5 g-cat also increased in the same AN range, probably because of the enhancement of  $\text{CO}_2$  solubility. These results indicate that the addition of 120 mmol AN is most effective for the enhancement of catalytic activity and equilibrium yield.

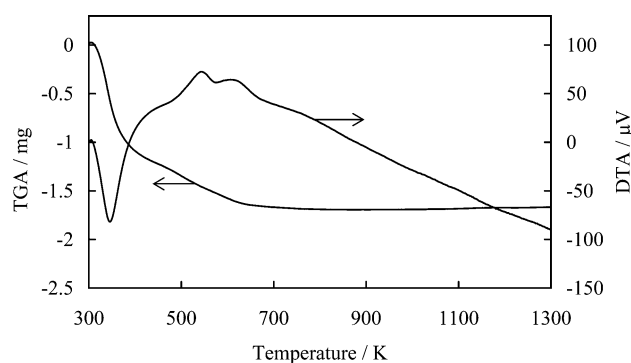
**Table 6** Effect of AN amount in PG+ $\text{CO}_2$  reaction at 403 K

$\text{CH}_3\text{CN}$ amount/mmol	Catalyst weight/g	Reaction time/h	Formation amount/mmol	
			PC	DPGs
0	0.05	2	0.37	n. d.
	0.5	2	0.50	n. d.
60	0.05	2	0.51	n. d.
	0.5	2	1.4	n. d.
120	0.05	2	0.67	n. d.
	0.5	2	2.0	n. d.
180	0.05	2	0.62	n. d.
	0.5	2	2.1	n. d.

Reaction conditions: PG :  $\text{CO}_2$  :  $\text{CH}_3\text{CN}$  = 100 : 200 :  $x$  mmol ( $x = 0\text{--}180$  mmol). Catalyst:  $\text{CeO}_2\text{-ZrO}_2$  ( $\text{Ce}/(\text{Ce}+\text{Zr}) = 0.33$ ), calcination temperature 1273 K. n. d.; not detected by FID-GC.

### Catalyst characterization

Fig. 6 shows the thermogravimetric analysis of Ce and Zr hydroxide. Weight loss occurred in the range of 298–673 K. This



**Fig. 6** TGA-DTA profiles of Ce-Zr hydroxide ( $\text{Ce}/(\text{Ce}+\text{Zr}) = 0.33$ ). Initial sample weight: 10 mg, heating rate: 15  $\text{K min}^{-1}$ .

behavior is similar to Zr hydroxide in the previous report.<sup>24</sup> The endothermic DTA peak was observed at 298–423 K. This corresponds to the desorption of water. At 520–650 K, the exothermic DTA peak and the weight loss was observed. This seems to be assigned to solid reaction and/or the phase transition for the formation of solid solution, although the details are not clear. The amount of desorbed  $\text{H}_2\text{O}$  was estimated to be about 1.5 mol per 1.0 mol metal cation in  $\text{CeO}_2\text{-ZrO}_2$  ( $\text{Ce}/(\text{Ce}+\text{Zr}) = 0.33$ ). An important point is that  $\text{H}_2\text{O}$  desorption finished below 673 K. Since we used the catalyst calcined at higher temperature than 673 K, we evaluated the catalytic performance of oxide catalyst which did not contain hydroxide.

Fig. 7 shows XRD patterns of  $\text{ZrO}_2$ ,  $\text{CeO}_2$  and  $\text{CeO}_2\text{-ZrO}_2$  ( $\text{Ce}/(\text{Ce}+\text{Zr}) = 0.33$ ) calcined at various temperatures. In the case of  $\text{ZrO}_2$ , only a small amount of metastable tetragonal structure due to the diffraction peak at  $30.3^\circ$  was observed when the sample was calcined at a low temperature such as 673 K. According to the XRD patterns of  $\text{ZrO}_2$  (Fig. 7(I)), the sample mainly consisted of monoclinic zirconia. The peak width decreased with increasing the calcination temperature because of crystal growth. This corresponds to the decrease of BET surface area from  $93 \text{ m}^2 \text{ g}^{-1}$  at 673 K to  $9 \text{ m}^2 \text{ g}^{-1}$  at 1273 K. As shown in Fig. 7(II), the XRD patterns confirm that  $\text{CeO}_2$  has the fluorite lattice structure at all the temperatures.<sup>32</sup> The peak width decreased with increasing the calcination temperature, and this behavior agrees with the BET surface area listed in Table 1. The BET surface area of  $\text{CeO}_2$  was very low ( $3 \text{ m}^2 \text{ g}^{-1}$ ) at 1273 K, although it was  $53 \text{ m}^2 \text{ g}^{-1}$  at 673 K. In addition, XRD patterns of  $\text{CeO}_2\text{-ZrO}_2$  ( $\text{Ce}/(\text{Ce}+\text{Zr}) = 0.33$ ) were very similar to those of  $\text{CeO}_2$ . The peaks assigned to  $\text{ZrO}_2$  were not observed at all, although the content of Zr is rather high. This indicates that all the Zr ions are incorporated into the  $\text{CeO}_2$  structure to form a solid solution in  $\text{CeO}_2\text{-ZrO}_2$  ( $\text{Ce}/(\text{Ce}+\text{Zr}) = 0.33$ ) calcined at any temperatures. The diffraction angle of the



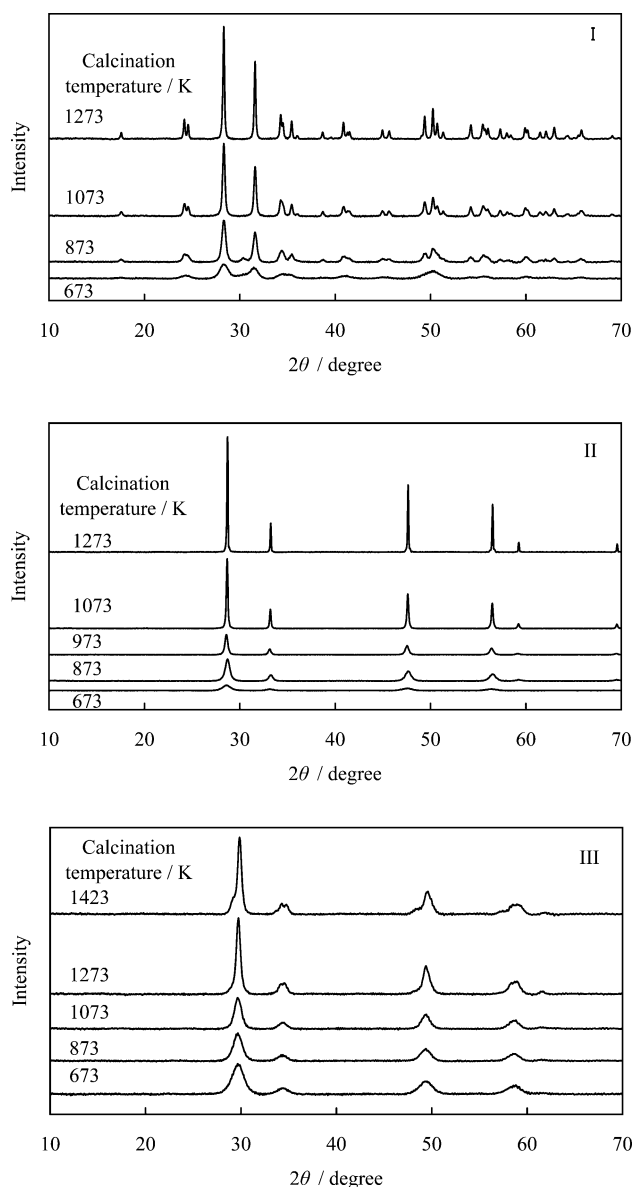
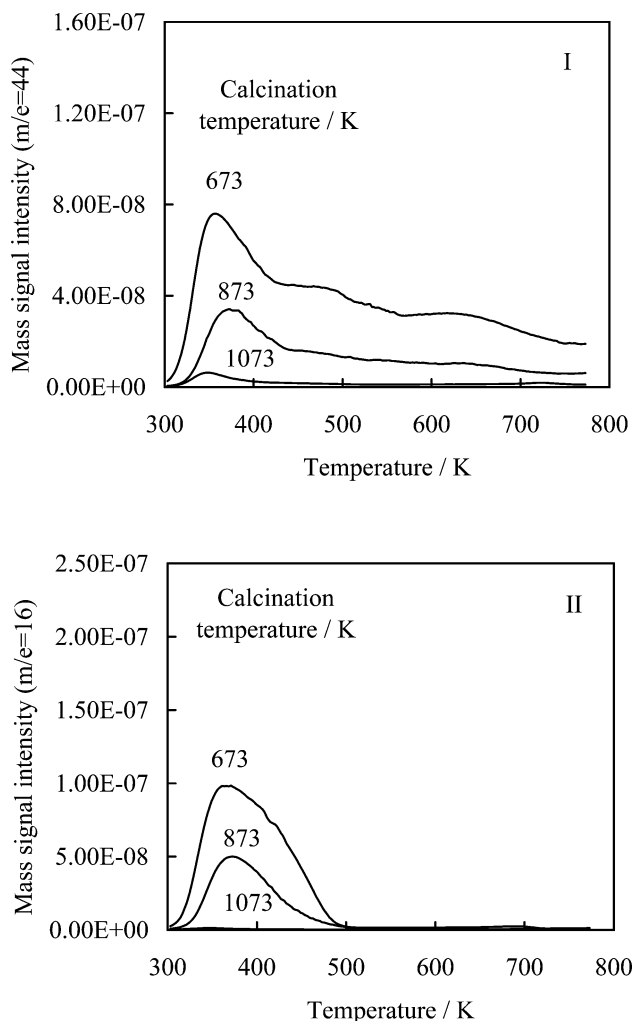


Figure 7. K. Tomishige, et al.

**Fig. 7** XRD patterns of catalysts prepared by the calcination of hydroxides at various temperatures. (I)  $\text{ZrO}_2$ , (II)  $\text{CeO}_2$ , (III)  $\text{CeO}_2\text{-ZrO}_2$  ( $\text{Ce}/(\text{Ce}+\text{Zr}) = 0.33$ ). X-Ray source:  $\text{Cu K}\alpha$ .

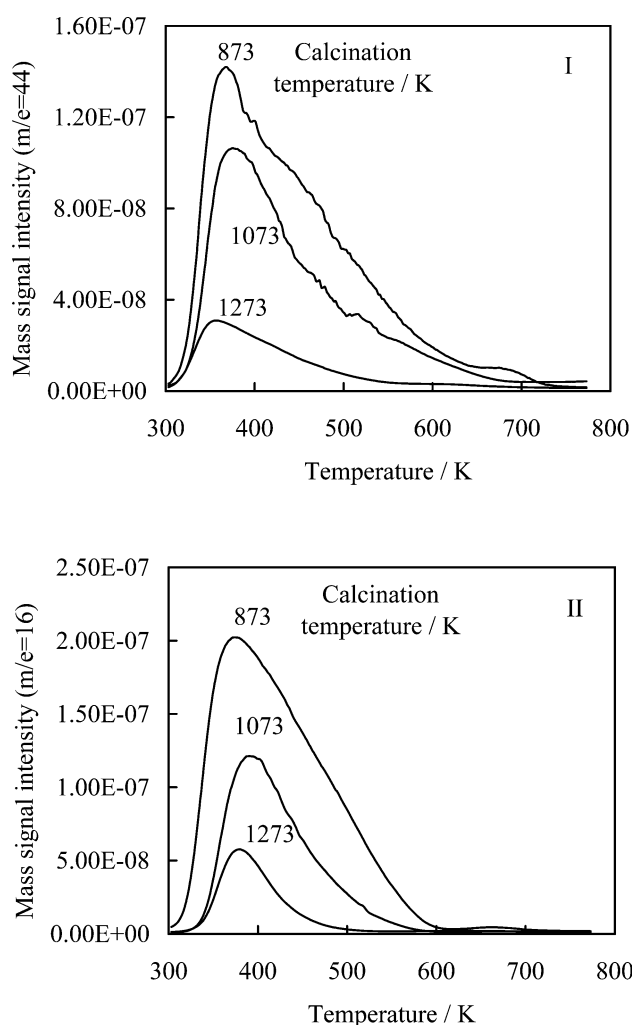
highest peak on  $\text{CeO}_2$  was 28.68 degree; in contrast, that on  $\text{CeO}_2\text{-ZrO}_2$  ( $\text{Ce}/(\text{Ce}+\text{Zr}) = 0.33$ ) was 29.75 degree. This is due to the smaller radius of the  $\text{Zr}^{4+}$  ion (0.084 nm) than that of the  $\text{Ce}^{4+}$  ion (0.097 nm).<sup>36</sup> The peak widths of  $\text{CeO}_2\text{-ZrO}_2$  ( $\text{Ce}/(\text{Ce}+\text{Zr}) = 0.33$ ) were much larger than that of  $\text{CeO}_2$  and  $\text{ZrO}_2$ . This tendency is consistent with the order of BET surface area:  $\text{CeO}_2 < \text{ZrO}_2 < \text{CeO}_2\text{-ZrO}_2$ . As a result, the addition of  $\text{ZrO}_2$  to  $\text{CeO}_2$  can inhibit the sintering of  $\text{CeO}_2$  and maintain a higher surface area, as reported previously.<sup>31,32</sup>

On the basis of our previous reports regarding dimethylcarbonate synthesis from methanol and  $\text{CO}_2$ , the acid-base properties are related to the catalyst performance.<sup>24,26</sup> In order to investigate the surface acid-base properties of the catalysts, we measured the temperature programmed desorption (TPD) of  $\text{NH}_3$  and  $\text{CO}_2$ . Fig. 8 and 9 show TPD profiles of  $\text{CeO}_2$  and  $\text{CeO}_2\text{-ZrO}_2$  ( $\text{Ce}/(\text{Ce}+\text{Zr}) = 0.33$ ) calcined at various temperatures, respectively. The peak intensities in TPD profiles of  $\text{CO}_2$  and  $\text{NH}_3$  decreased gradually with increasing the calcination temperature on both catalysts. In the case of  $\text{CeO}_2$ , desorption of  $\text{CO}_2$  was observed even at temperatures higher than 500 K, and this indicates that  $\text{CeO}_2$  has stronger basicity than  $\text{CeO}_2\text{-ZrO}_2$ . On the other hand, from the profiles of  $\text{NH}_3$  TPD,



**Fig. 8** Profiles of temperature-programmed desorption of  $\text{CO}_2$  (I) and  $\text{NH}_3$  (II) adsorbed on  $\text{CeO}_2$  calcined at 673–1073 K. The calcination temperature is described in the figure.  $\text{CO}_2$  and  $\text{NH}_3$  adsorption:  $P = 6.6$  kPa and 293 K. TPD conditions: heating rate =  $7 \text{ K min}^{-1}$  and sample weight = 0.1 g.

we found that  $\text{CeO}_2\text{-ZrO}_2$  has a little stronger acidity than  $\text{CeO}_2$ . For example, the desorption of  $\text{NH}_3$  was not observed at temperatures higher than 500 K over  $\text{CeO}_2\text{-ZrO}_2$  ( $\text{Ce}/(\text{Ce}+\text{Zr}) = 0.33$ ) calcined at 1273 K, however, the desorption of  $\text{NH}_3$  continued to 600 K over the catalyst calcined at 873 K. This suggests that the structural change of the surface can make the surface acidity and basicity weaker. Although the details are not elucidated yet, it is thought that the surface on the catalysts calcined at lower temperature has more roughness and higher temperature calcination makes the surface more plain. There are more coordination unsaturated cations and anions on rougher surfaces, and these sites give higher acidity and basicity.<sup>37</sup> Furthermore,  $\text{CeO}_2\text{-ZrO}_2$  ( $\text{Ce}/(\text{Ce}+\text{Zr}) = 0.33$ ) calcined at 1273 K and  $\text{CeO}_2$  calcined at 873 K gave higher performance in PC and EC formation from corresponding glycols and  $\text{CO}_2$  as shown in Fig. 1 and 4. TPD profiles of  $\text{NH}_3$  and  $\text{CO}_2$  over two catalysts are very similar to each other. The relation between carbonate formation and catalyst properties such as BET surface area, adsorption amount of  $\text{CO}_2$  and  $\text{NH}_3$  is shown in Fig. 10. Adsorption amount of  $\text{NH}_3$  and  $\text{CO}_2$  was measured by the volumetric methods and the results are summarized in Table 7. Interestingly, EC and PC amount, which represents formation rate, increased with decreasing surface area. A similar tendency was observed in the comparison with adsorption amount of  $\text{CO}_2$  and  $\text{NH}_3$ . These results suggest that the formation rate per acidic and/or basic sites significantly increased on the catalysts calcined at higher temperature with lower surface area. Combined with TPD results, weak acid and base sites can give high PC and EC



**Fig. 9** Profiles of temperature-programmed desorption of CO<sub>2</sub> (I) and NH<sub>3</sub> (II) adsorbed on CeO<sub>2</sub>-ZrO<sub>2</sub> (Ce/(Ce+Zr) = 0.33) calcined at 873–1273 K. The calcination temperature is described in the figure. CO<sub>2</sub> and NH<sub>3</sub> adsorption:  $P = 6.6$  kPa and 293 K. TPD conditions: heating rate = 7 K min<sup>-1</sup> and sample weight = 0.1 g.

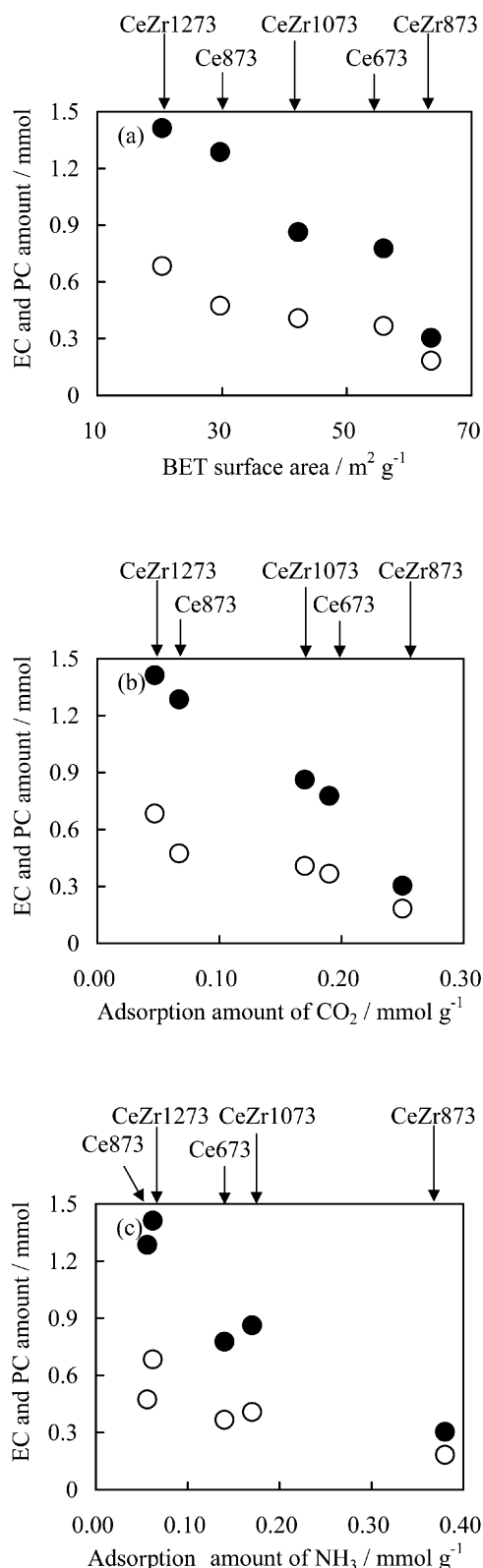
formation rate. We have reported that weak Brønsted acid sites exhibited high activity of dimethyl carbonate from methanol and CO<sub>2</sub> over H<sub>3</sub>PO<sub>4</sub>/ZrO<sub>2</sub>.<sup>26</sup> We are going to elucidate the reaction mechanism over these weak acid and base sites and their roles in PC+CO<sub>2</sub> and EC+CO<sub>2</sub> reaction.

In terms of the productivity, the yield of EC and PC is very low and also limited by the equilibrium; the maximum PG conversion was about 2% under our reaction conditions. This problem is also pointed in the direct synthesis of DMC from methanol and CO<sub>2</sub>.<sup>29,38</sup> The challenge of obtaining a higher yield has been addressed, and two successful methods have been reported: one is the removal of H<sub>2</sub>O using molecular sieves,<sup>38</sup> and the other is the removal of H<sub>2</sub>O through the reaction between H<sub>2</sub>O and 2,2-dimethoxy propane.<sup>29</sup> It is thought that these methods are also promising for the increase of PC yield in the reaction system since, in principle, a higher yield of PC is available if H<sub>2</sub>O is removed from the system.

## Conclusions

1. Propylene carbonate (PC) and ethylene carbonate (EC) were synthesized by the reaction of CO<sub>2</sub> with propylene glycol (PG) and ethylene glycol (EG), respectively, using ceria based catalysts.

2. Catalytic activity of PC and EC formation was much dependent on the composition and calcination temperature of the CeO<sub>2</sub>-ZrO<sub>2</sub> solid solution. On the basis of the catalyst characterization, it is suggested that the active sites could be weak acid–base



**Fig. 10** Correlation in catalyst performance and properties of CeO<sub>2</sub> and CeO<sub>2</sub>-ZrO<sub>2</sub> (Ce/(Ce+Zr) = 0.33) catalysts. ●: PC amount, ○: EC amount. (a) EC and PC amount vs. BET surface area, (b) EC and PC amount vs. adsorption amount of CO<sub>2</sub> (c) EC and PC amount vs. adsorption amount of NH<sub>3</sub>, EC and PC amounts originate from Fig. 1 and 4. Ce673 and Ce873 are CeO<sub>2</sub> calcined at 673 and 873 K, respectively. CeZr873, CeZr1073, and CeZr1273 are CeO<sub>2</sub>-ZrO<sub>2</sub> (Ce/(Ce+Zr) = 0.33) calcined at 873, 1073 and 1273 K, respectively. Ethylene carbonate and propylene carbonate can be synthesized with high selectivity by the reaction of CO<sub>2</sub> with ethylene glycol and propylene glycol using ceria based catalysts.

sites which are present on the plain surface of the catalysts calcined at high temperature. On the other hand, catalyst calcined at too high

**Table 7** Adsorption amount of CO<sub>2</sub> and NH<sub>3</sub> on the catalysts

Catalyst	Calcination	CO <sub>2</sub> /mmol g <sup>-1</sup>	NH <sub>3</sub> /mmol g <sup>-1</sup>
	temperature/K		
CeO <sub>2</sub>	673	0.19	0.14
	873	0.067	0.056
CeO <sub>2</sub> -ZrO <sub>2</sub> (Ce/(Ce+Zr) = 0.33)	873	0.25	0.38
	1073	0.17	0.17
	1273	0.047	0.062

Irreversible adsorption amount measured by volumetric method at room temperature.

temperature exhibited low activity due to very low surface area. The addition of Zr to CeO<sub>2</sub> was very effective at maintaining the high surface area of the catalysts calcined at high temperature, and this is related to the calcination temperature dependence of the catalytic activity.

3. In PG+CO<sub>2</sub> and EG+CO<sub>2</sub> reactions, ether and polycarbonate are expected by-products. According to the GC analysis, diethylene glycol in the EG+CO<sub>2</sub> reaction was observed at high reaction temperature (423–463 K). However, it was not observed at all under optimum reaction conditions. In contrast, dipropylene glycol in the PG+CO<sub>2</sub> reaction was not observed in all the temperature range (383–463 K). Furthermore, polycarbonate was not observed at all in both reactions from the FTIR measurement. Cyclic carbonate formation such as EC and PC was highly selective.

4. The production of EC and PC from corresponding glycols and CO<sub>2</sub> using CeO<sub>2</sub> based catalysts is limited by the reaction equilibrium. In order to obtain high yields of PC and EC, the removal of H<sub>2</sub>O from the reaction system is essential and this becomes a subject in the future.

## References

- 1 J. H. Clements, *Ind. Eng. Chem. Res.*, 2003, **42**, 663.
- 2 A.-A. Shaikh and S. Sivaram, *Chem. Rev.*, 1996, **96**, 951.
- 3 T. Nishikubo, A. Kameyama, J. Yamashita, M. Tomoi and W. Fukada, *J. Polym. Sci. Part A Polym. Chem.*, 1993, **31**, 939.
- 4 T. Yano, H. Matsui, T. Koike, H. Ishiguro, H. Fujihara, M. Yoshikara and T. Maeshima, *Chem. Commun.*, 1997, 1129.
- 5 B. M. Bhanage, S. Fujita, Y. Ikushima and M. Arai, *Appl. Catal. A: Gen.*, 2001, **219**, 259.
- 6 K. Yamaguchi, K. Ebitani, T. Yoshida, H. Yoshida and K. Kaneda, *J. Am. Chem. Soc.*, 1999, **121**, 4526.
- 7 E. J. Doskocil, S. V. Bordawekar, B. G. Kaye and R. J. Davis, *J. Phys. Chem. B*, 1999, **103**, 6277.
- 8 M. Tu and R. J. Davis, *J. Catal.*, 2001, **199**, 85.
- 9 H. Yasuda, L. N. He and T. Sakakura, *J. Catal.*, 2002, **209**, 547.
- 10 S. Fukuoka, M. Kawamura, K. Komiya, M. Tojo, H. Hachiya, K. Hasegawa, M. Aminaka, H. Okamoto, I. Fukawa and S. Konno, *Green Chem.*, 2003, **5**, 497.
- 11 D. Delledonne, F. Rivetti and U. Romano, *Appl. Catal. A*, 2001, **221**, 241.
- 12 P. T. Anastas and J. C. Warner, *Green Chemistry: Theory and Practice*, Oxford Univ. Press, Oxford, 1998.
- 13 M. Aresta and E. Quaranta, *CHEMTECH*, 1997, 32.
- 14 Y. Ono, *Appl. Catal. A*, 1997, **155**, 133.
- 15 M. A. Pacheco and C. L. Marshall, *Energy Fuels*, 1997, **11**, 2.
- 16 U. Romano, R. Tesei, M. M. Mauri and P. Rebora, *Ind. Eng. Chem. Prod. Res. Dev.*, 1980, **19**, 396.
- 17 T. Matsuzaki and A. Nakamura, *Catal. Surv. Jpn.*, 1997, **1**, 77.
- 18 X. B. Lu, X. J. Feng and R. He, *Appl. Catal. A*, 2002, **234**, 25.
- 19 J. Gao and S. H. Zhong, *Prog. Chem.*, 2002, **14**, 107.
- 20 B. M. Bhanage, S. Fujita, Y. Ikushima and M. Arai, *Appl. Catal. A*, 2001, **219**, 259.
- 21 M. S. Han, B. G. Lee, B. S. Ahn, K. Y. Park and S. I. Hong, *React. Kinet. Catal. Lett.*, 2001, **73**, 33.
- 22 T. Tatsumi, Y. Watanabe and K. A. Koyano, *Chem. Commun.*, 1996, 2281.
- 23 K. Tomishige, T. Sakaihorii, Y. Ikeda and K. Fujimoto, *Catal. Lett.*, 1999, **58**, 225.
- 24 K. Tomishige, Y. Ikeda, T. Sakaihorii and K. Fujimoto, *J. Catal.*, 2000, **192**, 355.
- 25 Y. Ikeda, T. Sakahori, K. Tomishige and K. Fujimoto, *Catal. Lett.*, 2000, **66**, 59.
- 26 Y. Ikeda, K. Fujimoto and K. Tomishige, *J. Phys. Chem. B*, 2001, **105**, 10653.
- 27 Y. Ikeda, Y. Furusawa, K. Tomishige and K. Fujimoto, *ACS Symp. Ser.*, 2002, **809**, 71.
- 28 K. Tomishige, Y. Furusawa, Y. Ikeda, M. Asadullah and K. Fujimoto, *Catal. Lett.*, 2001, **76**, 71.
- 29 K. Tomishige and K. Kunimori, *Appl. Catal. A*, 2002, **237**, 103.
- 30 Jpn. Kokai Tokkyo Koho, 1999, 11-292538.
- 31 V. Perrichon, A. Laachir, S. Abouarnadasse, O. Touret and G. Blanchard, *Appl. Catal. A: Gen.*, 1995, **129**, 69.
- 32 C. Leitenburg, A. Trovarelli, J. Llorca, F. Cavani and G. Bini, *Appl. Catal. A: Gen.*, 1996, **139**, 161.
- 33 D. J. Darensbourg, J. C. Yarbrough, C. Ortiz and C. C. Fang, *J. Am. Chem. Soc.*, 2003, **125**, 7586.
- 34 R. D. Shannon and C. T. Prewitt, *Acta Crystallogr., Sect. B*, 1969, **25**, 925.
- 35 C. J. Angell, *Trans. Faraday Soc.*, 1956, **52**, 1178.
- 36 G. Fini, P. Mirone and B. Fortunato, *J. Chem. Soc., Faraday Trans.*, 1973, **69**, 69.
- 37 H. Kawakami and S. Yoshida, *J. Chem. Soc., Faraday Trans.*, 1984, **2(80)**, 921.
- 38 J.-C. Choi, L. N. He, H. Yasuda and T. Sakakura, *Green Chem.*, 2002, **4**, 230.



# Palladium-free and ligand-free Sonogashira cross-coupling

Mehul B. Thathagar, Jurriaan Beckers and Gadi Rothenberg\*

van't Hoff Institute for Molecular Sciences, University of Amsterdam, Nieuwe Achtergracht 166, 1018 WV Amsterdam, The Netherlands. E-mail: gadi@science.uva.nl; Fax: +31 20 525 5604

Received 3rd February 2004, Accepted 3rd March 2004

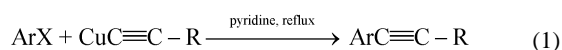
First published as an Advance Article on the web 19th March 2004

Copper nanoclusters catalyse the cross-coupling of alkynes and aryl halides to give the corresponding disubstituted alkynes. No palladium, ligand, or co-catalyst is needed, and products are isolated in good yields (80–85%) and high selectivity. The clusters are simple to prepare, stable and can be applied to a variety of iodo- and bromoaryls. Mechanistic pathways for homocoupling and cross-coupling of alkynes are examined by comparing the activity of different catalyst and co-catalyst combinations. The copper clusters show different catalytic properties than their homogeneous analogues.

## Introduction

The ever-growing search for new drugs and polymers is bringing alkyne chemistry forward. In the fine-chemical industry, C–C triple bonds are sought because they can be easily functionalised using multiple addition reactions. In materials science, polyalkyne derivatives are used to make organic LEDs,<sup>1</sup> new carbon allotropes and carbon-rich materials.<sup>2</sup>

The key reaction here is the formation of an alkyne–carbon bond, *i.e.* the attachment of an alkyl or aryl group onto the triple bond without destroying it. In 1963, Stephens and Castro<sup>3</sup> demonstrated the coupling of aryl halides with alkynylcopper(i) species to obtain arylacetylenes (eqn. 1). Since then, much effort has been directed to elucidate the mechanism of the Stephens–Castro reaction, and to develop synthetic protocols that would not require stoichiometric copper.<sup>4</sup> Sonogashira and co-workers found that combining catalytic amounts of Pd(PPh<sub>3</sub>)<sub>4</sub> and CuI enabled the same coupling without the need for stoichiometric copper or for isolating the alkynylcopper(i) intermediate.<sup>5</sup> Many variations of this reaction have since been reported<sup>6–10</sup> including palladium-catalysed copper-free versions<sup>11–16</sup> and, notably, palladium-free versions.<sup>17–22</sup> This seems already like an optimal solution, but for large-scale synthesis the phosphine ligands themselves are a problem. They are usually unrecoverable and can complicate further synthetic steps. In fact, the ligand problem is one reason why homogeneous catalysis, so popular in the lab, is often shunned by the fine-chemical industry.<sup>23</sup>

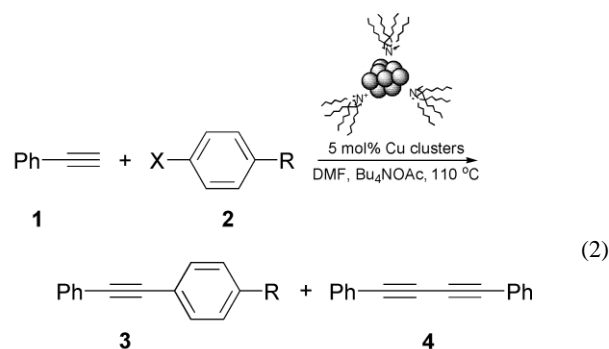


However, while ligands are ubiquitous in homogeneous catalysis, ligand–metal complexes are not always the only active catalytic species. This is especially true in the case of C–C coupling reactions, where catalysis by metal nanoclusters (2–10 nm in diameter) is often observed.<sup>24</sup> These clusters often exhibit unique catalytic properties due to their high surface area and the possibility of charge distribution in electron transfer reactions.<sup>25</sup> For the past two years, our group has been developing metal nanoclusters as alternative cross-coupling catalysts.<sup>26,27</sup> Here we report the first palladium-free and ligand-free Sonogashira cross-coupling, using stable copper nanoclusters as catalysts.

## Results and discussion

The metal clusters (Cu, Cu/Pd and Pd) were prepared by reducing solutions of the chloride salt precursors with tetraoctylammonium formate (TOAF) in DMF at 65 °C.<sup>27,28</sup> TOAF also acts simultaneously as a stabiliser, forming an organic corona around the clusters that prevents their aggregation. The clusters were used as is in the

coupling of phenylacetylene **1** with various aryl halides (eqn. 2). In a typical reaction, 1.5 equiv. of **1** and one equiv. of aryl halide **2** were mixed in the presence of 1.5 equiv. base and 0.05 equiv. of metal clusters at 110 °C. Reaction progress was monitored by GC. After 24 h, the clusters were separated and the substituted diphenylalkyne **3** was isolated and analysed by GC/MS and <sup>1</sup>H NMR.



X = I, Br

R = H, Me, Perfluoro, CF<sub>3</sub>, NO<sub>2</sub>, OMe, CN

Table 1 shows the conversion and yield obtained for various aryl iodides and bromides in the presence of 5 mol% Cu clusters. Iodoarenes gave quantitative yields, while bromoarenes gave good to moderate yields. Chloroarenes, unfortunately, were inactive (no reaction was observed even when using the activated *p*-nitrochlorobenzene). Control experiments confirmed that no conversion occurs without Cu clusters. The cross-coupling product accounted for 100% of the haloarene (the limiting reagent). In some cases, the excess phenylacetylene reacted to give 10–15% of the homocoupling (Hay coupling<sup>29</sup>) product **4**, as well as small amounts (2–4%) of a heavy (not identified) product. Copper clusters performed better than their homogeneous analogues, not only with iodoarenes but also with the activated bromoarene substrates *p*-Br-C<sub>6</sub>H<sub>4</sub>-CN and *p*-Br-C<sub>6</sub>H<sub>4</sub>-CF<sub>3</sub> (92% and 55% conversion with Cu clusters, *cf.* with <25% reported<sup>18</sup> for CuI/PPh<sub>3</sub> and no reaction observed using Cu 1,10-phenanthroline complexes<sup>19</sup>). However, attempts to perform the cross-coupling of phenylacetylene with electron rich bromoarenes using 10 mol% Cu clusters gave only modest yields (15–20%), and no conversion was observed also for triisopropylsilyl acetylene with iodoarenes (in the latter case, large aggregates formed within 15 min). To check if triisopropylsilyl acetylene interacts with the clusters and destabilises them, we stirred triisopropylsilyl acetylene, tetra-*n*-butylammonium acetate

**Table 1** Cross-coupling of aryl halides with **1** using Cu nanoclusters.<sup>a</sup>

Entry	Substrate	Conversion (%) <sup>b</sup>	Yield (%) <sup>b</sup>
1		100	82 <sup>c</sup>
2		100	84 <sup>c</sup>
3		100	> 99
4		100	> 99
5		100	94 <sup>c</sup>
6		100	> 99
7		100	> 99
8		100	88 <sup>c</sup>
9		55	53
10		100	> 99
11		92	91
12		20 <sup>d</sup>	20
13		16 <sup>d</sup>	16

<sup>a</sup> Reaction conditions: 0.25 mmol substrate, 0.38 mmol **1**, 0.40 mmol TBAA, 0.012 mmol copper nanoclusters, 2.5 mL DMF, N<sub>2</sub> atmosphere, 110 °C, 24 h (time was not optimised). <sup>b</sup> Conversion of **2** and yield of **3**, respectively, based on GC, corrected for the presence of an internal standard. <sup>c</sup> Isolated yield. <sup>d</sup> 10 mol% of Cu clusters was used.

(TBAA) and Cu clusters at 110 °C. No aggregation was observed even after 24 h.

The facile cross-coupling and the product specificity in the presence of copper clusters raise some interesting questions regarding similarities and differences between the coupling mechanisms using copper and palladium, and regarding the role of cuprous iodide. To try and answer these questions, we performed a series of cross-coupling experiments between phenylacetylene and iodotoluene, using various nanocluster/co-catalyst combinations (Table 2).

**Table 2** Cross-coupling of **1** with 4-iodotoluene<sup>a</sup>

Entry	Catalyst (mol%)	Base	Time/h	Conversion (%) <sup>b</sup>
1	none	TBAA	24	0
2	Cu (5)	none	24	0
3	CuI (5)	TBAA	24	18
4	CuI + TOAB (5 + 5)	TBAA	24	20
5	Cu (5)	TBAA	8	90
6	Cu + CuI (5 + 5)	TBAA	8	72
7	Cu (5)	TBAF	24	75
8	Cu (5)	Et <sub>3</sub> N	24	25
9	Cu (5)	Na(OAc) <sub>2</sub>	24	22
10	Pd (2)	TBAA	2	100
11	Pd + CuI (2 + 5)	TBAA	2	100
12	Pd + Cu (2 + 5 <sup>c</sup> )	TBAA	2	86
13	{CuPd} (2 <sup>d</sup> )	TBAA	2	92

<sup>a</sup> Reaction conditions: 0.25 mmol 4-iodotoluene, 0.38 mmol **1**, 0.40 mmol tetra-*n*-butylammonium acetate (TBAA), 2.5 mL DMF, N<sub>2</sub> atmosphere, 110 °C. <sup>b</sup> GC conversion of the 4-iodotoluene, corrected for the presence of an internal standard. <sup>c</sup> A mixture of Cu clusters (5 mol%) + Pd clusters (2 mol%). <sup>d</sup> Pre-prepared bimetallic {Cu/Pd} clusters (2 mol%).

Palladium clusters were active in the Sonogashira cross-coupling (Table 2, entry 10), but they aggregated as Pd black at the end of the reaction. The copper clusters, on the other hand, remained stable – no aggregation was observed – and could be re-used. Adding CuI did not improve the performance of either cluster catalyst (entries 6, 11). Moreover, CuI as sole catalyst gave only 18% conversion after 24 h (entry 3). Bimetallic Cu/Pd and mixed<sup>30</sup> clusters gave nearly

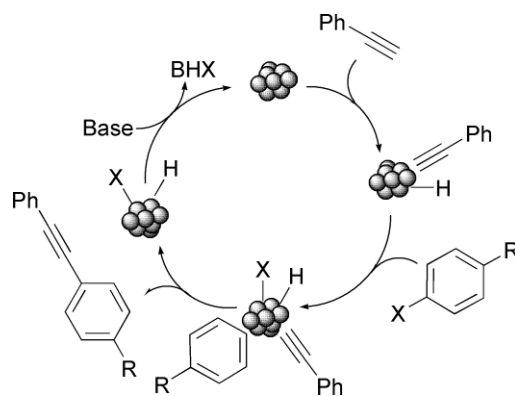
the same conversions and were both less active than pure Pd clusters.† The presence and type of base proved crucial to the reaction. No reaction occurred in absence of base, and only ~25% conversion was observed when TBAA was substituted with Et<sub>3</sub>N or with Na(OAc)<sub>2</sub> (entries 8, 9). Tetra-*n*-butylammonium fluoride gave good conversion but was not as effective as TBAA.

One important question is: Do the tetraoctylammonium cations ligate to Cu(I) that could possibly leach out from the clusters, pairing with iodide that originates in the iodoarene? If this is so, the clusters would be merely ‘copper reservoirs’ rather than catalysts. This possibility, however, was ruled out by control experiments using CuI and CuI + tetraoctylammonium bromide (TOAB) (Table 2, entries 3 and 4). Both experiments gave only ~20% conversion, showing that the tetraoctylammonium cations are not good ligands for cuprous ions as far as Sonogashira cross-coupling is concerned. We used TOAB in these tests instead of TOAF, because TOAF can reduce cuprous ions to form clusters, which would void the results.

The Hay coupling of phenylacetylene **2** to diphenyldiacetylene **4** requires the presence of oxygen.<sup>29,31</sup> 10–15% homocoupling was observed under a dry N<sub>2</sub> atmosphere, indicating that oxygen was still present in the system. We managed to prevent the homocoupling entirely by degassing the solvent and the stock suspension of the copper nanoclusters with dry N<sub>2</sub> for 1 h prior to reaction. In theory copper can oxidise to form copper oxide clusters, but in our case it is highly unlikely as all syntheses and reactions were performed under nitrogen. Moreover, Okuro *et al.*<sup>18</sup> showed that copper oxide catalysts are ineffective in Sonogashira coupling.

We also tested the reusability of the Cu clusters in the coupling of **1** with *p*-I-C<sub>6</sub>H<sub>4</sub>-CF<sub>3</sub>. In each re-run, we added another equivalent of reactants and base. The clusters could be used three times without deactivation, giving a final TON of 73.

The above experiments shed some light on the cross-coupling mechanism with copper nanoclusters. Although we do not have a detailed mechanistic picture yet, the mechanism is certainly different from that proposed by Okuro *et al.* for CuI + phosphine ligands<sup>18</sup> and also from that involving both copper and palladium.<sup>30</sup> We suggest that phenylacetylene co-ordinates to the copper cluster, forming an {alkenyl–Cu cluster} species. This then reacts with the aryl halide, after which the product is removed and HX eliminates from the cluster in the presence of a base (Scheme 1). One

**Scheme 1** Suggested cycle for cluster-catalysed Sonogashira cross-coupling (the stabilising tetraoctylammonium ions are omitted for clarity).

important difference between clusters and monoatomic complexes is that the positive charge created in the oxidative addition can be shared among the copper atoms in the cluster. This may facilitate the product formation and the reductive elimination steps. Further studies on this mechanism and on the catalyst deactivation process will be done in our laboratory. As the isolation and drying of nanoclusters can cause major changes in their catalytic properties,

† Cf. the synergistic effect observed in the case of Suzuki cross-coupling (ref. 24).

we want to track the active catalytic species *in operando*, rather than *via* a post-reaction characterisation. We are currently developing spectroscopic tools for this purpose.<sup>32</sup>

In conclusion, we show here that copper nanoclusters are good catalysts for Sonogashira cross-coupling. The lower price of copper compared to palladium, plus the fact that no phosphine ligands are needed, make this an interesting catalytic alternative for the synthesis of substituted carbon-carbon triple bonds.

## Experimental

### Materials and instrumentation

<sup>1</sup>H NMR spectra were recorded in CD<sub>2</sub>Cl<sub>2</sub> on a 300 MHz Varian Inova instrument. Chemical shift values are in ppm relative to Me<sub>4</sub>Si. Melting points were measured on a Gallenkamp melting point apparatus and are uncorrected. GC analysis was performed using an Interscience GC-8000 gas chromatograph with a 100% dimethylpolysiloxane capillary column (DB-1, 30 m × 0.325 mm). GC/MS analysis was performed using a Hewlett-Packard 5890/5971 GC/MS equipped with a ZB-5 (zebron) column (15 m × 0.25 mm). All products are known compounds and were identified by comparison of their spectral properties to those of authentic samples. Samples for GC were added in equivalent amount of water, extracted with hexanes and filtered through an alumina plug prior to injection. GC conditions: isotherm at 105 °C (2 min); ramp at 30 °C min<sup>-1</sup> to 280 °C; isotherm at 280 °C (5 min). All reactions were carried out under N<sub>2</sub> atmosphere. Unless noted otherwise, chemicals were purchased from commercial firms and were used as received. The nanoclusters were synthesised and characterised according to a previously published procedure.<sup>27</sup> In all cases, the metal core diameter was between 1.6 and 2.5 nm, with a distribution of ±0.1 nm.

### Preparation of tetra-*n*-octylammonium formate (TOAF)

This is a modification of procedure reported by Reetz *et al.*<sup>28</sup> 40 g of ion exchange resin suspended in a 1.5 M NaOH solution were charged to a column that was subsequently flushed with 3 L of 1.5 M NaOH. A slight N<sub>2</sub> overpressure was applied. The elute was tested for Cl<sup>-</sup> using AgNO<sub>3</sub>. The colour of the resin changed from yellow (Cl<sup>-</sup> form) to orange (OH<sup>-</sup> form). The column was then flushed with 3 L of distilled water followed by 500 mL of 0.2 M formic acid solution (without using N<sub>2</sub> overpressure), 3 L distilled water and finally 1 L MeOH to switch to an organic medium. The resin was left to swell for 1 h and the column was subsequently flushed with an 18 mM solution of tetra-*n*-octylammonium bromide (TOAB) in MeOH, until the elute tested positive for Br<sup>-</sup> using AgNO<sub>3</sub>. The MeOH was evaporated on a rotavapor and the crude TOAF (light oil) was dried for 24 h under vacuum.

### Parallel screening of catalysts and substrates

Sets of 16 reactions were performed using a Chemspeed Smartstart 16-reactor block, modified in-house for efficient reflux and shaking/stirring. The reactors were charged with a cluster suspension prepared in DMF (1.25 mL, 10.0 mM, 5.0 mol%), phenylacetylene **2** (0.50 mL, 745 mM, 0.38 mmol), tetra-*n*-butylammonium acetate (TBAA) (1.0 mL, 400 mM, 0.40 mmol) and aryl halide **2** (0.50 mL, 495 mM, 0.25 mmol). Glass beads were added in each reactor and the reactors were placed on an electronic shaker. The reactors were evacuated and refilled with N<sub>2</sub> three times and the mixture was shaken at 110 °C for 24 h under a slight N<sub>2</sub> overpressure. Reaction progress was monitored by GC (pentadecane internal standard).

### Copper-catalysed Sonogashira cross-coupling

**Example (1). 4-Nitrodiphenylethyne.** The Cu cluster suspension and DMF were degassed before use. A Schlenk-type glass vessel equipped with a rubber septum and a magnetic stirrer was evacuated and refilled with N<sub>2</sub>. The vessel was then charged with a

Cu cluster suspension prepared in DMF (12.0 mL, 10.0 mM, 5.0 mol%), phenylacetylene (0.35 g, 3.40 mmol), TBAA (1.02 g, 3.40 mmol) and 12 mL of DMF. 4-Iodonitrobenzene (0.56 g, 2.25 mmol) was added and the mixture was stirred at 110 °C for 6 h under a slight overpressure of N<sub>2</sub>. Reaction progress was monitored by GC and GC/MS. After 6 h the reaction mixture was poured into a separatory funnel, diluted with water (20 mL) and extracted with hexanes (3 × 15 mL). The organic layers were combined and dried over anhydrous MgSO<sub>4</sub> and concentrated under vacuum at 25 °C to yield 0.53 g of yellow product (94% yield based on 4-iodonitrobenzene). The crude material was recrystallised from hot ethanol to give a light yellow solid, mp = 112–114 °C (lit.<sup>31</sup> 114–116 °C). <sup>1</sup>H NMR δ<sub>H</sub> 7.416 (d, 3H, *J* = 8.7 Hz), 7.592 (m, 2H), 7.717 (d, 2H, *J* = 8.7 Hz), 8.22 (d, 2H, *J* = 8.7 Hz). Good agreement was found with literature values.<sup>31</sup>

**Example (2). 4-Acetyldiphenylethyne.** Reaction and work-up were performed as above, but using 4-iodoacetophenone (0.55 g, 2.25 mmol) to give 0.48 g of product (88% yield based on 4-iodoacetophenone). The crude material was recrystallised from hot ethanol to give cream coloured needles, mp = 95–97 °C (lit.<sup>31</sup> 96–98 °C). <sup>1</sup>H NMR δ<sub>H</sub> 7.406 (m, 3H), 7.593 (m, 4H), 7.956 (d, 2H, *J* = 8.6 Hz), 2.604 (s, 3H). Good agreement was found with literature values.<sup>31</sup>

**Example (3). Diphenylethyne.** Reaction and work-up were performed as above, but using 4-iodobenzene (0.45 g, 2.25 mmol) to give 0.37 g of product (82% yield based on 4-iodobenzene). The crude material was recrystallised from hot ethanol to give a white needles, mp = 57–58 °C (lit.<sup>19</sup> 59 °C). <sup>1</sup>H NMR δ<sub>H</sub> 7.34 (m, 6H), 7.52 (m, 4H). Good agreement was found with literature values.<sup>19</sup>

**Example (4). 4-Methyldiphenylethyne.** Reaction and work-up were performed as above, but using 4-iodotoluene (0.49 g, 2.25 mmol) to give 0.41 g of product (84% yield based on 4-iodotoluene). The crude material was recrystallised from hot ethanol to give a cream coloured solid, mp = 72–73 °C (lit.<sup>19</sup> 71 °C). <sup>1</sup>H NMR δ<sub>H</sub> 7.15 (m, 2H), 7.35 (m, 3H), 7.42 (d, 2H, *J* = 8.3 Hz), 7.55 (m, 2H), 2.38 (s, 3H). Good agreement was found with literature values.<sup>19</sup>

### Catalyst reusability

The reaction set-up and the pre-reaction procedure were similar to that used in Sonogashira cross-coupling on a preparative scale. The vessel was then charged with a Cu cluster suspension prepared in DMF (2.5 mL, 10.0 mM, 5.0 mol%), phenylacetylene (0.07 g, 0.75 mmol), TBAA (0.22 g, 0.75 mmol) and 5 mL of DMF. 4-iodobenzotrifluoride (0.13 g, 0.5 mmol) was added and the mixture was stirred at 110 °C for 24 h under a slight overpressure of N<sub>2</sub>. After complete conversion of 4-iodobenzotrifluoride the same amount of fresh reactants were added to the reaction mixture and sample was analysed every 24 h. The procedure was repeated until conversion lower than 100% was observed. Reaction samples were analysed by GC and GC/MS.

## References and notes

- 1 R. E. Martin and F. Diederich, *Angew. Chem., Int. Ed.*, 1999, **38**, 1350.
- 2 P. Siemsen, R. C. Livingston and F. Diederich, *Angew. Chem., Int. Ed.*, 2000, **39**, 2633.
- 3 R. D. Stephens and C. E. Castro, *J. Org. Chem.*, 1963, **28**, 2163.
- 4 K. Sonogashira, in *Metal-catalyzed Cross-coupling Reactions*, ed. F. Diederich and P. J. Stang, Wiley-VCH, Weinheim, 1997, pp. 203.
- 5 K. Sonogashira, Y. Tohda and N. Hagihara, *Tetrahedron Lett.*, 1975, **50**, 4467.
- 6 Y. Mori and M. Seki, *J. Org. Chem.*, 2003, **68**, 1571.
- 7 A. Köllhofer and H. Plenio, *Chem. Eur. J.*, 2003, **9**, 1416.

- 8 M. Erdélyi and A. Gogoll, *J. Org. Chem.*, 2001, **66**, 4165.
- 9 T. Hundertmark, A. F. Littke, S. L. Buchwald and G. C. Fu, *Org. Lett.*, 2000, **2**, 1729.
- 10 A. Köllhofer, T. Pullmann and H. Plenio, *Angew. Chem., Int. Ed.*, 2003, **42**, 1056.
- 11 D. Méry, K. Héuze and D. Astruc, *Chem. Commun.*, 2003, 1934.
- 12 X. Fu, S. Zhang, J. Yin and D. P. Schumacher, *Tetrahedron Lett.*, 2002, **43**, 6673.
- 13 D. A. Alonso, C. Nájera and M. C. Pacheco, *Tetrahedron Lett.*, 2002, **43**, 9365.
- 14 B. M. Choudary, S. Madhi, N. S. Chowdari, M. L. Kantam and B. Sreedhar, *J. Am. Chem. Soc.*, 2002, **124**, 14127.
- 15 N. E. Leadbeater and B. J. Tominack, *Tetrahedron Lett.*, 2003, **44**, 8653.
- 16 V. P. W. Böhm and W. A. Herrmann, *Eur. J. Org. Chem.*, 2000, 3679.
- 17 K. Okuro, M. Furuune, M. Miura and M. Nomura, *Tetrahedron Lett.*, 1992, **33**, 5363.
- 18 K. Okuro, M. Furuune, M. Enna, M. Miura and M. Nomura, *J. Org. Chem.*, 1993, **58**, 4716.
- 19 R. K. Gujadhur, C. G. Bates and D. Venkataraman, *Org. Lett.*, 2001, **3**, 4315.
- 20 S. K. Kang, S. K. Yoon and Y. M. Kim, *Org. Lett.*, 2001, **3**, 2697.
- 21 S. Cacchi, G. Fabrizi and L. M. Parisi, *Org. Lett.*, 2003, **5**, 3843.
- 22 I. P. Beletskaya, G. V. Latyshev, A. V. Tsvetkov and N. V. Lukashev, *Tetrahedron Lett.*, 2003, **44**, 5011.
- 23 A. H. M. de Vries, F. J. Parlevliet, L. Schmieder-van de Vondervoort, J. H. M. Mommers, H. J. W. Henderickx, M. A. M. Walet and J. G. de Vries, *Adv. Synth. Catal.*, 2002, **344**, 996.
- 24 (a) For a recent review on the role of metal nanoclusters in C–C bond formation reactions see M. Moreno-Mañas and R. Pleixats, *Acc. Chem. Res.*, 2003, **36**, 638; For cluster catalysis in Heck and Suzuki reactions see (b) M. T. Reetz and G. Lohmer, *Chem. Commun.*, 1996, 1921; (c) M. T. Reetz, R. Breinbauer and K. Wanninger, *Tetrahedron Lett.*, 1996, **37**, 4499; (d) M. Beller, H. Fischer, K. Kühlein, C. P. Reisinger and W. A. Herrmann, *J. Organomet. Chem.*, 1996, **520**, 257; (e) R. Narayanan and M. A. El-Sayed, *J. Am. Chem. Soc.*, 2003, **125**, 8340.
- 25 J. D. Aiken and R. G. Finke, *J. Mol. Catal. A: Chem.*, 1999, **145**, 1.
- 26 M. B. Thathagar, J. Beckers and G. Rothenberg, *J. Am. Chem. Soc.*, 2002, **124**, 11858.
- 27 M. B. Thathagar, J. Beckers and G. Rothenberg, *Adv. Synth. Catal.*, 2003, **345**, 979.
- 28 M. T. Reetz and M. Maase, *Adv. Mater.*, 1999, **11**, 773.
- 29 A. S. Hay, *J. Org. Chem.*, 1962, **27**, 3320.
- 30 C. Z. Cai and A. Vasella, *Helv. Chim. Acta*, 1995, **78**, 2053.
- 31 A. Elangovan, Y. H. Wang and T. I. Ho, *Org. Lett.*, 2003, **5**, 1841.
- 32 J. Wang, H. F. M. Boelens, M. B. Thathagar and G. Rothenberg, *ChemPhysChem*, 2004, **5**, 93.



# Aqueous *N*-alkylation of amines using alkyl halides: direct generation of tertiary amines under microwave irradiation

Yuhong Ju and Rajender S. Varma\*

Clean Processes Branch, National Risk Management Research Laboratory, U. S. Environmental Protection Agency, MS 443, 26 W. Martin Luther King Dr., Cincinnati, Ohio 45268, USA.

E-mail: Varma.Rajender@epa.gov

Received 3rd February 2004, Accepted 20th February 2004

First published as an Advance Article on the web 17th March 2004

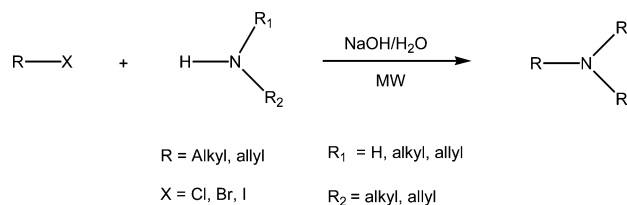
Direct formation of tertiary amines *via N*-alkylation of amines by alkyl halides occurs in aqueous media under microwave irradiation. This greener alternative is also a useful and powerful method to construct C–N bond without using any transition metal catalysts.

## Introduction

C–N bond formation is one of the most important transformations in organic synthesis. Amines are widely used as intermediates to prepare solvents, fine chemicals, agrochemicals, pharmaceuticals and catalysts for polymerization.<sup>1</sup> The nucleophilic attack of alkyl halides by primary and secondary amines is useful for the preparation of tertiary amines but the reaction requires longer reaction time and gives rise to a mixture of secondary and tertiary amines;<sup>2</sup> thermal reaction between alkyl halides and amines in the presence of base requires longer reaction time period and affords lower yields of desired products.<sup>3,4</sup> Although the relatively similar Ullmann and Goldberg reaction using copper catalysts,<sup>5,6</sup> and the Pd catalyzed Buchwald–Hartwig reaction have been studied,<sup>7</sup> transition metal-free microwave-assisted amination of electron-rich benzylic halides has been largely unexplored.<sup>8</sup>

Microwave (MW) irradiation has attracted considerable attention for rapid synthesis of a variety of organic compounds because of the selective absorption of microwave energy by polar molecules.<sup>9</sup> MW irradiation has been successfully utilized in the formation of a variety of carbon–heteroatom and carbon–carbon bonds.<sup>10</sup> During our ongoing efforts to explore organic syntheses using microwave irradiation,<sup>11</sup> we envisioned that the nucleophilic substitution reaction of alkyl halides with amines might be accelerated by microwave energy because of their polar nature. We wish to report herein an environmentally-friendlier synthesis of tertiary amines *via* direct *N*-alkylation of primary and secondary amines by alkyl

halides under microwave irradiation that proceeds in water without any phase transfer reagent<sup>12</sup> (Scheme 1).

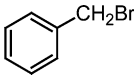

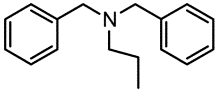
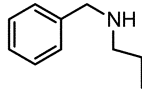
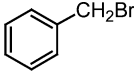

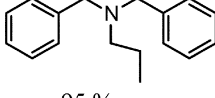
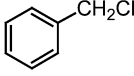
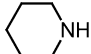
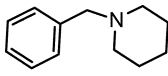
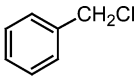
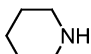
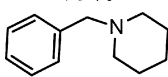


Scheme 1

## Results and discussion

In order to ascertain the comparative effectiveness of microwave heating with respect to conventional heating, a few representative reactions were conducted using conventional heating in an oil bath. Mixtures of alkyl halides and amines, in the presence of one equivalent of aqueous NaOH, were heated in a round-bottom flask for a period of 12 hours. On the other hand, the same reactions proceeded to completion under microwave irradiation condition within 20 minutes (Table 1). Further, it was observed that under conventional heating mixtures of products were formed (entry 1) in

Table 1 *N*-Alkylation of amines by alkyl halides using MW and conventional heating

Entry	Halide	Amine	Reaction conditions	Products and yields <sup>a</sup>
1			Heated at 50 °C, 12 h	 45 %  20 %
2			MW, 45–50 °C, 20 mins	 95 %
3			Heated at 95 °C, 12 h	 70 %
4			MW, 95–100 °C, 20 mins	 92 %

<sup>a</sup> Benzyl alcohol was observed by GC/MS analysis in entry 1 and entry 3.

addition to small amounts of side products such as benzyl alcohol (entries 1 and 3) as a result of hydrolysis of the alkyl halides in alkaline medium.<sup>13</sup>

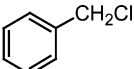
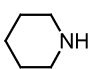
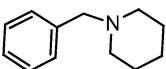
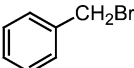
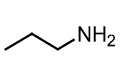
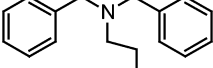
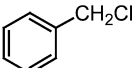
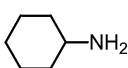
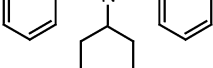
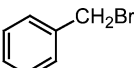
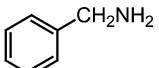
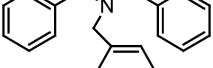
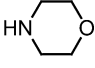
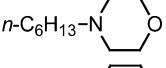
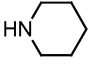
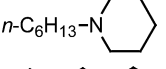
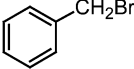
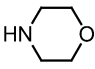
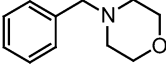
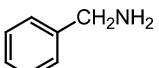
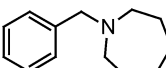
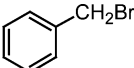
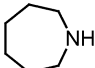
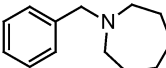
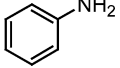
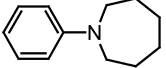
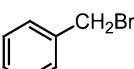
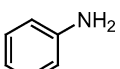
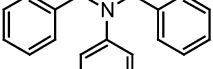
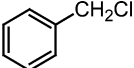
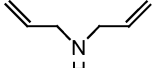
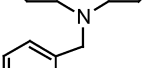
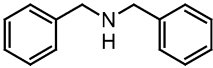
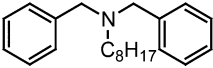
The microwave-assisted reaction was also examined under solventless conditions using water, polyethylene glycol with an average molecular weight of 300 (PEG 300) and acetonitrile as the reaction medium. Reactions under solventless conditions afforded very low yield (less than 20%) because of the insolubility of the base; volatile acetonitrile as reaction medium only gave rise to moderate products yields (50–70%); PEG 300 is a promising medium to replace volatile organic solvents for green chemical synthesis under microwave irradiation<sup>14</sup> but more expensive compared to water. Water is a good absorber for microwave energy<sup>15</sup> and has been successfully employed as solvent for various organic syntheses,<sup>16</sup> it turned out to be one of the best choices in view of its relatively environmentally-friendly characteristics.

The reaction is general in nature and is applicable to aliphatic halides and both aromatic and aliphatic amines as summarized in Table 2. Interestingly, the intramolecular double-alkylation of primary amines occurs in reaction with dihalides such as 1,6-dibromohexane thus providing a potentially useful approach to assemble cyclic amines in a single step (entries 8 and 10, Table 2).

## Conclusion

In summary, a direct *tert*-amine forming protocol has been developed that proceeds rapidly *via* microwave-assisted *N*-alkylation of amines by alkyl halides. Shorter reaction times, higher product yields and aqueous reaction medium are some of the relevant advantages that render this procedure a greener alternative to conventional chemical synthesis.

**Table 2** Aqueous *N*-Alkylation of amines using microwave irradiation<sup>a</sup>

Entry	Halide	Amine	Product amine <sup>b</sup>	Isolated yields (%) <sup>c</sup>
1				92
2				95
3				86
4				87
5	$n\text{-C}_6\text{H}_{13}\text{Br}$		$n\text{-C}_6\text{H}_{13}\text{-N}$ 	70
6	$n\text{-C}_6\text{H}_{13}\text{Br}$		$n\text{-C}_6\text{H}_{13}\text{-N}$ 	74
7				70
8	$\text{Br}(\text{CH}_2)_6\text{Br}$			71
9				90
10	$\text{Br}(\text{CH}_2)_6\text{Br}$			75
11				84
12				60
13	$n\text{-C}_8\text{H}_{17}\text{I}$			73

<sup>a</sup> All reactions were carried out at 1 mmol scale, MW power 250–300 Watt for 20–30 mins. <sup>b</sup> The NMR spectra of all synthesized amines are in accord with the literature. <sup>c</sup> Isolated yields based on starting halides (for entries 2, 3, 4, and 11, a halide : amine ratio of 2 : 1 has been used; 2 equivalents of base were used for entries 2, 3, 4, 8, 10 and 11).

## Experimental

### General

All the starting amines and alkyl halides were obtained from Aldrich Chemical Co. and were used as such. The synthesized products were identified by GC/MS qualitative analysis based on the Wiley library database using an HP 6890 GC system with an HP 5872 Mass selective detector. The identities were further confirmed by  $^1\text{H}$  and  $^{13}\text{C}$  NMR spectra that were recorded for the pure products in chloroform-*d* ( $\text{CDCl}_3$ ) with TMS as internal reference using a Bruker 300 MHz NMR spectrometer.

### Typical procedure

The representative experimental procedure is as follows: 1 mmol benzyl chloride (0.127 g), 1 mmol piperidine (0.085 g) and 1.1 mmol NaOH in water (2.20 mL 0.5 M solution) were placed in a round-bottom glass flask equipped with a condenser and a magnetic stirrer. The flask was placed in a CEM Discover Focused Microwave Synthesis System, and subjected to MW irradiation at 80–100 °C (power 250 Watt) for 25 minutes. After completion of the reaction (monitored by TLC), the product was extracted into ethyl acetate. Removal of the solvent under reduced pressure, followed by flash column chromatography using hexane–ethyl acetate (4/1) as eluent afforded 1-benzylpiperidine (0.161 g, 92%) as product as confirmed by satisfactory  $^1\text{H}$  and  $^{13}\text{C}$  NMR spectra.

### Acknowledgments

We wish to thank Tom Deinlein, Julius Enriquez, Albert Foster and Amy Zhao for their assistance. This research was supported, in part, by the Postgraduate Research Program at the National Risk Management Research Laboratory administered by the Oak Ridge Institution for Science and Education through an interagency

agreement between the U.S. Department of Energy and the U.S. Environmental Protection Agency.

### References

- (a) A. Seayad, M. Ahmed, H. Klein, R. Jackstell, T. Gross and M. Beller, *Science*, 2002, **297**, 1676; (b) F. Y. Rachinskii, T. G. Potapenko, O. D. Shapilov, V. T. Osipyan and A. A. Krupenina, *USSR, Zhurnal Prikladnoi Khimii (Sankt-Peterburg, Russian Federation)*, 1968, **41**, 1072; (c) F. Kiuchi, S. Nishizawa, H. Kawanishi, S. Kinoshita, H. Ohsima, A. Uchitani, N. Sekino, M. Ishida, K. Kondo and Y. Tsuda, *Chem. Pharm. Bull. Jpn.*, 1992, **40**, 3234.
- T. E. Muller and M. Beller, *Chem. Rev.*, 1998, **98**, 675.
- W. J. Hickinbottom, *J. Chem. Soc.*, 1930, 992.
- S. Caspe, *J. Am. Chem. Soc.*, 1932, **54**, 4457.
- F. Ullmann, *Ber. Dtsch. Chem. Ges.*, 1903, **36**, 2382.
- I. Goldberg, *Ber. Dtsch. Chem. Ges.*, 1906, **39**, 1691.
- (a) B. Y. Yang and S. L. Buchwald, *J. Organomet. Chem.*, 1999, **576**, 125; (b) J. F. Hartwig, *Angew. Chem., Int. Ed.*, 1998, **37**, 2406.
- L. Shi, M. Wang, C.-A. Fan, F.-M. Zhang and Y.-Q. Tu, *Org. Lett.*, 2003, **5**, 3515.
- C. Gabriel, S. Gabriel, E. H. Grant, B. S. J. Halstead and D. M. P. Mingos, *Chem. Soc. Rev.*, 1998, **27**, 213.
- M. Larhed, C. Moberg and A. Hallberg, *Acc. Chem. Res.*, 2002, **35**, 717.
- (a) R. S. Varma, *Organic Synthesis using Microwaves and Supported Reagents in Microwaves in Organic Synthesis*, ed. A. Loupy, Wiley-VCH, Weinheim, 2002, pp. 181; (b) R. S. Varma, *Advances in Green Chemistry: Chemical Syntheses Using Microwave Irradiation*, AstraZeneca Research Foundation India, Bangalore, India, 2002 (free copy available from: azrefi@astrazeneca.com). (c) R. S. Varma, *Pure Appl. Chem.*, 2001, **73**, 193; (d) R. S. Varma, *Green Chem.*, 1999, **1**, 43.
- (a) D. Bogdal, J. Pielichowski and K. Jaskot, *Heterocycles*, 1997, **45**, 715; (b) P. de la Cruz, A. de la Hoz, L. M. Font, F. Langa and M. C. Perez-Rodriguez, *Tetrahedron Lett.*, 1998, **39**, 6053.
- J. March, *Advanced Organic Chemistry: Reactions, Mechanisms, and Structure*, John Wiley & Sons, Inc., New York, 1992, pp. 370.
- V. V. Nambodiri and R. S. Varma, *Green Chem.*, 2001, **3**, 146.
- B. L. Hayes, *Microwave Synthesis – Chemistry at the Speed of Light*, CEM Publishing, Mathews, NC, 2002, pp. 29–36.
- (a) C. J. Li and T. H. Chan, *Organic Reaction in Aqueous Media*, John Wiley & Sons, New York, 1997; (b) C. J. Li, *Chem. Rev.*, 1993, **93**, 2023.



# Synthesis of *p*-isopropenylphenol in high-temperature water

Shawn E. Hunter, Claire A. Felczak and Phillip E. Savage\*

Department of Chemical Engineering, University of Michigan, Ann Arbor, MI 48109-2136, USA.

E-mail: psavage@umich.edu; Tel: +1 734 764 3386; Fax: +1 734 763 0459

Received 27th October 2003, Accepted 10th March 2004

First published as an Advance Article on the web 23rd March 2004

The synthesis of *p*-isopropenylphenol (IPP) from bisphenol A (BPA) cleavage typically requires an alkaline catalyst and results in a mixture of IPP oligomers. Using high-temperature (200–350 °C) liquid water (HTW) as the reaction medium, we synthesized IPP from BPA without catalyst and without oligomerization. IPP and phenol are primary products from BPA cleavage, whereas acetone forms from IPP hydrolysis as a secondary product.

## Introduction

*p*-Isopropenylphenols are unstable compounds that polymerize readily, but are useful in the synthesis of unsymmetrically alkylated isopropylidenebisphenols<sup>1</sup> and in the production of plastics, pesticides,<sup>2</sup> and photochemicals.<sup>3</sup> *p*-Isopropenylphenols can be synthesized by the dehydrogenation of the respective alkylphenol,<sup>4</sup> as a by-product of dihydric phenol synthesis,<sup>5</sup> and through catalytic or thermal decomposition of bishydroxyaryllkanes.<sup>6</sup> Bishydroxyaryllkane decomposition provides the least difficult method for synthesis of the parent compound *p*-isopropenylphenol (IPP) (**1**).<sup>7</sup> Classically, IPP synthesis *via* bisphenol A (BPA) (**2**) cleavage is carried out under reduced pressure at temperatures above 150 °C and in the presence of catalytic amounts of base. Both phenol (**3**) and IPP are formed, and the phenol must be removed *via* fractional distillation to yield pure IPP.<sup>6</sup> Due to the tendency for IPP to polymerize spontaneously, even at room temperature,<sup>4</sup> high yields of IPP are difficult to obtain using this method of synthesis. Cooling of IPP gas formed from BPA cleavage typically results in a mixture of *p*-isopropenylphenol oligomers.<sup>8,9</sup> Only low yields of IPP, with respect to the initial amount of BPA, can be obtained through recrystallization of the oligomer mixture.<sup>8</sup> Radical inhibitors do not prevent the formation of oligomers.<sup>8</sup> However, oligomerization can be avoided by using polar solvents such as ethylene glycol to absorb the IPP gas.<sup>8</sup> This technique results in an IPP solution, from which the IPP must be separated.

An alternative means of producing *p*-isopropenylphenol in high yield is by conducting the reaction in a supercritical fluid. Cleavage of BPA occurs in supercritical propane at 227 °C and with a modified magnesium oxide catalyst.<sup>9</sup> Cooling of the supercritical mixture enables precipitation of the reaction products including IPP and phenol, with a yield of less than one percent of dimerized isopropenylphenol.<sup>9</sup> To obtain IPP in high purity, further separation is necessary. While eliminating the problem of oligomer formation, this method maintains the use of a catalyst and requires multiple separation steps. Development of a method for IPP synthesis that avoids oligomerization, requires no catalyst, and enables facile product separation would be both useful from a practical perspective and desirable from a green engineering standpoint.

High-temperature water (HTW) is an interesting and useful reaction medium in which both organic synthesis and chemical decomposition reactions occur.<sup>10</sup> As a liquid above 200 °C, water possesses several properties that differ from those of water at room temperature. For example, the dielectric constant decreases from about 80 at 20 °C to roughly 27 at 250 °C.<sup>11</sup> This decrease in solvent polarity gives rise to increased solubility of small organic compounds.<sup>12,13</sup> Also, the native hydronium and hydroxyl ion concentrations increase by a factor of 25 over the same temperature range.<sup>14</sup> This natural abundance of H<sup>+</sup> and OH<sup>-</sup>, coupled with the

elevated temperature, enables some acid- and base-catalyzed reactions to proceed in the absence of added catalyst.<sup>10,15–18</sup> Above the critical temperature of 374 °C, water offers the unique possibility of shifting the dominant reaction mechanism from thermal to ionic, by simply manipulating the water density.<sup>19,20</sup>

These unique features of HTW suggest that IPP synthesis from BPA might be accomplished using a HTW medium in the absence of catalyst. Similar to reaction in supercritical propane, IPP synthesis in HTW should occur without oligomer formation. Additionally, a HTW-based method could offer easy product separation. The solubility of IPP in water at 25 °C should be on the same order of magnitude as that of *p*-isopropylphenol (**4**), which is only 0.01 M.<sup>21</sup> The solubility of phenol, the other cleavage product, in 25 °C water is almost 1 M.<sup>21</sup> This two order of magnitude difference in solubility implies that the IPP could be separated from the hot aqueous product mixture by simply reducing temperature.

The reactivity and decomposition of organic compounds in HTW has received a great deal of attention. Decomposition reactions in HTW can occur by several pathways, the most common of which are hydrolysis and pyrolysis. Hydrolysis, which usually requires catalytic amounts of acid or base, or addition of hydrolytic enzymes in room temperature water, can occur in HTW without catalyst. Ethers<sup>22</sup> and esters<sup>15</sup> are easily hydrolyzed to the corresponding acids and alcohols. Pyrolysis can occur in conjunction with hydrolysis, and is most significant at low water density and high temperatures in supercritical ( $T > 374$  °C) water (SCW).<sup>19,20,23</sup> HTW decomposition<sup>24</sup> and gasification<sup>25</sup> have been further examined as techniques for converting biomass into more chemically useful compounds. Chemical recycling of thermoplastics,<sup>26</sup> thermosets,<sup>27</sup> and rubber<sup>28</sup> into monomers has also been achieved *via* reaction in HTW. Other decomposition pathways in HTW include dehydration,<sup>29</sup> decarboxylation,<sup>30</sup> and dealkylation.<sup>31</sup>

While decomposition chemistry of organic compounds in HTW has been studied widely, hydrothermal cleavage of bishydroxyaryllkanes has received little attention. Adschiri *et al.*<sup>32</sup> examined BPA cleavage under SCW conditions ( $T = 400$  °C). At this temperature, BPA reacted without catalyst, but 2-(4-hydroxyphenyl)-2-propanol (HPP), rather than IPP, formed as the major cleavage product. In contrast, Tagaya *et al.*<sup>33</sup> concluded that BPA was stable in HTW at 250 °C. These results do not clarify the potential for HTW to be used as an effective medium for IPP synthesis from BPA. Furthermore, preliminary experiments in our laboratory indicated that IPP could be obtained by hydrothermal cleavage of BPA at temperatures below 300 °C. Thus, we conducted an experimental study to probe the extent to which HTW can be used as a medium for deriving IPP from BPA.

In this paper, we present experimental evidence to show that IPP can be obtained from BPA in HTW, and we deduce the reaction pathway. In a related publication,<sup>34</sup> we explore the kinetics and

mechanism of IPP synthesis in HTW, and discuss methylene bridge cleavage under hydrothermal conditions.

## Experimental

### Methods and materials

We conducted reactions in batch reactors assembled from  $\frac{1}{4}$ " stainless steel Swagelok parts. Port connectors were sealed with a cap on each end, giving a reactor volume of about 0.6 mL. Prior to use in any experiments, reactors were rinsed with acetone, dried, loaded with 380  $\mu$ L of water, and conditioned at 300 °C for 30 minutes. BPA, phenol, and *p*-isopropylphenol were purchased from Sigma-Aldrich and used as received. HPLC grade methanol and acetone (5) were obtained from Fisher Scientific and also used as received. For typical experiments, 14 mg of BPA was loaded into each reactor. Deionized water used for reaction was sparged with helium for 25 minutes to remove dissolved gases. The amount of water loaded was such that the expanded aqueous phase occupied 95% of the reactor volume at reaction conditions, based on the saturation densities<sup>11</sup> of pure water at reaction temperature.

Sealed reactors containing BPA and water were placed in a Techne SBL-2 fluidized sand bath preheated to the reaction temperature. Temperature control to within 1 °C was achieved by a Techne TC-8D temperature controller. The time required for these reactors to reach reaction temperature was roughly 2 minutes. After reaction was completed, the reactors were removed from the sand bath and submerged in a water bath at ambient temperature. The reactors were then placed in a refrigerator for at least 30 minutes prior to opening to maximize recovery of volatile products. The reactor contents were transferred to a flask containing about 2 mL of methanol, and the reactors were subsequently rinsed with methanol until the total volume collected was 10 mL.

All products, except for IPP, were identified by fragmentation patterns from an Agilent 5970 Mass Spectrometric (MS) detector and by matching retention times with known standards. Product separation was achieved using an Agilent 6890 gas chromatograph (GC) equipped with a 50 m  $\times$  0.2 mm  $\times$  0.33  $\mu$ m HP-5 capillary column. The temperature program consisted of a 9 minute soak at 70 °C followed by a 70 °C min<sup>-1</sup> ramp up to 240 °C, which was held for 28 min. Samples from the flasks were quantitatively analyzed using an Agilent 6890 GC with flame ionization detection (FID) and autoinjection. Quantitative analysis was performed using calibration curves for each product. The FID response was linear for each component over the concentration ranges used. Because IPP was not available commercially, we used the calibration curve of *p*-isopropylphenol to quantify IPP.

Product molar yields were calculated as the number of moles of product recovered divided by the initial number of moles of BPA loaded into the reactor. Uncertainties reported herein are 95% confidence intervals, obtained from replicate experiments. Each data point represents the average result from at least three independent experiments.

### Identification of *p*-isopropenylphenol

IPP was identified using MS fragmentation patterns, infrared (IR) spectroscopy, and GC retention times. The mass spectrum for the product determined to be IPP gave strong signals at  $m/z = 134$ , 119, and 91. A mass spectrum of IPP was not available in our spectrum database, but the peak at  $m/z = 134$  is consistent with the molecular ion for IPP. To verify the identity of this product, we obtained its IR spectrum. IR spectroscopy is useful for identifying the presence of functional groups. For example, conjugation of a double bond with an aromatic ring, a feature that is present in IPP, yields an enhanced absorption near 1625 cm<sup>-1</sup>.<sup>35</sup> Hence, IR absorption near 1625 cm<sup>-1</sup> serves as a consistency test for the presence of IPP. We generated IPP by conducting the reaction at 300 °C and 30 min. The reaction product mixture (aqueous slurry) was filtered to remove the water, and the resulting filter cake was collected. Neither phenol

nor BPA were present in the resulting solid. GC-MS analysis showed the solid consisted of a single compound. Using a Perkin-Elmer Spectrum BX FT-IR spectrometer, we obtained an IR spectrum for the solid product. The spectrum revealed an enhanced absorption at 1624 cm<sup>-1</sup>. This analysis suggests that the solid material formed in the BPA cleavage experiments is IPP.

Further evidence for the assignment of this product identity is given by the product retention times from the GC using the HP-5 column. The retention time of *p*-isopropylphenol, a compound chemically very similar to IPP, was 17.2 minutes. The retention time of the product determined to be IPP was 17.7 min. This spacing is expected for an alkane/olefin pair. Based on the MS, retention time, and IR evidence, we conclude that IPP formed from BPA cleavage in our experiments.

## Results and discussion

### *p*-Isopropenylphenol synthesis

Fig. 1–4 show the temporal variation of product molar yields obtained for IPP synthesis in HTW at 200, 250, 300, and 350 °C,

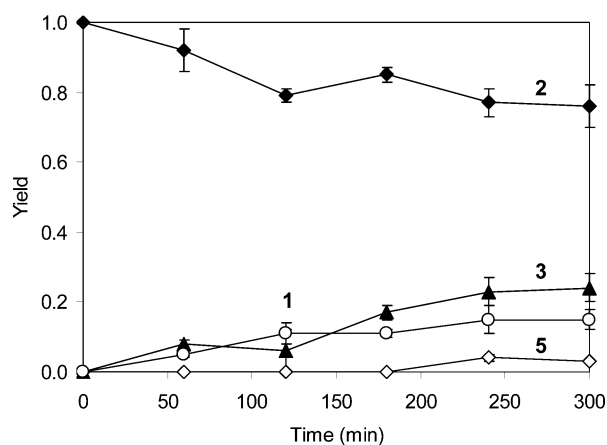
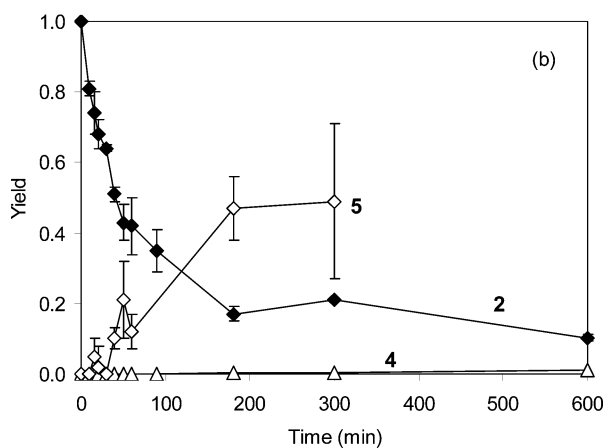
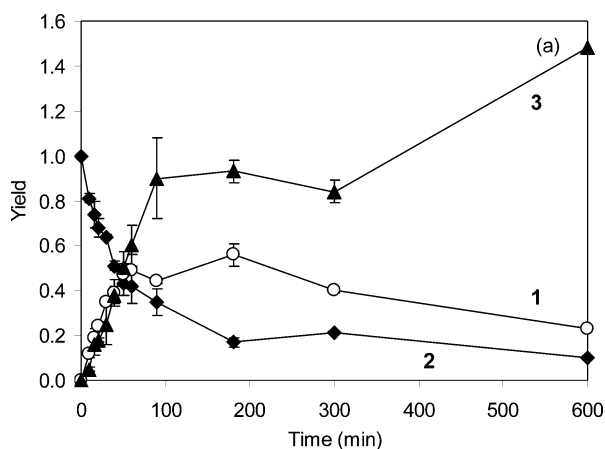


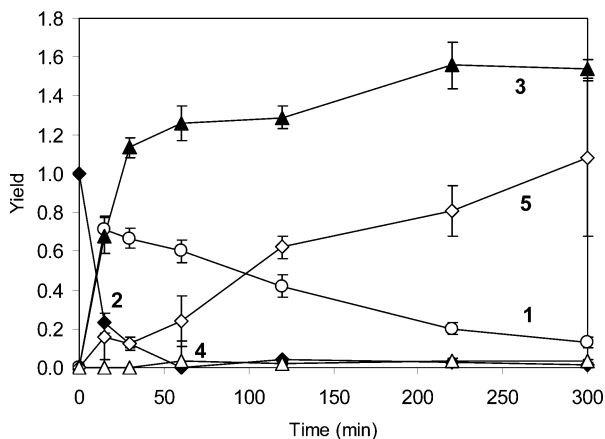
Fig. 1 Molar yields of IPP (1), BPA (2), phenol (3), and acetone (5) at 200 °C.

respectively. Mass balances, calculated based on product molar yields, were typically near 100%, and the average mass balance for all experiments was 96%. The figures show that BPA reacted readily in HTW without added catalyst at temperatures as low as 200 °C. The main products were phenol, IPP, and acetone. In some experiments, there were small amounts of *p*-isopropylphenol produced. In contrast, HPP did not appear in any of our experiments. Further, we observed no solid residue in the reactors, and found no mass spectral evidence to suggest that oligomerization of IPP had occurred. At short times and low temperatures, the disappearance of BPA was accompanied by the appearance of phenol and IPP in roughly equimolar yields, as shown in Fig. 1 and 2. As the reaction proceeded further, acetone appeared, and the ratio of the phenol yield to the IPP yield increases past unity. At 250 °C, the acetone yield at 600 min was not reliable, and is omitted from Fig. 2. At higher temperatures and longer times, the yield of IPP displayed a maximum, which implies that it is reactive in HTW. Fig. 3 and 4 demonstrate that *p*-isopropylphenol is slowly formed at higher temperatures, even after BPA has completely disappeared. Fig. 4 shows that BPA was completely converted after 30 minutes at 350 °C, but the yields of phenol and acetone continued to increase. This increase in phenol and acetone coincides with a decrease in IPP yield, and suggests a relationship between these compounds.

To examine the reversibility of the decomposition pathway, we attempted the synthesis of BPA in HTW from acetone and phenol. Commercial production of BPA occurs through the acid-catalyzed condensation of acetone and phenol.<sup>7</sup> This fact suggests that high-temperature water may be a suitable medium for performing the synthesis. BPA synthesis from phenol and acetone does not occur



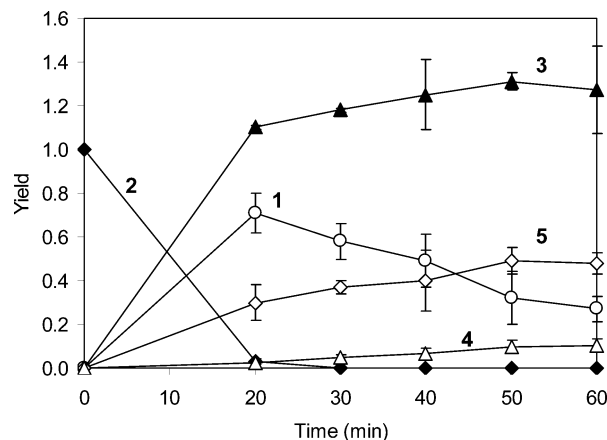
**Fig. 2** Molar yields at 250 °C. (a) IPP (1), BPA (2), and phenol (3). (b) BPA (2), *p*-isopropylphenol (4), and acetone (5).



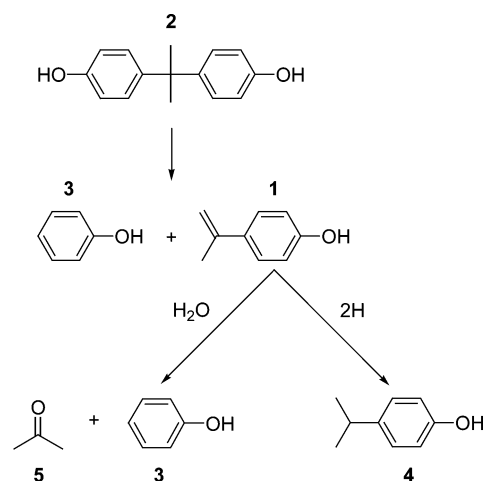
**Fig. 3** Molar yields of IPP (1), BPA (2), phenol (3), *p*-isopropylphenol (4), and acetone (5) at 300 °C.

in SCW at 400 °C,<sup>36</sup> but experiments at lower temperatures have not been reported. We conducted experiments without catalyst at 250 °C, 350 °C, and 380 °C, for 60 minutes, and for 24 hours at 350 °C. The water density at the supercritical temperature was 0.5 g mL<sup>-1</sup>. Sulfuric acid at initial concentration 1 mM was added to a 60-minute experiment at 350 °C, and 5 mM sulfuric acid was added to a 24-hour experiment at 350 °C. In all condensation experiments, the initial molar ratio of phenol to acetone was 3. None of these experiments yielded measurable amounts of BPA, and acetone and phenol were the only post-reaction species present. Thus, the synthesis of BPA from acetone and phenol does not occur to a measurable extent in neutral or acidic HTW.

Taken collectively, the present results suggest that the reaction pathways in Scheme 1 are significant for BPA decomposition in



**Fig. 4** Molar yields of IPP (1), BPA (2), phenol (3), *p*-isopropylphenol (4), and acetone (5) at 350 °C.



**Scheme 1** Reaction pathway for BPA decomposition in HTW.

HTW. BPA first decomposes to yield one mole each of phenol and IPP. IPP then reacts further with water to yield phenol and acetone. *p*-Isopropylphenol forms in low quantities from hydrogenation of IPP, perhaps through IPP disproportionation.<sup>6</sup>

The network rank  $N$  of the products, which is defined<sup>37</sup> as the minimum number of slow steps between a reactant and product, can be identified from Scheme 1. Based on this network, IPP and phenol are primary products having  $N = 1$ , whereas acetone and *p*-isopropylphenol are exclusively secondary products with  $N = 2$ .

Having proposed a network for BPA decomposition in HTW, we used the delplot methodology<sup>37,38</sup> to verify the network rank of the major products. This method uses plots of  $Y_i/X^r$  vs.  $X$ , where  $Y_i$  is the molar yield of product  $i$ ,  $X$  is the conversion of the reactant, and  $r$  is a positive integer. The delplot rank  $D$ , for a given product, is the value of  $r$  for which the delplot exhibits a finite intercept as  $X$  approaches zero. For reactions of integral order  $\geq 1$ , delplot intercepts will be 0 for  $r < D$ , finite for  $r = D$ , and will diverge for  $r > D$ . For  $r = 1$ , any reaction product having a finite intercept is a primary product, regardless of reaction order, and hence  $N = D$ . For  $r > 1$ , the network rank of products having finite intercept can be less than the delplot rank if any of the steps leading to the product are of order greater than one.

Fig. 5 and 6 show first and second rank delplots. We omitted the low-conversion data for acetone because this volatile product was difficult to recover completely and quantify when present in low yield. Both phenol and IPP show non-zero intercepts on the first-rank delplot (Fig. 5(a) and 5(b)). Furthermore, Fig. 6(a) and 6(b) show that the data on the second-rank delplot for these two products diverge as the conversion approaches zero. These behaviors verify that both phenol and IPP are primary products, as shown in Scheme 1. Fig. 5(a) shows the first-rank delplot for acetone. As the

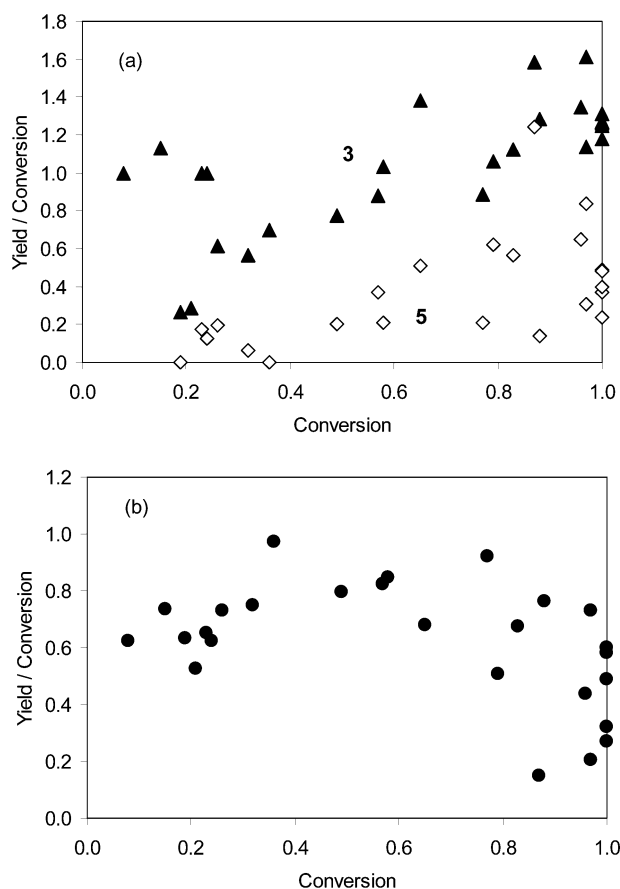


Fig. 5 First-rank delplots. (a) Phenol (3) and acetone (5). (b) IPP.

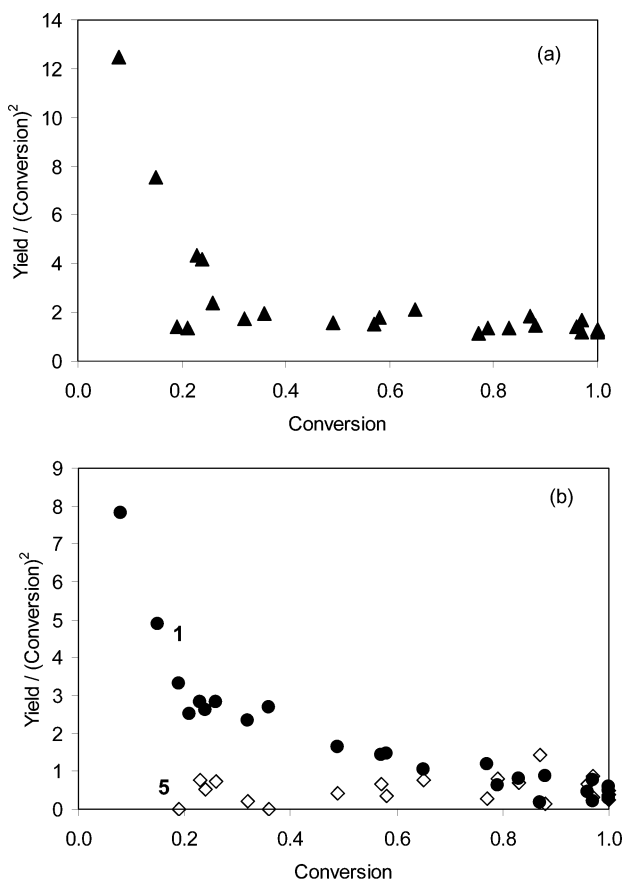


Fig. 6 Second-rank delplots. (a) Phenol. (b) IPP (1) and acetone (5).

conversion approaches zero, the y-intercept decreases and quite likely goes to zero. This zero intercept indicates that acetone is not a primary product, and that it appears later in the reaction network. The second-rank delplot for acetone shown in Fig. 6(b) implies a non-zero intercept as  $X$  approaches zero, and hence the delplot rank for acetone is two. The delplot rank for acetone, being two, requires its network rank to be two or lower. Thus, because acetone is not a primary product, it must have network rank equal to two. Scheme 1 shows acetone as a secondary product, which agrees with the delplot result.

Fig. 5(b) shows the selectivity of *p*-isopropenylphenol as a function of BPA conversion. At conversions less than 0.8, the selectivity of IPP is about 80% in most cases. The highest IPP selectivity was  $97 \pm 4\%$ , which was obtained at  $250^\circ\text{C}$  and 30 minutes, with  $36 \pm 1\%$  conversion of BPA. These results show that IPP can be obtained from BPA in high selectivity, without oligomerization, and without catalyst, using HTW as the reaction medium.

### Comparison with the literature

**BPA cleavage at  $250^\circ\text{C}$ .** Tagaya *et al.*<sup>33</sup> reported the conversion of BPA in HTW after 60 minutes of reaction at  $250^\circ\text{C}$  to be only 3%. In contrast, we found BPA to be quite reactive at  $250^\circ\text{C}$ , with a conversion of  $58 \pm 8\%$  at the same time. The apparent stability of BPA observed by Tagaya *et al.* can be explained when considering the heat-up time of their 10 mL-batch reactors. They did not measure the time required for these reactors to reach the reaction temperature once exposed to the heating source. Rather, they cited Townsend *et al.*,<sup>20</sup> whose measured reactor heat-up time was about two minutes. The 10 mL reactors used by Tagaya *et al.* are quite massive in comparison to the 0.6 mL reactors used by Townsend *et al.* Thus, it is likely that the temperature of the reactors used by Tagaya *et al.* was less than  $250^\circ\text{C}$  for a significant portion of the nominal reaction time. This lower temperature led to lower reaction rates for BPA, and hence a lower observed reactivity.

**Subcritical versus supercritical experiments.** The pathway presented in Scheme 1 for BPA conversion in hot ( $200\text{--}350^\circ\text{C}$ ) liquid water differs from that proposed by Adschiri *et al.*<sup>32</sup> for BPA conversion in supercritical water ( $T = 400^\circ\text{C}$ ). They observed HPP and phenol as the major products, with only small amounts of IPP forming. In contrast, we find that IPP and phenol are the sole primary products, and that HPP did not form at subcritical temperatures. This apparent disagreement can be resolved by considering the probable mechanism of BPA decomposition in supercritical water. Experiments conducted in argon<sup>32</sup> revealed that HPP, IPP, and phenol formed at  $400^\circ\text{C}$  even in the absence of water. The formation of significant amounts of HPP and IPP in argon suggests that BPA cleavage in SCW can occur through a thermal process, rather than solely *via* an ionic mechanism. However, at the lower temperatures used in the present work, BPA is thermally stable, and reacts in water through a primarily base-catalyzed reaction.<sup>34</sup> Hence, there is a shift in mechanism for BPA. In hot, liquid water, the cleavage is primarily base-catalyzed. At higher temperatures in supercritical water, a thermal pathway becomes available and contributes to the product distribution.

Another interesting difference between the two pathways is the reported stability of IPP. Adschiri *et al.*<sup>32</sup> concluded that IPP was stable in SCW at  $400^\circ\text{C}$  under the conditions employed in their study. In contrast, our analysis indicated that IPP hydrolysis occurred at temperatures as low as  $200^\circ\text{C}$ . One explanation for this variation in reported reactivity is that the reaction times at  $400^\circ\text{C}$  were not long enough to observe reaction of IPP. Another possibility is that IPP was misidentified as the corresponding alkylphenol, *p*-isopropylphenol. *p*-Isopropylphenol is stable<sup>17</sup> under the conditions employed by Adschiri *et al.*, and thermal decomposition<sup>6</sup> of BPA results in the formation of *p*-isopropylphenol, rather than IPP. An additional explanation is simply



that IPP is, in fact, stable in SCW and reactive in hot liquid water. The water density in the supercritical experiments did not exceed  $0.5 \text{ g mL}^{-1}$ . In the present subcritical experiments, where IPP was reactive, the water density was higher (up to  $0.86 \text{ g mL}^{-1}$ ). The mechanism of IPP decomposition in HTW is not known, and competing effects associated with increased temperature and decreased water density may lead to IPP stability in SCW.

## Conclusions

In high-temperature liquid water at 200–350 °C, IPP is synthesized without oligomerization *via* bisphenol A cleavage in the absence of catalyst. Phenol is formed as a co-product. The IPP can react further with water to yield phenol and acetone. This work demonstrates a more environmentally benign method for IPP synthesis from BPA that uses water as the reaction medium, avoids oligomerization, and does not require a catalyst. Additionally, separation of IPP from the product mixture can be easily achieved by cooling the product mixture to room temperature, and recovering the solid IPP that precipitates.

## Acknowledgement

This work was supported through a graduate fellowship to S. E. H. provided by the NSF. Additional support was provided by NSF (CTS-0218772) and the ACS-PRF (37603-AC9). Finally, we thank G. B. Less for assistance with the FT-IR spectrometer.

## References

- 1 J. Kahovec, H. Pivcová and J. Pospíšil, *Collect. Czech. Chem. Commun.*, 1961, **36**, 1986.
- 2 H. Krimm and H. Schnell, Br. Patent 905 994, 1962.
- 3 H. W. Voges, in *Ullmann's Encyclopedia of Industrial Chemistry*, vol. 25, 6<sup>th</sup> edn., Wiley-VCH, Weinheim, 2003, p. 636.
- 4 B. B. Corson, W. J. Heintzelman, L. H. Schwartzman, H. E. Tiefenthal, R. J. Lokken, J. E. Nickels, G. R. Atwood and F. J. Pavlik, *J. Org. Chem.*, 1958, **23**, 544.
- 5 D. I. H. Jacobs, US Patent 2 736 753, 1956.
- 6 H. Schnell and H. Krimm, *Angew. Chem., Int. Ed.*, 1963, **2**, 373.
- 7 H. J. Buysch, in *Ullmann's Encyclopedia of Industrial Chemistry*, vol. 25, 6<sup>th</sup> edn., Wiley-VCH, Weinheim, 2003, pp. 644–646.
- 8 K. Mimaki, T. Takase, M. Iwasa and T. Yamamori, US Patent 4 054 611, 1977.
- 9 K. Inoue, US Patent 4 594 459, 1986.
- 10 P. E. Savage, *Chem. Rev.*, 1999, **99**, 603.
- 11 *NIST Standard Reference Database 10*, version 2.2, National Institute of Standards and Technology, Boulder, CO, 1996.
- 12 J. F. Connolly, *J. Chem. Eng. Data*, 1966, **11**, 13.
- 13 K. Chandler, B. Eason, C. L. Liotta and C. A. Eckert, *Ind. Eng. Chem. Res.*, 1998, **37**, 3515.
- 14 W. L. Marshall and E. U. Franck, *J. Phys. Chem. Ref. Data*, 1981, **10**, 295.
- 15 P. Krammer and H. Vogel, *J. Supercrit. Fluids*, 2000, **16**, 189.
- 16 J. D. Taylor, F. A. Pacheco, J. I. Steinfeld and J. W. Tester, *Ind. Eng. Chem. Res.*, 2002, **41**, 1.
- 17 T. Sato, G. Sekiguchi, T. Adschiri and K. Arai, *Ind. Eng. Chem. Res.*, 2002, **41**, 3064.
- 18 S. A. Nolen, C. L. Liotta, C. A. Eckert and R. Gläser, *Green Chem.*, 2003, **5**, 663.
- 19 W. Bühler, E. Dinjus, H. J. Ederer, A. Kruse and C. J. Mas, *J. Supercrit. Fluids*, 2002, **22**, 37.
- 20 S. H. Townsend, M. A. Abraham, G. L. Huppert and M. T. Klein, *Ind. Eng. Chem. Res.*, 1988, **27**, 143.
- 21 S. H. Yalkowsky and Y. He, *Handbook of Aqueous Solubility Data*, CRC Press, Boca Raton, FL, 2003.
- 22 J. M. L. Penninger, R. J. A. Kersten and H. C. L. Baur, *J. Supercrit. Fluids*, 1999, **16**, 119.
- 23 C. J. Martino and P. E. Savage, *Ind. Eng. Chem. Res.*, 1997, **36**, 1385.
- 24 H. Ando, T. Sakaki, T. Kokusho, M. Shibata, Y. Uemura and Y. Hatate, *Ind. Eng. Chem. Res.*, 2000, **39**, 3688.
- 25 M. J. Antal Jr., S. G. Allen, D. Schulman and X. Xu, *Ind. Eng. Chem. Res.*, 2000, **39**, 4040.
- 26 S. G. Kazarian and G. G. Martirosyan, *Phys. Chem. Chem. Phys.*, 2002, **4**, 3759.
- 27 Y. Suzuki, H. Tagaya, T. Asou, J. Kadodawa and K. Chiba, *Ind. Eng. Chem. Res.*, 1999, **38**, 1391.
- 28 Y. Park, J. N. Hool, C. W. Curtis and C. B. Roberts, *Ind. Eng. Chem. Res.*, 2001, **40**, 756.
- 29 X. Xu, C. P. DeAlmeida and M. J. Antal Jr., *Ind. Eng. Chem. Res.*, 1991, **30**, 1478.
- 30 J. B. Dunn, M. L. Burns, S. E. Hunter and P. E. Savage, *J. Supercrit. Fluids*, 2003, **27**, 263.
- 31 T. Sato, G. Sekiguchi, M. Saisu, M. Wantanabe, T. Adschiri and K. Arai, *Ind. Eng. Chem. Res.*, 2002, **41**, 3124.
- 32 T. Adschiri, R. Shibata and K. Arai, *Sekiyu Gakkaishi*, 1997, **40**, 291.
- 33 H. Tagaya, K. Katoh, J. Kadokawa and K. Chiba, *Polym. Degrad. Stab.*, 1999, **64**, 289.
- 34 S. E. Hunter and P. E. Savage, *J. Org. Chem.*, (submitted).
- 35 R. M. Silverstein, G. C. Bassler and T. C. Morrill, in *Spectrometric Identification of Organic Compounds*, 5<sup>th</sup> edn., John Wiley & Sons, New York, 1991, p. 106.
- 36 T. Sato, G. Sekiguchi, T. Adschiri and K. Arai, *J. Chem. Eng. Jpn.*, 2003, **36**, 339.
- 37 N. A. Bhole, M. T. Klein and K. B. Bischoff, *Chem. Eng. Sci.*, 1990, **45**, 2109.
- 38 N. A. Bhole, M. T. Klein and K. B. Bischoff, *Ind. Eng. Chem. Res.*, 1990, **29**, 313.



# Kinetics of crossed aldol condensations in high-temperature water

Craig M. Comisar and Phillip E. Savage\*

Department of Chemical Engineering, University of Michigan, Ann Arbor, Michigan.  
E-mail: psavage@umich.edu

Received 13th November 2003, Accepted 1st March 2004

First published as an Advance Article on the web 22nd March 2004

We examined two crossed aldol condensations in pure liquid water at temperatures of 250, 300, and 350 °C. We synthesized benzalacetone from benzaldehyde and acetone, and chalcone from benzaldehyde and acetophenone. We provide evidence that these reactions are acid and base catalyzed in high-temperature water. Benzalacetone was always the major reaction product in its experiments and chalcone was almost always the major product in its synthesis experiments. At 350 °C and long reaction times (5 and 8 hours) the chalcone yields were surpassed by those of 3-phenylpropiophenone. The maximum molar yield from the benzalacetone synthesis was 24% at 250 °C and 5 hours, and the maximum yield of chalcone was 21% at 250 °C and 15 hours. At higher temperatures, the yield of the unsaturated ketone products was lower due to formation of degradation products such as benzoic acid, benzyl alcohol, benzylacetone, acetophenone, *E*-stilbene, propiophenone and diphenylethane. A reaction network with reversible formation of the unsaturated ketone, its degradation, and a path for benzaldehyde disproportion provided the basis for a quantitative reaction model. These results provide another illustration of the ability of HTW to facilitate acid- and base-catalyzed reactions without any added acid or base.

## Introduction

High-temperature water (HTW), defined here as liquid water above 200 °C, is a useful medium for chemical reactions. Relative to water at room temperature, HTW has a low dielectric constant, increased solubility for small organic compounds, and an increased ion product. All of these properties are temperature dependent and can be manipulated to optimize the reaction environment. In addition, the low solubility of most organic compounds in water at room temperature facilitates post-reaction separation of reaction products from the aqueous phase. The use of pure HTW also eliminates the waste salt generated in standard acid/base-catalyzed reactions, as the acidity or basicity of HTW is reduced by lowering the temperature rather than adding a neutralizing agent.

Acetone and benzaldehyde react *via* a crossed aldol condensation to produce benzalacetone, an industrial photoinitiator. Benzalacetone is also a key ingredient in warfarin, an anticoagulant and an additive in rat poison. Commercial production of benzalacetone proceeds through a standard carbonyl condensation with benzaldehyde and acetone.<sup>1</sup> This process requires an acid or base to catalyze the reaction, and the post-reaction addition of base or acid to neutralize the solution. A production method that eliminates the need for the base and acid would make this reaction more environmentally benign.

HTW, which has elevated levels of both hydronium and hydroxide ions, is an interesting medium for this reaction. Although HTW and supercritical water ( $T > 374$  °C,  $P > 218$  atm) have been investigated for numerous acid-catalyzed reactions, much less research has been dedicated to exploring base-catalyzed reaction systems. Because the crossed aldol condensation of benzaldehyde and acetone can be either acid or base catalyzed, it is an ideal system to study in HTW.

Zhu *et al.* previously studied benzalacetone synthesis in HTW.<sup>2</sup> They observed a 46.2% yield after 6 hours of reaction at 260 °C. This article is written in Chinese and could not be acquired, so we know little about their reaction system. Nolen *et al.*<sup>3</sup> recently reported results from benzalacetone synthesis in HTW at 250 °C. The work described herein explores the parameter space (effect of temperature and pH) in greater depth than done previously and provides the reaction kinetics of the benzalacetone system. We know of no previous accounts of chalcone synthesis in the archival chemical literature.

## Results and discussion

Table 1, which contains representative experimental results, shows the molar yields of acetone, benzaldehyde, benzalacetone, benzylacetone, and acetophenone obtained at different temperatures and batch holding times for benzalacetone synthesis. The uncertainties shown here and throughout the article are experimentally determined standard deviations. Benzalacetone is the most abundant reaction product at all conditions. Benzylacetone and acetophenone are minor products at high temperatures and long reaction times. Other products formed at 350 °C, but in even lower yields. These products, the yields of which were not quantified, include benzoic acid, benzyl alcohol, *E*-stilbene, diphenylethane, and dibenzalacetone.

Table 1 also displays the ring balance for each experimental condition. This quantity is the fraction of the total number of moles of aromatic rings initially added to the reactor that appear in the quantified products. The ring balance generally decreased as reaction severity increased. Several factors may have contributed to this trend. There was a notable release of gas and loss of some liquid upon opening reactors that had been at 350 °C. The reactors were not designed to collect gas samples so the mass associated with the gas phase could not be measured. In addition, not all of the minor products could be identified with our analytical instruments. Some mass loss was certainly due to the formation of products that could not be measured. Finally, at 350 °C, there was a brown/black char on the side of the reactors that did not dissolve in methanol. These factors combine to suggest that char, gas, and minor product formation most likely account for ring balances less than 100%.

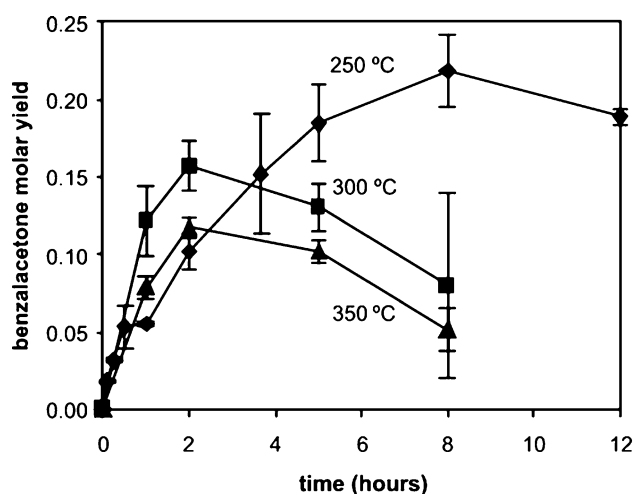
Fig. 1 shows the temporal variation of the yield of benzalacetone at 250, 300, and 350 °C with no acid or base added. The product yield increases steadily at 250 °C and reaches what appears to be an equilibrium value of about 20%. At 250 °C, benzalacetone is the only reaction product detected.

At 300 °C, the yield of benzalacetone at short times exceeded that at 250 °C, which indicates a faster formation rate at the higher temperature. There is also a clear maximum in Fig. 1, which indicates that benzalacetone reacts to form other products. At 350 °C, the yield follows a trend similar to that seen in the 300 °C experiments, but decomposition products form more readily at 350 °C. The two main degradation products are benzylacetone and acetophenone. Benzylacetone is identical in structure to benzalace-

**Table 1** Molar yields of reactants and products from benzalacetone synthesis in HTW

Temperature/°C	t/h	Molar yields					Ring balance
		Acetone	Benzaldehyde	Benzalacetone	Benzylacetone	Acetophenone	
250	0.08	1.00 ± 0.02	0.91 ± 0.03	0.02 ± 0.01	n.d. <sup>a</sup>	n.d. <sup>a</sup>	0.93 ± 0.04
	0.25	0.99 ± 0.02	0.88 ± 0.01	0.03 ± 0.01	n.d. <sup>a</sup>	n.d. <sup>a</sup>	0.91 ± 0.02
	0.50	0.92 ± 0.02	0.86 ± 0.02	0.05 ± 0.01	n.d. <sup>a</sup>	n.d. <sup>a</sup>	0.91 ± 0.03
	1.00	0.86 ± 0.06	0.92 ± 0.08	0.06 ± 0.01	n.d. <sup>a</sup>	n.d. <sup>a</sup>	0.98 ± 0.10
	2.00	0.76 ± 0.07	0.75 ± 0.06	0.10 ± 0.01	n.d. <sup>a</sup>	n.d. <sup>a</sup>	0.85 ± 0.09
	3.66	0.69 ± 0.05	0.65 ± 0.07	0.15 ± 0.04	n.d. <sup>a</sup>	n.d. <sup>a</sup>	0.80 ± 0.09
	5.00	0.70 ± 0.06	0.68 ± 0.11	0.18 ± 0.03	n.d. <sup>a</sup>	n.d. <sup>a</sup>	0.86 ± 0.13
	8.00	0.58 ± 0.04	0.50 ± 0.08	0.22 ± 0.02	n.d. <sup>a</sup>	n.d. <sup>a</sup>	0.72 ± 0.09
300	1.00	0.92 ± 0.10	0.93 ± 0.06	0.12 ± 0.02	trace	trace	1.05 ± 0.12
	2.00	0.79 ± 0.05	0.75 ± 0.04	0.16 ± 0.02	trace	trace	0.91 ± 0.07
	5.00	0.65 ± 0.07	0.60 ± 0.09	0.13 ± 0.02	0.021 ± 0.005	trace	0.75 ± 0.12
	8.00	0.80 ± 0.20	0.41 ± 0.25	0.08 ± 0.06	0.036 ± 0.002	0.016 ± 0.002	0.54 ± 0.33
350	1.00	0.73 ± 0.04	0.67 ± 0.04	0.08 ± 0.01	trace	trace	0.75 ± 0.06
	2.00	0.69 ± 0.10	0.69 ± 0.05	0.12 ± 0.01	0.020 ± 0.001	trace	0.83 ± 0.11
	5.00	0.60 ± 0.04	0.53 ± 0.03	0.10 ± 0.01	0.020 ± 0.001	0.025 ± 0.001	0.68 ± 0.05
	8.00	0.27 ± 0.15	0.29 ± 0.06	0.05 ± 0.01	0.031 ± 0.006	0.043 ± 0.012	0.41 ± 0.16

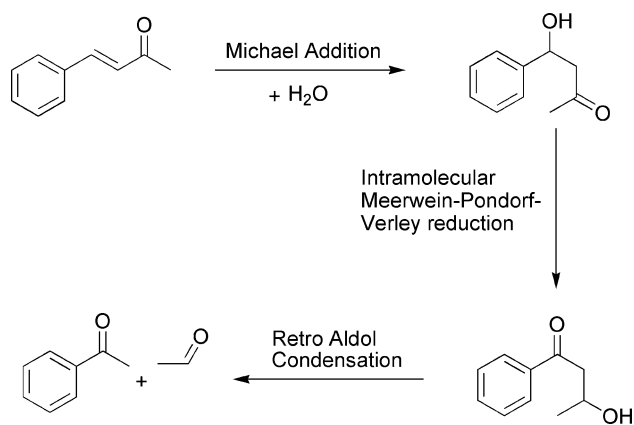
<sup>a</sup> n.d. - not detected.



**Fig. 1** Temporal variation of benzalacetone yields at different temperatures.

tone except that the double bond between the aliphatic carbons has been hydrogenated. Water is a likely source of the hydrogen.

The formation of acetophenone might be caused by a series of



**Fig. 2** Potential reaction pathway to form acetophenone.

reactions, as outlined in Fig. 2. A Michael addition of water to benzalacetone followed by an intramolecular Meerwein-Ponndorf-Verley reduction would form an aldol product. This intermediate undergoes a reverse aldol condensation to form acetophenone and

acetaldehyde. Like acetone, acetophenone has an acidic hydrogen alpha to the carbonyl group, which can participate in condensation reactions. Thus acetophenone can also undergo a crossed aldol condensation with benzaldehyde in HTW. The product of this reaction is chalcone. Hydrogenation of chalcone forms 3-phenylpropiofenone, a reaction product observed in small amounts at 350 °C in the benzalacetone experiments.

The presence of 3-phenylpropiofenone prompted us to investigate the possibility of synthesizing chalcone in HTW using acetophenone as a reactant. Table 2 shows the molar yields of acetophenone, benzaldehyde, chalcone, and 3-phenylpropiofenone from the chalcone experiments. Fig. 3 displays the temporal variation of the yield of chalcone. The chalcone yield increases with time at 250 °C and reaches what appears to be an equilibrium value of about 21%. At 300 °C, the chalcone yield increases more quickly than at 250 °C but then reaches a maximum of 14% at 5 hours. At 350 °C formation of decomposition products limits the chalcone yield at all times. There is a steady decrease in the chalcone yield with time and a steady increase in the yield of 3-phenylpropiofenone.

We also performed background experiments in HTW starting with benzaldehyde, acetophenone, and acetone individually. At 250 °C none of these three compounds reacted after 8 hours. At 350 °C, we observed no reaction for acetone or acetophenone after 8 hours, but benzaldehyde did react. Benzyl alcohol and benzoic acid were the main products, each occurring at approximately 3–5% yield after 8 hours reaction time. This result is consistent with previous work on the noncatalytic disproportionation of benzaldehyde to form benzyl alcohol and benzoic acid in HTW.<sup>4</sup>

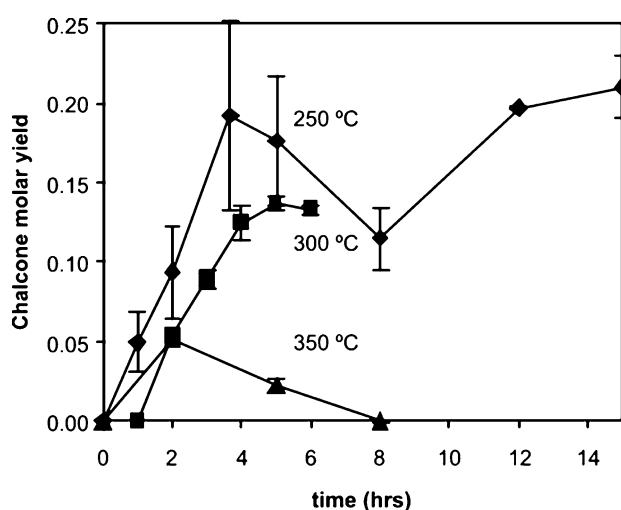
Experiments at 250 °C revealed that benzalacetone undergoes a reverse aldol condensation to form benzaldehyde and acetone in a 7–11% yield at a reaction time of 2 hours. Chalcone underwent a similar reverse aldol condensation to form benzaldehyde and acetophenone in 48–56% yield at a reaction time of 1 hour. The average ring balance in both experiments was about 97%.

The crossed aldol condensation reaction can be catalyzed by either acid or base. We performed experiments at different pH values to probe the relative contribution of the two routes for benzalacetone synthesis. To alter the pH of the reaction system we added either hydrochloric acid or sodium hydroxide. We used the dissociation constant for hydrochloric acid,<sup>5</sup> and the ion product of water<sup>6</sup> to calculate the amount of hydrochloric acid dissociated at reaction conditions. Due to the small amount of acid added and the relatively mild reaction conditions, 99.98% of the hydrochloric acid dissociated. Because NaOH is an equivalently strong base, we

**Table 2** Molar yields of reactants and products from chalcone synthesis in HTW

Temperature/°C	t/h	Molar yields				
		Acetophenone	Benzaldehyde	Chalcone	3-Phenyl propiophenone	Ring balance
250	1.00	0.99 ± 0.02	0.95 ± 0.02	0.05 ± 0.02	n.d. <sup>a</sup>	1.02 ± 0.03
	2.00	0.92 ± 0.02	0.88 ± 0.03	0.09 ± 0.03	n.d. <sup>a</sup>	0.99 ± 0.05
	3.66	0.90 ± 0.02	0.88 ± 0.08	0.19 ± 0.06	trace	1.08 ± 0.10
	5.00	0.71 ± 0.05	0.71 ± 0.07	0.18 ± 0.04	trace	0.89 ± 0.09
	8.00	0.71 ± 0.08	0.64 ± 0.08	0.12 ± 0.02	trace	0.80 ± 0.11
	12.00	0.60 ± 0.03	0.58 ± 0.02	0.20 ± 0.01	trace	0.79 ± 0.04
	15.00	0.62 ± 0.09	0.66 ± 0.07	0.21 ± 0.02	0.007 ± 0.004	0.86 ± 0.12
300	0.50	0.86 ± 0.02	0.73 ± 0.02	0.05 ± 0.01	0.008 ± 0.001	0.85 ± 0.03
	1.00	0.61 ± 0.01	0.89 ± 0.01	0.09 ± 0.01	0.012 ± 0.002	0.85 ± 0.02
	2.00	0.90 ± 0.05	0.79 ± 0.05	0.12 ± 0.01	0.008 ± 0.003	0.97 ± 0.07
	5.00	0.81 ± 0.01	0.74 ± 0.03	0.14 ± 0.01	0.012 ± 0.011	0.93 ± 0.03
	8.00	0.82 ± 0.01	0.75 ± 0.01	0.13 ± 0.01	0.018 ± 0.010	0.93 ± 0.02
350	2.00	0.84 ± 0.05	0.67 ± 0.05	0.05 ± 0.01	0.009 ± 0.002	0.81 ± 0.07
	5.00	0.60 ± 0.11	0.38 ± 0.06	0.02 ± 0.01	0.028 ± 0.006	0.54 ± 0.13
	8.00	0.56 ± 0.02	0.18 ± 0.02	trace	0.060 ± 0.005	0.43 ± 0.03

<sup>a</sup> n.d.-not detected.

**Fig. 3** Temporal variation of chalcone yields at different temperatures.

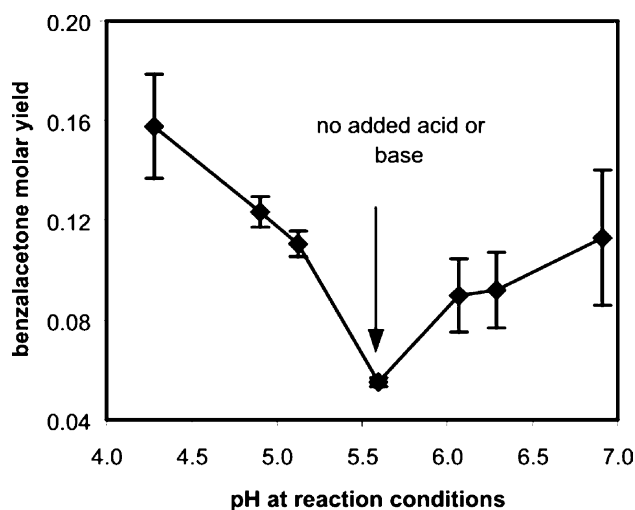
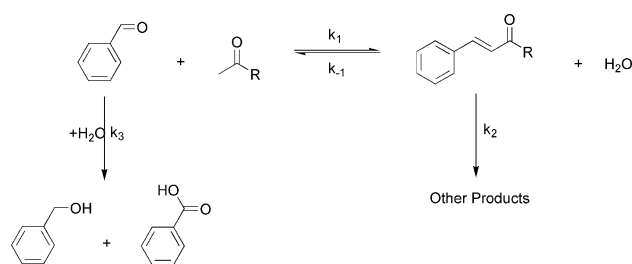
assumed it also dissociated completely. We did not observe any new products from the experiments with added acid or base (no sodium-containing or chlorinated products).

Fig. 4 shows results from the reaction of benzaldehyde and acetone in HTW with added acid or base. All experiments were done at 250 °C for 1 hour. The average ring balance in these experiments was 102 ± 3%. The experiments show that the benzalacetone yield increased with the addition of either acid or base indicating that the reaction was not exclusively acid or base catalyzed in HTW. Since the benzalacetone yields increased by addition of both acid and base, the reaction is likely being catalyzed by both H<sup>+</sup> and OH<sup>-</sup> ions in pure HTW.

### Reaction network and kinetics model

The reaction network for this system appears in Fig. 5. Benzaldehyde (B) reacts reversibly with a ketone (A) to form benzalacetone or chalcone (C). These products can react further to form other products. Additionally, benzaldehyde can react to form benzyl alcohol and benzoic acid. Given this network, one can write the differential equations that govern species' concentrations during reaction in a constant-volume batch reactor.

$$\frac{dC_A}{dt} = -k_1 C_A C_B + k_{-1} C_C \quad (1)$$

**Fig. 4** Effect of pH on benzalacetone yield at 250 °C and 1 hour.**Fig. 5** Reaction network for crossed aldol condensations in HTW. R = CH<sub>3</sub> for benzalacetone synthesis and R = Ph for chalcone synthesis.

$$\frac{dC_B}{dt} = -k_1 C_A C_B - k_3 C_B^2 + k_{-1} C_C \quad (2)$$

$$\frac{dC_C}{dt} = -k_2 C_C - k_{-1} C_C + k_1 C_A C_B \quad (3)$$

The disproportionation of benzaldehyde is second order,<sup>4</sup> so we used this rate equation in the model. The rate of the reverse reaction in pathway 1 depends on the water concentration. This quantity does not change appreciably during an experiment, so the water concentration was embedded in the reverse rate constant for pathway 1. These differential equations provide a mathematical model for this chemical reaction system. We used these model

equations along with the experimental data to find values of the rate constants at each temperature that provided the best fit of the data. We used SCIENTIST, a commercial software package, to simultaneously solve the differential equations and perform the parameter estimation. The objective function that was minimized was the sum of the squared differences between the calculated and experimental concentrations of benzaldehyde, acetone/acetophenone, and benzalacetone/chalcone in each reactor.

Fig. 6 and 7 show that the model captured quantitatively the trends in the experimental data for benzalacetone synthesis. The

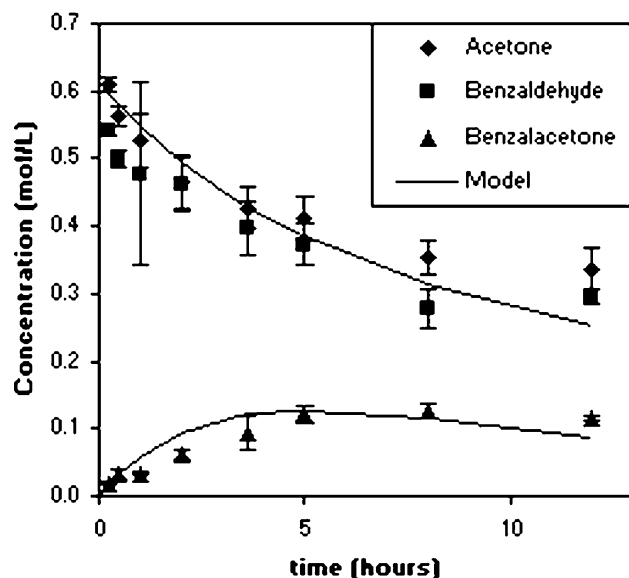


Fig. 6 Comparison of model and experimental results for benzalacetone synthesis at 250 °C.

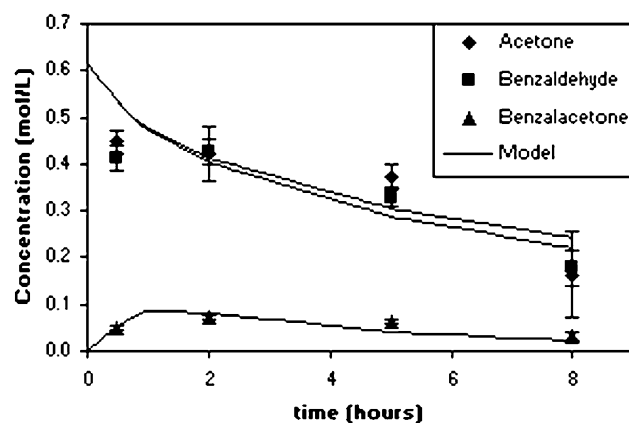


Fig. 7 Comparison of model and experimental results for benzalacetone synthesis at 350 °C.

model showed the same ability to fit the data from the chalcone experiments. Tables 3 and 4 display the optimized values of the rate

Table 3 Optimized values  $\times 10^5$  of rate constants for reaction network in Fig. 4, R = CH<sub>3</sub>

T/°C		250 °C	300 °C	350 °C
$k_1$	L mol <sup>-1</sup> s <sup>-1</sup>	5.3 ± 0.6	6.7 ± 1.1	17.5 ± 1.7
$k_{-1}$	s <sup>-1</sup>	0.8 ± 0.8	4.4 ± 3.1	18.9 <sup>a</sup>
$k_2$	s <sup>-1</sup>	6.1 ± 0.8	9.4 ± 1.9	23.3 ± 5.6
$k_3$	L mol <sup>-1</sup> s <sup>-1</sup>	0 <sup>a</sup>	0 <sup>a</sup>	0.6 ± 0.8

<sup>a</sup> Value fixed in the model.

constants for each path at each of the three temperatures. Note that  $k_3$  was set to zero when working with the data obtained at 250 and 300 °C, because there was no evidence of benzaldehyde dis-

Table 4 Optimized values  $\times 10^5$  of rate constants for reaction network in Fig. 4, R = Ph

T/°C		250 °C	300 °C	350 °C
$k_1$	L mol <sup>-1</sup> s <sup>-1</sup>	3.1 ± 0.3	6.1 ± 0.3	13.6 ± 4.7
$k_{-1}$	s <sup>-1</sup>	1.9 ± 0.8	15.0 ± 1.9	61.4 <sup>a</sup>
$k_2$	s <sup>-1</sup>	2.2 ± 0.6	2.8 ± 0.6	57.2 ± 38.9
$k_3$	L mol <sup>-1</sup> s <sup>-1</sup>	0 <sup>a</sup>	0 <sup>a</sup>	6.7 ± 0.8

<sup>a</sup> Value fixed in the model.

proportionation at these temperatures. The values of  $k_3$  at 350 °C are  $5.6 \times 10^{-6}$  and  $6.7 \times 10^{-5}$  L mol<sup>-1</sup> s<sup>-1</sup>, which are in reasonable agreement with the value of  $2.0 \times 10^{-5}$  reported previously<sup>4</sup> for the reaction at 352 °C. The value of  $k_{-1}$  was fixed at 350 °C rather than allowing it to remain a fitted parameter, as it was at the lower temperatures. The reason for this change is that the parameter estimation routine set  $k_{-1}$  to zero when fitting the data at 350 °C. We believe this behavior is an artifact of the modelling program (the ability to fit the data at 350 °C is not very sensitive to the value, or even presence, of  $k_{-1}$ ). Therefore, to ensure chemically meaningful values of  $k_{-1}$  at 350 °C, we used the Arrhenius equation and the values of  $k_{-1}$  determined at 250 and 300 °C to extrapolate to 350 °C. These extrapolated values are the ones that appear in Tables 3 and 4.

We used the equilibrium constants ( $k_1/k_{-1}$ ) and the van't Hoff equation to estimate the heats of reaction for the unsaturated ketone syntheses. The resulting reaction enthalpies are -53 and -54 kJ mol<sup>-1</sup>, respectively, for benzalacetone and chalcone synthesis, respectively. The literature<sup>7</sup> provides an experimental value of  $-65 \pm 2$  kJ mol<sup>-1</sup> for the heat of reaction for chalcone synthesis. Thus, the reaction enthalpy determined from the model shows good agreement with this experimental measurement from calorimetry.

The activation energy for  $k_1$ , which is the path to the desired product, is 32 kJ mol<sup>-1</sup> for benzalacetone and 40 kJ mol<sup>-1</sup> for chalcone. These values are higher than the values of 20–25 kJ mol<sup>-1</sup> that previous workers<sup>2</sup> reported for a condensation reaction between benzaldehyde and 2-butanone. The discrepancies in the activation energies might be explained by differences in the reactants and in the two reaction models employed. The previous model used data only at short times, covered a 50 °C range of temperatures, and included only the forward and reverse rates for the main reaction. The present model, on the other hand, included experimental data at long times, spanned a 100 °C temperature range, and included reaction paths for decomposition of the unsaturated ketone product and for benzaldehyde disproportionation along with the main reaction.

## Experimental

We performed batch reactor experiments in  $\frac{1}{4}$  inch stainless steel Swagelok tube fittings. These reactors consisted of a port connector and two caps, which provided 0.59 cm<sup>3</sup> reactor volume. Prior to their use in experiments, all the reactors were loaded with water and conditioned for 1 hour at 300 °C to remove any lubricants/oils that remained from the manufacture of the Swagelok parts. These reactors were then cleaned with methanol and dried prior to use. All chemicals were purchased from Aldrich and used as received. Benzaldehyde, acetophenone, and benzalacetone were 99% pure, and chalcone was 97% pure. Methanol and acetone were HPLC grade.

All reactants were added to the reactors inside a glove box filled with purified helium. In addition, for 25 minutes helium was bubbled through the deionized water used in the experiments to remove any dissolved oxygen and carbon dioxide, which could affect the reaction rate. Carbon dioxide forms carbonic acid in water, which alters the pH. Because we were interested in the kinetics of the synthesis reaction we wanted to remove any uncontrolled effect of acid catalysis.

We loaded 322–448  $\mu\text{l}$  of water in the reactors. The water loadings were selected such that 95% of the reactor volume would be occupied with liquid water at the reaction temperature. Water densities were taken from steam tables.<sup>8</sup> Next 35  $\mu\text{l}$  of benzaldehyde was loaded into the reactors. Acetone, the more volatile reactant, was added last to minimize evaporative losses. The reactors were immediately capped after the addition of 25.5  $\mu\text{l}$  of acetone. In the chalcone experiments, 40  $\mu\text{l}$  of acetophenone was added instead of acetone. The volumes of benzaldehyde and acetone/acetophenone added corresponded to an initial concentration of 0.614 M for each reactant. In benzalacetone synthesis, if much more than the stoichiometric amount (1 : 1) of benzaldehyde is added, then benzalacetone may react with benzaldehyde to form dibenzalacetone.<sup>1,9</sup> Several independent runs were done at each set of reaction conditions.

In some experiments acid or base solution was added to the reactor. A Beckman  $\Phi$  45 pH Meter was calibrated at pH 4.0 and 10.0 with commercial buffer solutions and then used to measure the pH of standard acid and base solutions. Standard solutions were created at pH values of 4.5, 5.0, 5.5, 8.5, 9.0, and 9.5 at ambient conditions.

Once loaded and capped, the reactors were stored in a  $-10\text{ }^{\circ}\text{C}$  freezer (12 hours or less) until they could be placed in a Techné SBL-2 fluidized sand bath, preheated to the reaction temperature  $\pm 1\text{ }^{\circ}\text{C}$ . The reactor heat-up time is of the order of a few minutes,<sup>10</sup> which is very short compared to the reaction times investigated. Following the heating period, the reactors were removed from the sand bath and submerged in room temperature water for 30–60 seconds. The reactors were then stored in the freezer until they were opened and their contents recovered and analyzed.

Upon being opened, the reactors were filled with methanol (for benzalacetone synthesis) or acetone (for chalcone synthesis). The reactor contents were then stirred to dissolve any solids in the reactors. This process was repeated 5–8 times. The solutions were then analyzed by an Agilent model 6890 gas chromatograph. A 50 m  $\times$  0.2 mm  $\times$  33  $\mu\text{m}$  HP-5 capillary column with helium carrier gas separated the sample constituents. We used a mass spectrometric (GC-MS) detector for product identification and a flame ionization detector (GC-FID) for quantitative analysis. An auto injector was used with both devices. The GC-FID injected 2  $\mu\text{l}$  and used a split ratio of 25 : 1. The GC-MS injected 4  $\mu\text{l}$  in splitless mode. The temperature program in both instruments was 5 minutes at 70  $^{\circ}\text{C}$ , a temperature ramp of 70  $^{\circ}\text{C}$  per minute to 240  $^{\circ}\text{C}$ , and then holding the final temperature for 23 minutes. Analysis of standard solutions containing known amounts of reactants and products provided calibration curves, which were used to determine the amount of recovered chemicals in the reaction samples. Molar yields were calculated as the moles of product formed per mole of acetone/acetophenone loaded into the reactor.

## Conclusions

The crossed aldol condensation of benzaldehyde and acetone forms benzalacetone in HTW. The condensation of benzaldehyde and acetophenone forms chalcone in HTW. No acid or base need be added to cause the reaction to occur, but adding either acid or base increased the reaction rate.

These condensation products form in HTW in high selectivity at the milder reaction conditions. Thus, a large-scale continuous process could give a high selectivity. The process can also give the desired product in high yields if there is post-reaction separation of the product and unconverted reactants. This separation is conceptually simple for the present system wherein the product is a solid and all other components are liquids. After the solid product has been removed, the liquid stream can be recycled to the reactor to convert more of the reactants.

Using HTW as the medium for this reaction can make the process more environmentally benign because it eliminates the need for added acid or base, the subsequent neutralization of the excess acid or base, and disposal of the salt so formed. HTW is a promising medium for aldol condensations and for acid and base-catalyzed green syntheses.

## Acknowledgements

We thank Professor Edwin Verdejs for helpful discussions. This work was supported in part by the American Chemical Society Petroleum Research Fund (37603-AC9) and by the U.S. National Science Foundation (CTS0218772).

## References

- 1 R. D. Ashford, *Ashford's Dictionary of Industrial Chemicals*, Wave-length Publications Ltd, London, England, 1994, p. 123.
- 2 Z. Q. Zhu, J. Q. Zeng, Y. Q. Li and L. M. Liu, *Youji Huaxue*, 2003, **23**(1), 72.
- 3 S. A. Nolen, C. L. Liotta, C. A. Eckert and R. Gläser, *Green Chem.*, 2003, **5**, 663.
- 4 Y. Ikushima, K. Hatakeda, O. Sato, T. Yokoyama and M. Arai, *Angew. Chem., Int. Ed.*, 2001, **1**, 210.
- 5 B. R. Tagirov, A. V. Zotov and N. N. Akinfiev, *Geochim. Cosmochim. Acta.*, 1997, **20**, 4267.
- 6 W. L. Marshall and E. U. Franck, *J. Phys. Chem. Ref. Data*, 1981, **2**, 295.
- 7 J. Hao, J. Chang, K. Wang, Y. Liu and G. Zhong, *Huaxue Tongbao*, 1985, 15.
- 8 Y. Cengel and M. A. Boles, *Thermodynamics an Engineering Approach 3<sup>rd</sup> edition*, McGraw-Hill, New York, 1998, p. 905.
- 9 C. R. Conard and M. A. Dolliver, *Org. Synth.*, 1943, **CV 2**, 167.
- 10 J. R. Lawson and M. T. Klein, *Ind. Eng. Chem. Fundam.*, 1985, **24**, 203.